2008

Erosion rate of chemically stabilised soils incorporating tensile stress-deformation behaviour

Thevaragavan Muttuvel
University of Wollongong

EROSION RATE OF CHEMICALLY STABILISED SOILS INCORPORATING TENSILE STRESS - DEFORMATION BEHAVIOUR

A thesis submitted
in fulfilment of the requirements for the Award of the Degree

DOCTOR OF PHILOSOPHY

from

UNIVERSITY OF WOLLONGONG

by

Thevaragavan Muttuvel, BSc Eng (Hons)

School of Civil, Mining and Environmental Engineering
University of Wollongong, Australia.

2008

THESIS CERTIFICATION

I, Thevaragavan Muttuvel, declare that this thesis, submitted in fulfillment of the requirements for the award of Doctor of Philosophy, in the School of Civil, Mining and Environmental Engineering, Faculty of Engineering, University of Wollongong, is wholly my own work unless otherwise referenced or acknowledged. The document has not been submitted for qualification at any other academic institution.

……

Thevaragavan Muttuvel

April 2008

ACKNOWLEDGEMENTS

I would first like to express my gratitude to my supervisor Prof. Buddhima Indraratna for his constant support, encouragement, and enthusiastic guidance throughout this research project. His availability for fruitful discussion and thesis editing, despite his heavy workload, is very much appreciated. His support during difficult times and outside academia is gratefully acknowledged.

I would also like to extend thanks to my co-supervisor Dr. Hadi Khabbaz for taking the time for open discussion and mentoring during tough moments.

My thanks also go to the University of Wollongong and the Australian Government *IPRS* scheme for financially supporting this thesis to completion.

I wish to express my gratitude to technical staff Alan Grant, Ian Laird and Jason Knust for their assistance during the experimental work. I also extend my thanks to technical officers Bob Rowlan, Ian Bridge, Ken, Peter, Des, Leonie and the EEC staff.

I wish to thank past and current postgraduate companions including Dr. Jayanathan Mylvaganam, Kalyani Dissanayake, Dr. Ashok Raut, Dr. Behzad Fatahi, and Linda for their support, and social interaction outside the "geotechnical" world. My appreciation is also extended to all past and present members of the School of Civil, Mining and Environmental Engineering, University of Wollongong for their warm hearted cooperation.

Finally, the author dedicates this piece of work to his mother and sister because without their support it would have been impossible to achieve this goal.

LIST OF PUBLICATIONS

The following publications were generated during my research period.

Indraratna, B., Thevaragavan, M., Khabbaz, H., and Armstrong, R. (2007). “Predicting the erosion rate of chemically treated soil using a process simulation apparatus for internal crack erosion”, Journal of Geotechnical & Geo-environmental Engineering, ASCE, Accepted for publication.

Indraratna, B., Thevaragavan, M., and Khabbaz, H. (2007). “Modelling the erosion rate of chemically stabilised soil incorporating tensile stress-deformation characteristics”, Canadian Geotechnical Journal, Submitted for publication.

Indraratna, B., Thevaragavan, M., and Khabbaz, H. (2008). “Investigating erosional behaviour of chemically stabilised erodible soils”, Geotechnical special publication 178, Geo-congress 2008, ASCE, 670-677.

ABSTRACT

Problems associated with erodible soils have been reported in Australia and many parts of the world since the early 1970s. Significant soil loss from embankments, internal erosion and piping are some of the problems that practicing engineers face during the construction and maintenance phase of earth structures constructed with erodible soils. It is therefore necessary to identify appropriate stabilisation techniques to control erosion. This study considers chemical stabilisation as an erosion control method and a rigorous testing program has been conducted to investigate how effectively two chemical agents (general purpose Portland cement and lignosulfonate) control the erosion rate of two natural erodible soils (a silty sand and dispersive clay).

In this study, a Process Simulation Apparatus for Internal Crack Erosion (*PSAICE*) has been designed and built to conduct tests on chemically treated and untreated soil samples. The effect of the degree of compaction and moulding water content on erosional behaviour of soils has also been addressed. In addition, the tensile stress-deformation characteristics of chemically treated soil samples have been investigated using a uniaxial tensile testing apparatus, designed and built at University of Wollongong for this current research study.

One of the main objectives was to develop an analytical model for the erosion rate that incorporates the tensile stress-deformation characteristics of the soil. The model has been developed based on the law of the conservation of energy and validated using the results of erosion and uniaxial tensile tests conducted on chemically stabilised soil samples.

The results of the tests indicated that the erosion rate changes linearly with the hydraulic shear stress; slope of the line that represents the coefficient of soil erosion. The coefficient of soil erosion decreases, while the critical shear stress increases with an increasing amount of stabiliser,

irrespective of the soil type. It was also found that the coefficient of soil erosion of chemically treated soil has a strong relationship with its critical shear stress. Uniaxial tensile tests on chemically treated saturated samples showed that both stabilisers increase the tensile strength with a decrease in the displacement at failure.

Model validation demonstrated that only a fraction of flow energy (i.e. efficiency index) is used for the erosion process, and it depends on the hydraulic conditions of flow. Moreover, the proposed model can be used to predict the erosion rate of chemically treated erodible soils, if the tensile stress-deformation characteristics, mean particle diameter, dry density, and mean flow velocity through the crack are known.

TABLE OF CONTENTS

LIST OF FIGURES

LIST OF TABLES

LIST OF SYMBOLS AND ABBREVIATIONS

Symbols	Description
A_s	Cross-sectional area of the soil sample used for tensile test
a, b	Constants
CP	Amount of chemical stabiliser
D	Mean particle diameter of soil
c, d	Constants
e	Void ratio
F	Inter-particle bond strength
F_J	Friction at the joint of tensile testing apparatus
F_T	Tensile force acting on the fracture plane
f	Friction factor
g	Gravitational acceleration
J	Jet index
k	Mean coordination number
k_c	Empirical factor relating turbidity to the soil solids concentrated in the flow
k'	Average number of common contacts (inter-particle bonds) per particle
L	Applied tensile load
l	Length of the sample used for erosion test

M	Total amount of soil eroded during an erosion test
m	Proportionality coefficient used for the prediction of critical shear stress of treated soil
P	Unit stream power
P_c	Critical unit stream power
Q_i	Flow rate of i^{th} time step
R	Mean particle radius
r	Contact radius between particles
S_v	Vane shear strength
s	Hydraulic gradient across the crack
T_i	Effluent turbidity of i^{th} time step
u_*	Shear velocity of the flow
v	Mean velocity of the flow through crack
v_c	Critical mean velocity of the flow through crack
W_A	Weight of the upper part of the tensile testing apparatus
W_S	Weight of the soil in the upper part of the tensile testing apparatus
α	Coefficient of soil erosion
λ, β, γ	Constants
δ_T	Tensile deformation
δ_{Tf}	Failure tensile deformation
χ	Relative roughness
$\dot{\varepsilon}$	Erosion rate

μ	Dynamic viscosity of the eroding fluid
ρ_d	Dry density of the soil
ρ_s	Density of the particle
ρ_w	Density of the eroding fluid
σ_T	Applied tensile stress
σ_{Tf}	Tensile strength of the soil
τ_a	Hydraulic shear stress
τ_c	Critical shear stress
ϕ_i	Soil crack diameter at time *t*
ω	Efficiency index

Abbreviations

PSAICE	Process Simulation Apparatus for Internal Crack Erosion

CHAPTER 1

INTRODUCTION

1.1 Overview and Statement of the Problem

Earth structures such as embankment dams constructed with erodible soils are in danger of severe surface and internal erosion (piping). The erodible soils may be dispersive clayey soils, or non-cohesive silt and very fine sands. The degree of dispersion and subsequent erosion of cohesive clay depend on factors such as its mineralogy and the dissolved salt in pore and eroding water (Sherard *et al.* 1972). When a dispersive clay comes into contact with relatively pure water, the particles tend to separate because of an increasing repulsive force, which significantly reduces the strength of the inter-particle bond. Therefore, flowing water, even under a very mild hydraulic gradient, can remove these particles (ICOLD 1990). Apart from its mineralogy, the placement moisture content and the degree of compaction also influence the erodibility (e.g. Wan and Fell 2004; Kandiah and Arulananthan 1974). If, for example, the soil is poorly compacted especially near rigid structures such as outlet pipe in a dam, the reservoir water will erode the soil in these highly permeable zones and result in a piping incident.

Non-cohesive soils containing a vast amount of fine sand and silt such as silty sand, and flood deposits will also be erodible (Udomchoke 1991). Their erosion is controlled by the size and self weight of the particles, the placement moisture content, and the degree of compaction (e.g. Wan and Fell 2004; Briaud *et al.* 2001; Parker *et al.* 1995).

Internal and surface erosion are two important failure modes of earthfill dams all around the world. The internal erosion in dams occurs through concentrated leaks (e.g. cracks), backward erosion due to seepage, through internally unstable soils, and blow out, while surface erosion takes place over the slopes from runoff after rainfall (Fell *et al.* 2003; Foster 1999).

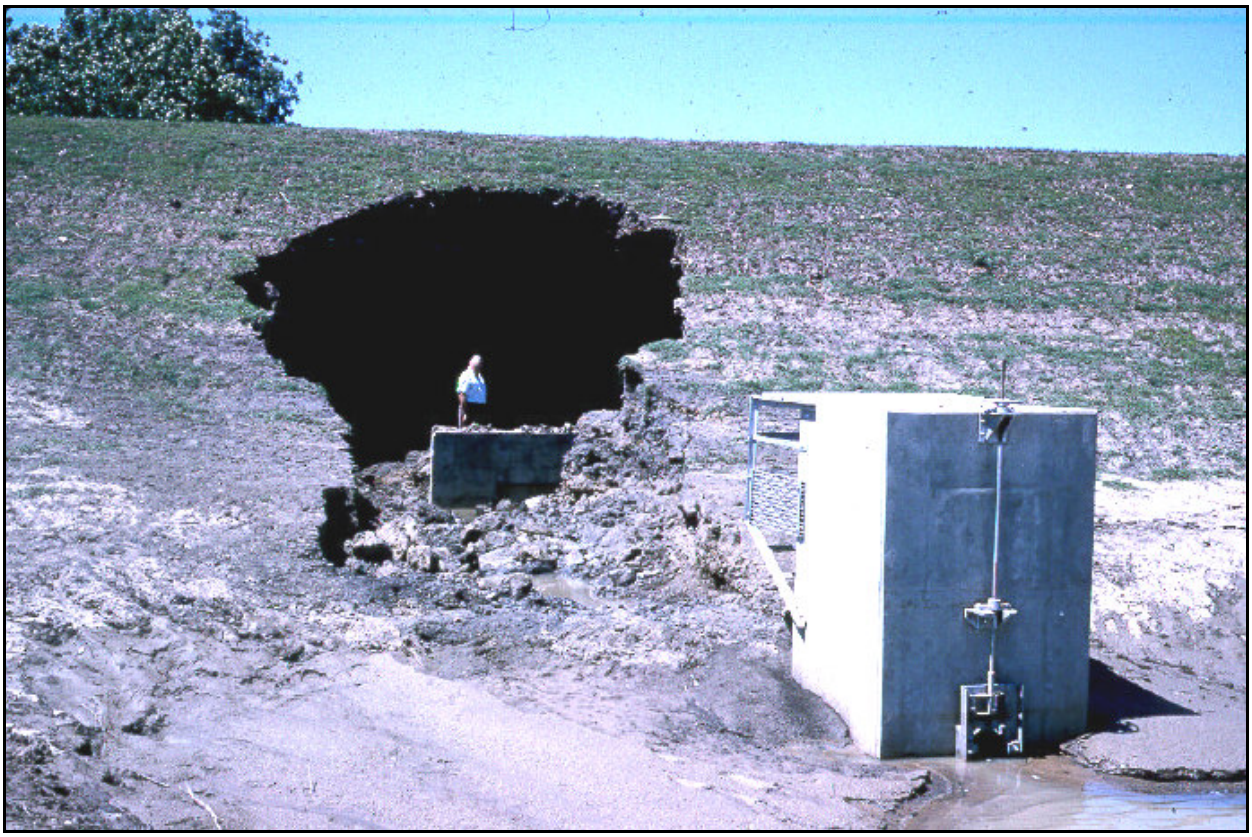

Figure 1.1 An example of piping failure at Upper Clear Boggy in the USA (Lim 2006)

Internal erosion and piping are recognised as major causes of failures of embankment dams. Figure 1.1 shows a dam at Upper Clear Boggy in the USA that failed from piping. Historically, around 0.5% (1 in 200) of embankment dams in the world have failed because of internal erosion and piping, while approximately 1.5% have experienced piping incidents. It was reported that

around half of the piping incidents had occurred through the embankment, while 40% through the foundations (Fell *et al.* 2003). They also reported that the internal erosion in an embankment may occur rapidly through cracks, while its progression depends on the type of soil. If the soil falls into following categories, then erosion progresses rapidly.

(a) Very uniform, fine cohesionless sand or well graded cohesionless soil with a plasticity index less than 6%. And soils contain low clay (less than 5%).

(b) A dispersive soil of class *D1* or *D2* (classified using the standard pinhole test).

It is clear that using erodible soils for embankment dams only increases the possibility of piping failure. Since problems associated with erodible soils can cause loss of lives, property, and high maintenance costs, using them as dam construction fills is not advisable, but sometimes it is unavoidable. Hence, it is essential that appropriate methods of reducing erosion be identified.

Chemical stabilisation is a promising method for protecting earth structures from erosion. Several investigations have been carried out (e.g. Indraratna *et al.* 1991; Indraratna 1996; Perry 1977; Biggs and Mahony 2004), and they all reported that stabilising erodible soils with traditional chemical agents such as lime, gypsum, milled slag, and pozzolanic fly ash (ASTM class C) is an effective method of controlling erosion. Because of economic considerations, this method can only be applied at selected locations of earthdams such as around outlet conduits, at the foundation interface, and on the slopes. However, using the traditional chemical stabilisers may cause problems such as (a) corrosion of steel structures (e.g. due to gypsum treatment), (b) milled slag requires stringent scrutiny from environmental bodies because of the presence of heavy metals and other impurities and (c) the effect of an acid or alkali environment on

vegetation from soils treated with lime (Indraratna 1996; Perry 1977; Sherard *et al.* 1972; Ryker 1977; Biggs and Mahony 2004). Hence, identifying an alternative chemical treatment to avoid some of these short comings is crucial. This study considers general purpose Portland cement (a traditional stabiliser) and lignosulfonate (a non-traditional stabiliser), a processed by-product of paper manufacturing industry.

Studying the erosion of soil in cracks will help to understand its resistance to flowing water under a given hydraulic condition. Tests have been conducted in the past to investigate the erosion of soils through cracks (e.g. Wan and Fell 2004; Sherard *et al.* 1976(a); Locke 2001), however they have not saturated the soil before testing. When water in a reservoir flows through a crack, the soil becomes saturated over time, and only true cohesion of the soil governs its erosional behaviour, as reported by Atkinson *et al.* (1990). True cohesion is the strength of the soil at zero effective normal stress, but if tested under unsaturated conditions the matric suction may produce higher normal stress, which ultimately increases resistance to erosion. Therefore, this study investigates erosion in cracks under saturated conditions.

Calculating the erosion rate of soil using its strength is an effective approach for geotechnical engineers to assess erosion related problems. Only a few empirical relationships for critical shear stress in terms of the shear strength of saturated soils are available in literature (e.g. Dunn 1959; Lyle and Smerdan 1965; Kamphuis and Hall 1983). Reddi and Bonala (1997) derived a theoretical model for the critical shear stress incorporating the cohesion of a saturated sand-kaolinite mix. To the writer's knowledge, however, no comprehensive model for the erosion rate in terms of the shear strength of soil has been developed. It was found from literature that developing a relationship between the erosion rate and the shear strength of soil is difficult for the following reasons:

- As discussed earlier, only true cohesion controls erosion under saturated conditions, but its measurement is complicated, because the test should be conducted under very low normal stresses. The conventional equipment such as direct shear apparatus measures cohesion intercept that includes both true cohesion (if tests are performed under normal stresses that do not destruct interparticle bonds) and cohesion resulting from particle interlocking. Hence, it is not possible to measure true cohesion using the conventional shear tests.

- When the soil comes into contact with the eroding fluid, it will lose the strength, and erode quickly, if the concentration of dissolved salt in the eroding fluid is below that of the pore fluid. Unless the sample for the shear strength test is prepared under the same conditions existing in the erosion process, the measured shear strength will not represent the strength that controls erosion. In the conventional shear tests such as triaxial test, however, it is difficult to attain those conditions.

Due to these limitations, this study considers tensile stress-deformation behaviour rather than shear behaviour to model erosion, because, the former is a direct measure of the inter-particle bond strength that controls erosion under saturated conditions.

1.2 Objectives of the Study

This study aims to improve the understanding of the soil erosion through the following tasks:

- A critical review of literature that describes previous experimental methods used for predicting soil erosion parameters, erosion modelling in terms of the shear strength of

soil, and erosion control measures, with an emphasis on chemical stabilisation. Identifying the knowledge gap in erosion modelling and chemical stabilisation based on the findings of the past studies is imperative.

- Developing an analytical model to capture erosion through cracks incorporating the tensile stress-deformation characteristics of soil.

- Executing a rigorous experimental program to investigate the erosion characteristics of two natural erodible soils treated with chemical stabilisers. This includes designing and building a new apparatus called "Process Simulation Apparatus for Internal Crack Erosion (*PSAICE*)" and developing a procedure for erosion testing and interpretation of observation.

- Optimising the amount of chemical agent and establishing stabilisation mechanism based on the results of a preliminary investigation, which includes Scanning Electron Microscopy (*SEM*) tests, Soil Conservation Service (*SCS*) dispersion tests, standard pinhole tests, standard compaction tests, and unconfined compression tests.

- Conducting a series of tensile tests on chemically treated erodible soils using a uniaxial tensile testing apparatus, designed and built for this study at University of Wollongong.

- Validating the writer's theoretical erosion model using the results of erosion and tensile tests conducted with the *PSAICE* and uniaxial tensile testing apparatus, respectively.

1.3 Thesis Structure

Following the Introduction in Chapter 1, Chapter 2 provides a critical review of past studies. The literature review includes factors controlling soil erosion, different experimental approaches used for predicting erosion parameters, erosion control techniques, stabilising the soil with chemical additives, and the tensile stress-strain behaviour of soil and its relevance to erosion related problems.

Chapter 3 elaborates on the development of an analytical model for erosion using the law of the conservation of energy by incorporating the tensile stress-deformation characteristics of soil, mean particle diameter, dry density, and hydraulic condition. This chapter also includes available empirical models to predict the critical shear stress using the shear strength of soil, the difficulties of correlating shear behaviour of soil to erosion rate, and the selection of an alternative strength property for modelling erosion.

Chapter 4 describes the methodology adopted in the experimental program conducted on chemically treated and untreated erodible soils. Description of the *PSAICE* and uniaxial tensile testing apparatus, sample preparation for erosion and tensile tests, and interpretation of observation are presented. The procedure used for the Scanning Electron Microscopy (*SEM*) tests and Soil Conservation Services (SCS) dispersion tests are also included in this chapter.

The experimental results are discussed in detail in Chapter 5. The effectiveness of lignosulfonate and cement in reducing the erosion rate of dispersive clay and silty sand, and the effect of the degree of compaction and moulding water content on erosion is presented. The mechanisms by which these chemical agents stabilise the selected erodible soils are explained. This chapter also includes the tensile stress-deformation characteristics of chemically treated erodible soils.

Chapter 6 presents the validation of the theoretical erosion model developed in Chapter 3. The quantification of model parameters based on the results of tensile and erosion tests are described in detail.

Chapter 7 presents the "Conclusions and Recommendations". It sets out the main findings of this study presented in Chapters 5 and 6, and outlines recommendations for the future studies in erosion modelling and chemical stabilisation of erodible soils.

The final section of the thesis includes Appendices A to C that provide additional information to supplement the contents described in Chapter 4.

CHAPTER 2

LITERATURE REVIEW

2.1 Introduction

Erodible soils are usually susceptible to being detached and transported by flowing water. They may be dispersive clayey soils which lose their cohesive strength upon contact with relatively pure water, or non-cohesive silt and very fine sands which do not possess cohesion to resist the force exerted by the water.

Some natural clayey soils are vulnerable to dispersion when exposed to relatively pure water and prone to erosion. The tendency for dispersive erosion depends on factors such as the mineralogy of the clay and dissolved salt in pore water and eroding water. When dispersive clay is immersed in water the clay particles tend to separate particle by particle because of an increasing repulsive force which causes a significant reduction in the inter-particle bond strength. This means they can easily be detached by flowing water even under a very mild hydraulic gradient (ICOLD 1990). Non-cohesive silt and very fine sands are at high risk of erosion by water due to a lack of cohesive bonds amongst the particles. Their entrainment and subsequent transportation is controlled by the self weight of the particles. Soils containing a vast amount of fine sand and silt such as silty sand, wind blown sand, flood deposits and man-made mound soil will be highly erodible (Udomchoke 1991).

In this chapter, problems associated with erodible soils, factors influencing erodibility, experimental methods to measure the erosion rate and critical shear stress, and erosion control

techniques, with the emphasise on chemical stabilization, are discussed in detail. This research study explores the relationship between the tensile stress-deformation behaviour and the erodibility of soil. Therefore, a brief description of experimental methods available to measure the tensile strength and factors affecting the tensile stress-strain behaviour is also included in this chapter.

2.2 Problems Associated with Highly Erodible Soils

Surface erosion and internal erosion, including piping, are two major problems that engineers face all around the world. If the slopes of dams, channels, sides of highway embankments and cut slopes contain highly erodible soils, then severe surface erosion is inevitable (Figure 2.1(a) and (b)).

(a) (b)

Figure 2.1 Severe surface erosion observed in embankment slopes (Kuganenthira 1990)

Crouch (1977) and Elliot (1977) reported that earth structures such as storm water channels in New South Wales, Australia, have been affected by tunnel and gulley erosion. Furthermore, colluvium soils on hilly terrains (loose landslide debris) in New South Wales, Australia, are often

subjected to considerable erosion and slope movement after rainfall, which causes environmental pollution (Indraratna 1996).

In past years, around 0.5% (1 in 200) of embankment dam failures and 1.5% (1 in 60) of piping incidents were caused by internal erosion and piping. Statistics show that about half the dams experienced internal erosion and piping suffered central core erosion, while about 40% were affected by foundation erosion (Fell *et al.* 2003). Many dams in New South Wales and Victoria, Australia affected by internal erosion and piping due to dispersive soils were documented by Philips (1977) and Rosewell (1977). They reported that about 10-16% of small dams failed by physical breach because of dispersive related erosion such as piping. Figures 2.2 and 2.3 show two different dams affected by internal erosion and piping in the USA.

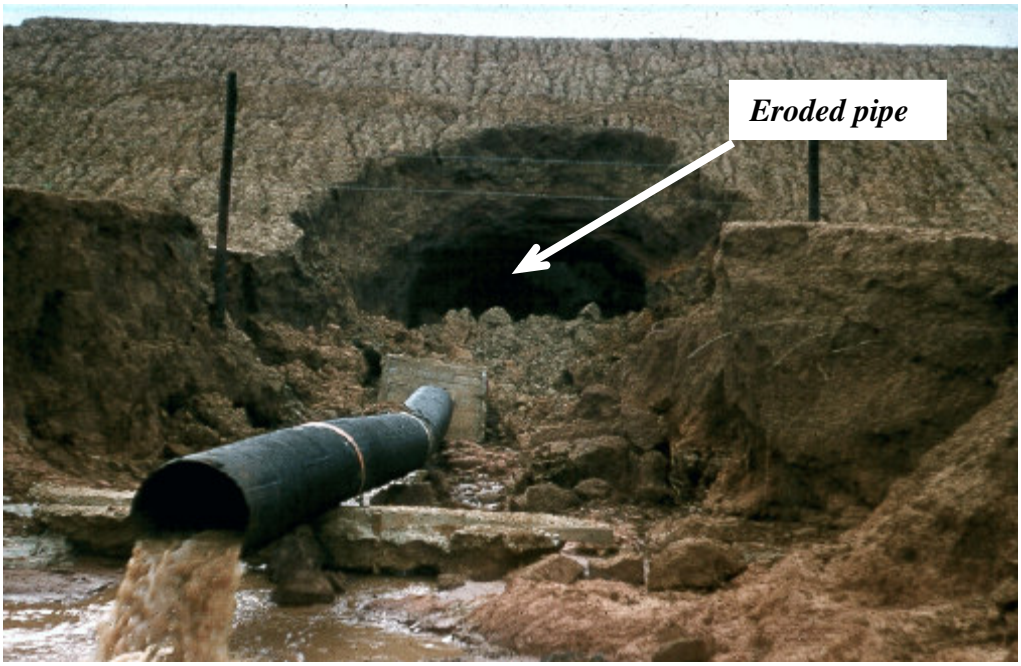

Figure 2.2 Piping incident of an embankment dam constructed with dispersive clay in Mississippi, USA (www.fema.gov/library)

Figure 2.3 Failure of Teton dam due to piping in Idaho, USA

(http://web.umr.edu/~rogersda/teton_dam)

Internal erosion and piping in earth structures can occur by erosion through concentrated leaks (e.g. cracks), seepage through internally unstable soil, backward erosion due to seepage, and blow out (Fell *et al.* 2003; Foster 1999). They are described briefly below.

(a) Piping through concentrated leaks

Cracks from desiccation and differential settlement will create a path for reservoir water to flow through. Other types of leakage channels are formed at high permeable zones such as around outlet conduits through embankments, at the foundation interface, and close to concrete structures where a high degree of compaction is normally not possible to achieve. Cracks may also occur close to concrete structures such as outlet conduits because of differential settlement induced by stiffness contrast. Consequently water seeps through these channels, detaching soil particles which are washed away by flowing water. Figure 2.4 shows an example of a concentrated leak involved in the internal erosion and piping.

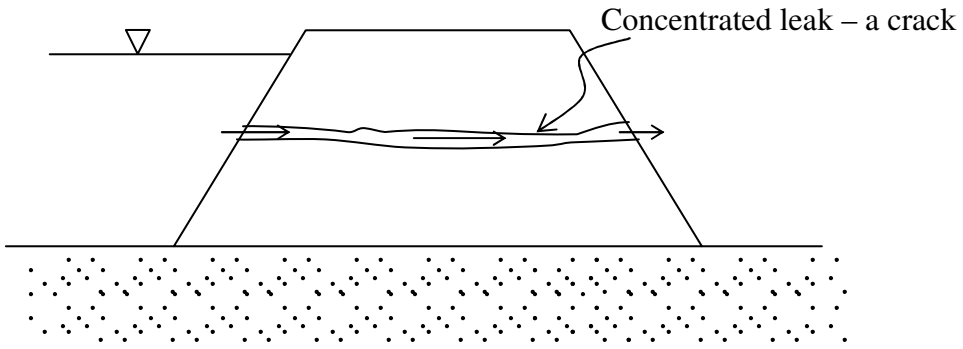

Figure 2.4 Piping through a concentrated leak

(b) Piping due to backward erosion

Piping associated with backward erosion occurs when seepage starts at an exit point (due to high exit hydraulic gradient) and gradually erodes back towards the source to form a continuous soil pipe, as shown in Figure 2.5.

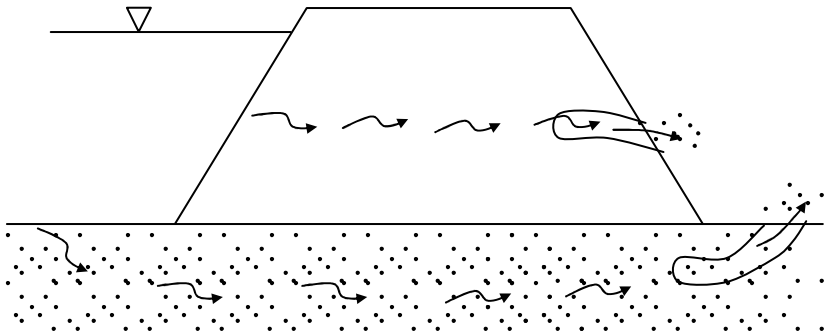

Figure 2.5 Backward piping erosion mechanism

(c) Piping through internally unstable soils

This type of erosion takes place by seepage through internally unstable soils which contain fine and coarse particles with the lack of intermediate size particles (Figure 2.6). Since internal erosion removes fines from the original soil, the stability of the structure diminishes over time.

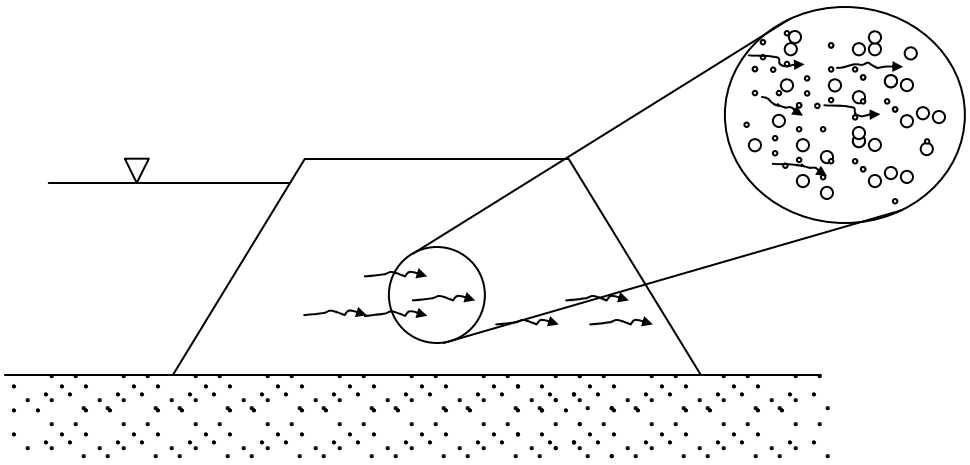

Figure 2.6 Seepage erosion through internally unstable soils

(d) Blow out

Blow out occurs due to high pressures in the foundations caused by a low permeable layer at the downstream toe of the dam (Figure 2.7). High pore pressure can lead to zero effective stress at the downstream toe which erodes the soil as a whole.

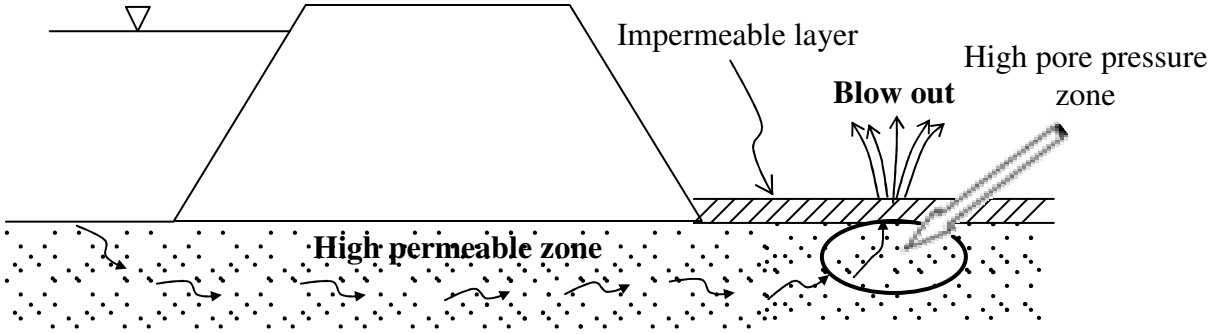

Figure 2.7 Piping caused by blow out

2.3 Identifying the Erodible Soils

Non-cohesive (e.g. silty sand and sands) and dispersive soils are generally called erodible soils. If a soil contains vast amount of silt and sand, then it will be highly erodible. Identification of this type of soil can be done based on the particle size distribution. However, it is difficult to identify dispersive soils based on particle size distribution or other engineering properties such as plasticity and shear strength which is why several field and laboratory methods were developed. A brief description of these methods is outlined below.

2.3.1 Emerson Class Test

This quick and simple test was developed by Emerson to identify dispersive soils. Soils are categorized into eight classes based on their coherence in the water. The standard testing method and classification are described in Australian Standard AS1289.3.8.1 (1997).

2.3.2 SCS Laboratory Dispersion Test

This test has been used extensively by the US Soil Conservation Service (SCS) for decades. It is a simple and easy method to perform in the laboratory. Particle size distribution will be determined from the standard hydrometer analysis by adding a chemical dispersant under strong mechanical agitation. Another hydrometer test will also be performed on a duplicate soil specimen, but without chemical dispersant and mechanical agitation. The "percent dispersion" is given by the ratio of percent finer than 5 microns measured in the second test to the first test. If the "percentage dispersion" is more than 30%, then the soil is susceptible to dispersion erosion (Decker and Dunnigan 1977; Sherard *et al.* 1972).

2.3.3 Standard Pinhole Test

This test was developed in the 1970's (Sherard *et al.* 1976a) to directly measure the dispersibility of compacted fine grained soils. Distilled water will be pushed through a 1 mm diameter hole in the compacted soil specimen. The soil is classified into six groups ranging from highly dispersive clay to completely erosion resistance clay based on the cloudiness of effluent and size of the hole at the end of the test. Detailed procedure and classification method are clearly explained in ASTM D 4647 (93).

2.3.4 Soil Chemical Test

The aim of this experiment is to determine Total Dissolved Salt (*TDS*) and Percent Sodium by measuring the four major cations (sodium, calcium, magnesium and potassium) in the pore water. These parameters will be used to classify dispersive soils, as described in Figure 2.8.

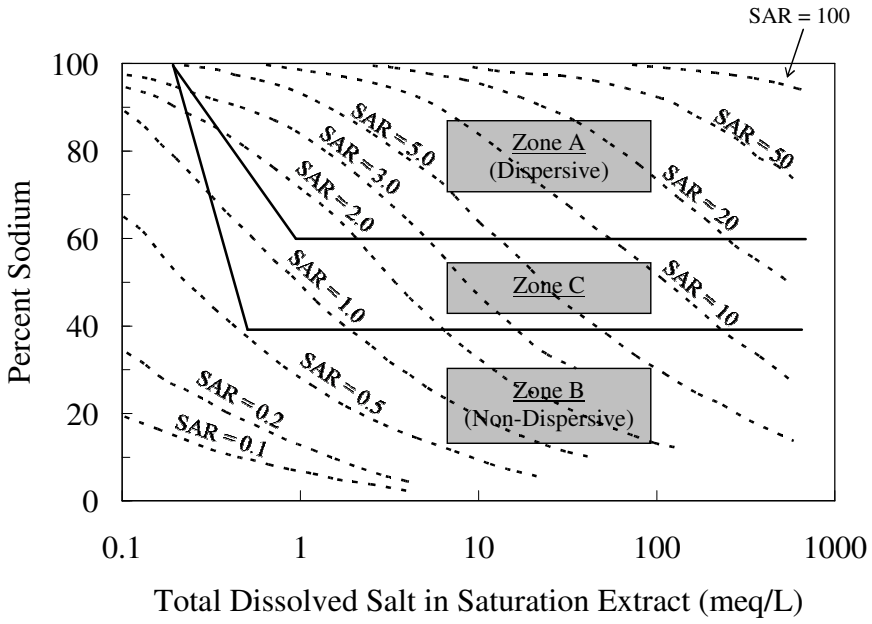

Figure 2.8 Classification of dispersive soils using percent sodium and total dissolved salt in the pore water (Sherard *et al.* 1976b)

This classification chart was introduced by Sherard *et al.* (1976b) based on laboratory results, including the pinhole test and field observations, on a number of dispersive soils. They mentioned that most soils are naturally dispersive or non-dispersive if the pore water salts fell into Zones A and B, respectively. It was also pointed out that soils in Zone C could be dispersive or non-dispersive. The *TDS* and percent sodium can be determined from Equations 2.1 and 2.2, respectively.

$$TDS = Na^{+} + Ca^{2+} + Mg^{2+} + K^{+} \tag{2.1}$$

$$Percent\ \ Sodium = \frac{Na^{+}}{TDS} \times 100 \tag{2.2}$$

The accuracy of all of these methods in identifying dispersive soils was discussed by Sherard *et al.* (1976b) based on the results obtained for many different fine grained soils. It was reported that the crumb test was a suitable method for checking the dispersion of a soil in one direction only, i.e., soils which showed dispersion according to the crumb test were dispersive, though the reverse was not always true. They also concluded that the SCS dispersion test was a reasonably accurate technique for classifying dispersive soils although somewhat less perfect than the pinhole test. Atkinson *et al.* (1990) questioned the reliability of the crumb test and pinhole test, all of which considered soil under unsaturated conditions. He pointed out that internal erosion was governed by true cohesion of the soil, which was defined as the strength of soil at zero effective normal stress. Hence, a rise in effective stress because of suction in unsaturated soil could influence the results of the pinhole test and crumb test. He therefore proposed a modified crumb test called a 'cylinder dispersion test', which was intended to evaluate the behaviour of soils at zero effective stress by submerging a saturated sample in water

for several months. He categorized soils into three different groups, namely non-dispersive cohesionless soils (Type N), non dispersive-cohesive soils (Type C) and dispersive soils (Type D) as described in Figure 2.9.

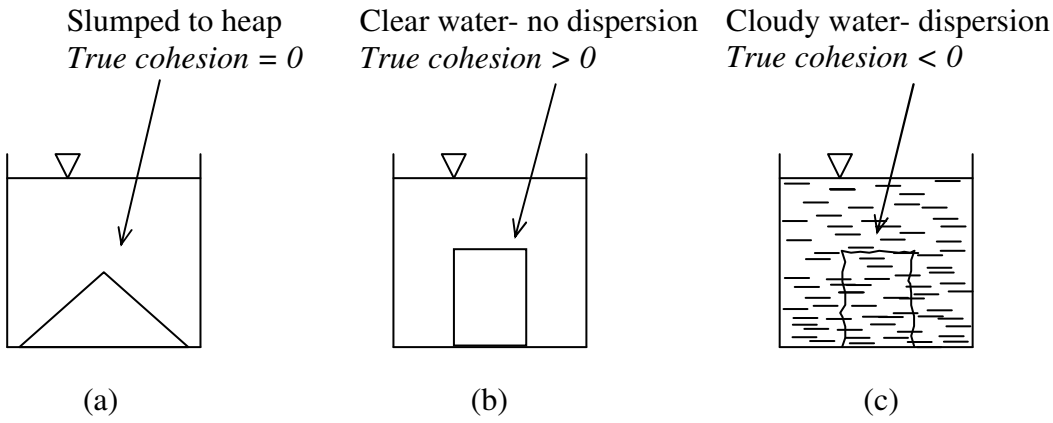

Figure 2.9 Dispersion behaviour of soils based on cylindrical dispersion tests (a) Type N: Non dispersive cohesionless (b) Type C: Non-dispersive cohesive and (c) Type D: Dispersive

2.4 Factors Influencing the Erodibility

Depending on its type (non-cohesive or cohesive), several factors influence the erodibility of a soil. In order to describe them, it is necessary to introduce the well known erosion parameters, hydraulic shear stress, critical shear stress, and erosion rate.

Erosion rate

This term was introduced by many previous researchers to explain how much soil was eroded during a unit time over unit surface area. This parameter indicates how fast a soil will be eroded under a certain hydraulic shear stress.

Hydraulic shear stress and critical shear stress

The hydraulic shear stress is the stress applied on the soil surface by flowing water. Critical shear stress is the minimum hydraulic shear stress necessary to initiate erosion and it depends on factors such as the type of eroding fluid, soil type, degree of compaction, and water content. Most previous researchers defined the critical shear stress as the threshold hydraulic shear stress below which no erosion was observed, as illustrated in Figure 2.10 (e.g. Arulananthan *et al.* 1975; Kandiah and Arulananthan 1974; Sargunan 1977; Wan and Fell 2004).

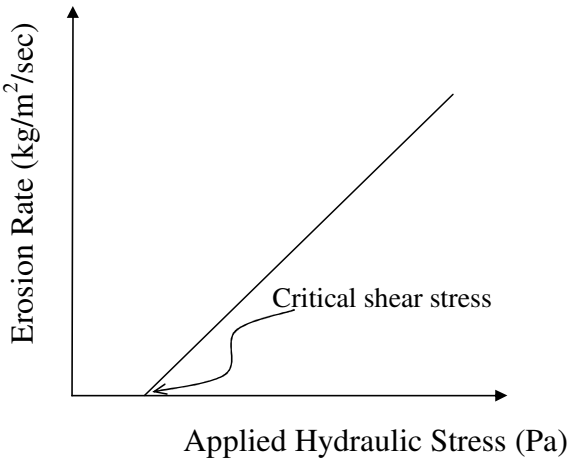

Figure 2.10 Typical curve for the variation of erosion rate with the hydraulic shear stress

2.4.1 Factors Affecting the Erodibility of Cohesive Soils

The erodibility of cohesive soils depends on factors such as hydraulic shear stress, eroding fluid and pore fluid properties, dry density, moisture content, and common soil properties such as the plasticity index and shear strength. They are described in detail in the following sections.

Hydraulic shear stress

As described in Figure 2.10, the erosion rate increases linearly with the hydraulic shear stress. It demonstrates that the hydraulic shear stress directly influences the soil's erodibility. The velocity of the flow, friction factor and density of the eroding fluid affect the magnitude of the hydraulic shear stress.

Eroding and pore fluid characteristics

The concentration of salt and sodium percent of the pore fluid, and the concentration of salt in eroding fluid are three of the main factors controlling the erosion characteristics of cohesive soils. Many previous studies were carried out to investigate how these parameters affected the critical shear stress (Arulananthan *et al.* 1975; Sargunan 1977; Shaikh *et al.* 1988). Arulananthan *et al.* (1975) concluded that an increase in the Sodium Absorption Ratio (it can be determined using Equation 2.3) at a certain concentration of salt in the pore fluid decreased the critical shear stress when the saturated soil was eroded with distilled water. Further, the critical shear stress increased with an increase in the concentration of salt in the pore fluid for a given sodium absorption ratio (Figure 2.11). They explained that a significant flocculation of clay particles occurred under highly concentrated salt for a given sodium absorption ratio and therefore, it was difficult to detach the particles. Similar conclusions were drawn by Sargunan (1977). Arulananthan *et al.* (1975) also showed that the higher the concentration of salt in an eroding fluid the lower the erosion rate, but the higher the critical shear stress for a given pore fluid properties (Figure 2.12). It was explained that the swelling of soil was controlled by the gradient existing between the eroding fluid and pore fluid salt concentrations (osmotic influence). The concentration of salt in an eroding fluid below that of pore fluid increased the swelling. Consequently, the inter-particle bond strength decreased and so too is the critical shear stress.

$$Sodium\ Absorption\ Ratio = \frac{Na^{+}}{\sqrt{0.5(Ca^{2+} + Mg^{2+})}} \times 100 \qquad (2.3)$$

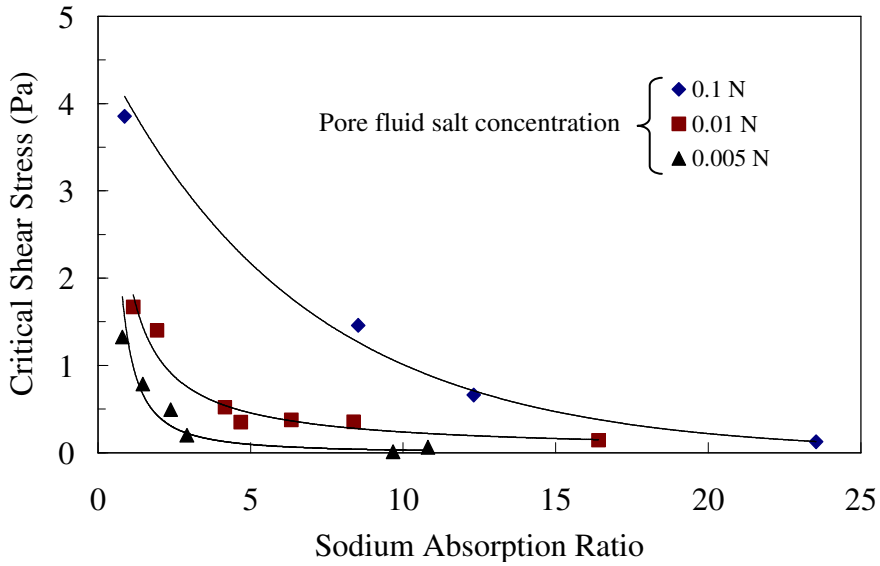

Figure 2.11 Effect of pore fluid salt concentration and sodium absorption ratio on the critical shear stress (After Arulananthan *et al.* 1975)

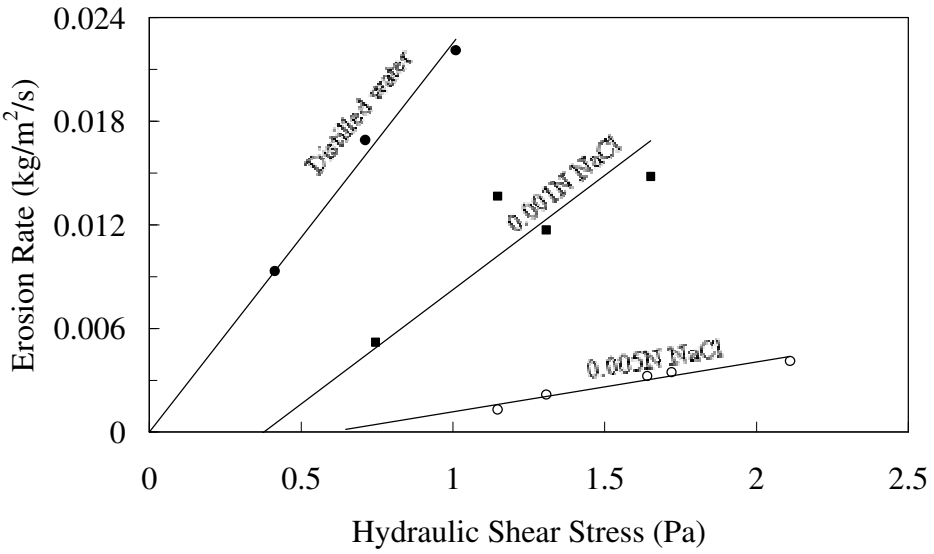

Figure 2.12 Effect of eroding fluid salt concentration on the critical shear stress and the erosion rate (After Arulananthan *et al.* 1975)

Shaikh *et al.* (1988) reported that the erosion rate of unsaturated compacted calcium monmorillonite (Classified as non dispersive) was two orders of magnitude higher than sodium monmorillonite (Classified as dispersive). He pointed out that with unsaturated compacted clayey soils slaking was the major cause of erosion, not dispersion. This result contradicts the findings of other investigations (e.g. Sherard *et al.* 1976b) which demonstrated that dispersive soils are highly erodible. Shrestha and Arulananthan (1989) commented on these results and explained that the calcium monmorillonite was in a higher state of flocculation than sodium monmorillonite and therefore slaked faster.

Dry density and moisture content

Many studies were performed to understand the erosion of unsaturated compacted clayey soils, including Kandiah and Arulananthan (1974) and Wan and Fell (2004). It was observed from their investigations that the water content played a crucial role on the erodibility of compacted unsaturated soils. In general, they all reported that the critical shear stress of a soil, compacted at a certain dry density, increased with the water content. Kandiah and Arulananthan (1974) reasoned that the swelling of soils decreased with an increase in the placement water content and it ultimately lead to an increase in the critical shear stress and a reduction in the erosion rate. In addition, they reported that the slaking or flaking phenomenon governed erodibility if the soil was compacted at the dry side of optimum water content.

The combined effects of compacted density and water content on the erosion characteristics of soil were analysed and plotted on a single graph (Figure 2.13) by Wan and Fell (2004). They drew contours to represent the erosion rate index. According to their classification, the higher the erosion rate index the less the erodibility. They summarised that compacting a soil at high dry

density (97% of the maximum dry density) and at the optimum or wet of optimum would significantly reduce erodibility.

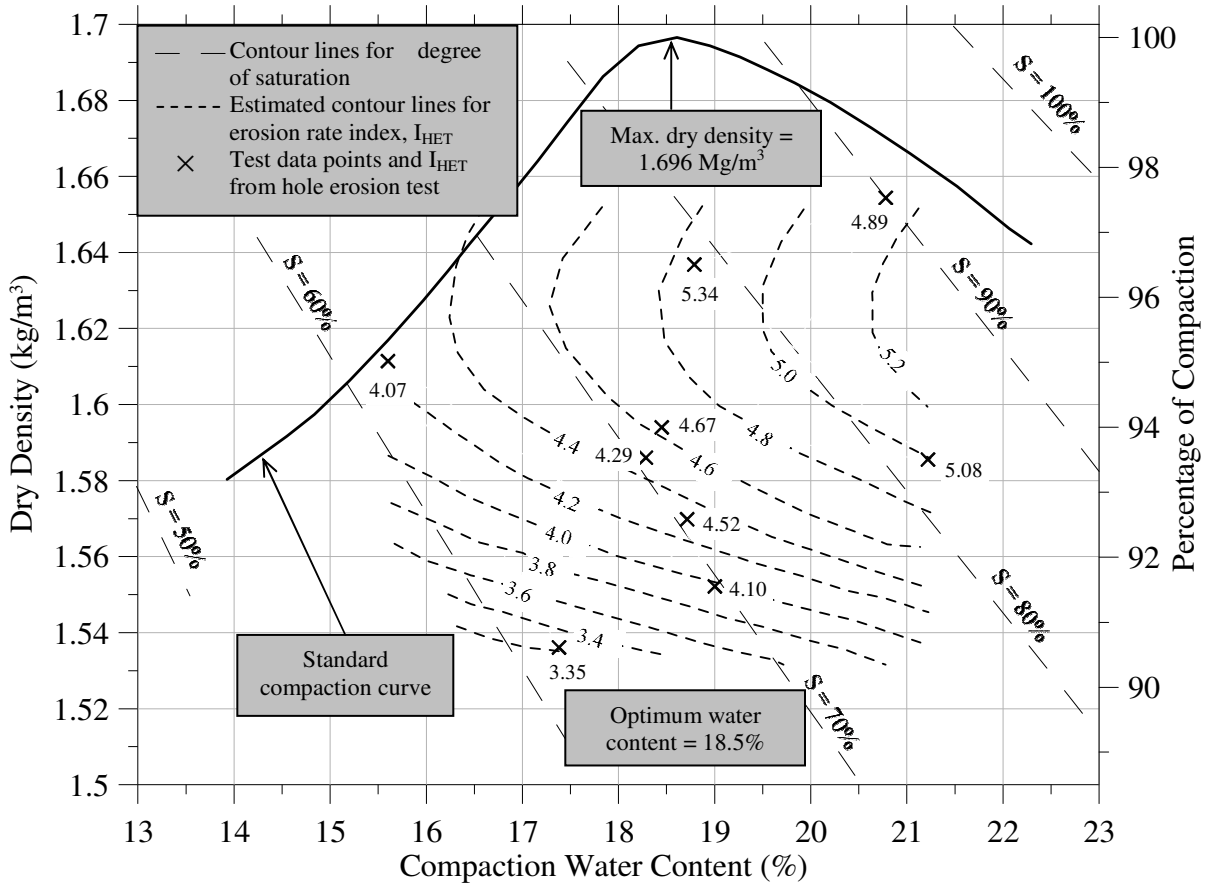

Figure 2.13 Variation of the erosion rate index with the compacted density and the moisture content (Wan and Fell 2004)

Common soil properties

Only a few researchers investigated the relationship between erodibility and common soil properties such as the plasticity index, void ratio, and shear strength (e.g. Dunn 1959; Lyle and Smerdon 1965; Reddi and Bonala 1997; Kamphuis and Hall 1983). Dunn (1959) conducted experiments to study the critical shear stress of saturated cohesive soils using a jet erosion test

and found a linear relationship between the vane shear strength and critical shear stress. The influence of the void ratio, vane shear strength, and plasticity index on the critical shear stress was investigated by Lyle and Smerdon (1965) based on erosion tests conducted on seven different types of soils. It was reported that the critical shear stress was a function of the vane shear strength and void ratio. They also concluded that the critical shear stress had a strong relationship with the plasticity index. Kamphuis and Hall (1983) used a flume to perform a set of erosion experiments on two different soils collected from a landslide location and the Mackenzie River bed in Canada. Tests were performed on the saturated cohesive soils, which were consolidated at different pressures. It was found that the critical shear stress changed linearly with the vane shear strength and unconfined compressive strength.

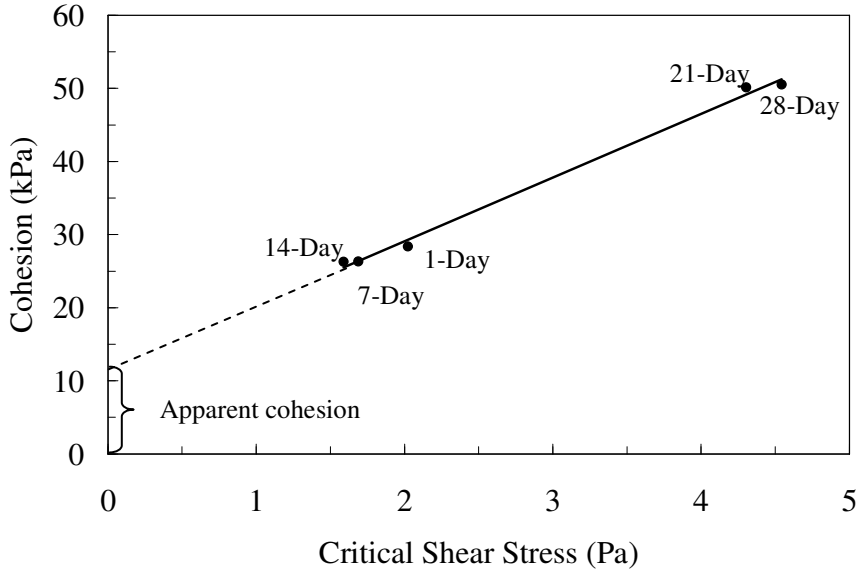

Figure 2.14 Relationship between the critical shear stress and the cohesion (Reddi and Bonala 1997)

Reddi and Bonala (1997) conducted erosion tests on saturated sand - kaolinite mixtures by pumping the eroding fluid through the soil matrix to study internal erosion (seepage erosion).

From these erosion tests and direct shear tests on five samples cured for periods of 1 day, 7 days, 14 days, 21 days, and 28 days, a linear relationship between cohesion and the critical shear stress was obtained, as described in Figure 2.14.

By way of contrast to above findings, Briaud *et al.* (2001) reported that the critical shear stress decreased with an increase in undrained shear strength, as shown in Figure 2.15. They also pointed out that a correlation between the erosion parameters and common soil properties such as plasticity and percentage passing sieve 200 was not convincing.

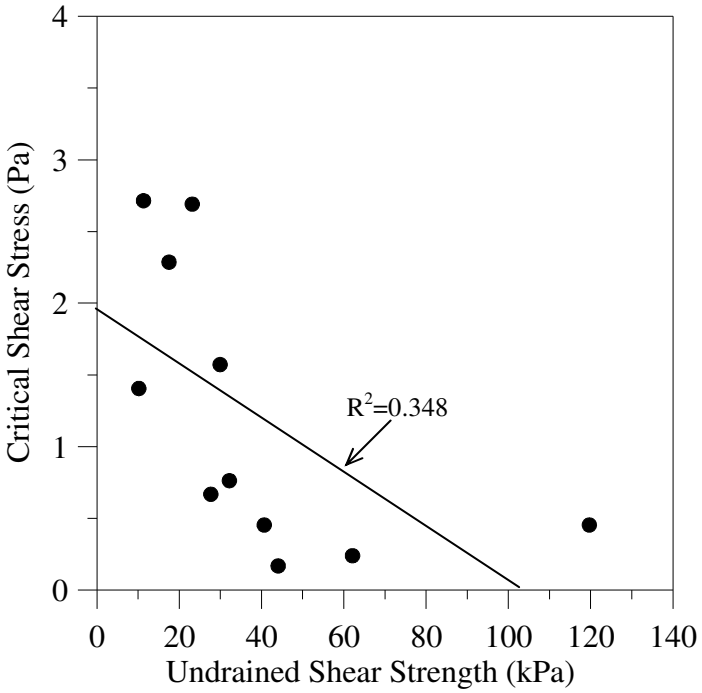

Figure 2.15 Variation of the critical shear stress with the undrained shear strength (Briaud *et al.* 2001)

2.4.2 Factors Affecting the Erodibility of Non-Cohesive Soils

The main factors controlling the erodibility of non-cohesive soils are hydraulic shear stress, size and self weight of the particles, compacted density and moisture content. The effect of these

parameters was explored previously by several investigators (e.g. Wan and Fell 2004; Briaud *et al.* 2001; Parker *et al.* 1995). A useful design chart was developed by Briaud *et al.* (2001) based on the experimental results obtained from the erosion function apparatus, as shown in Figure 2.16. According their classification, the critical shear stress of a soil with particles larger than 0.1 mm is equal to the mean particle diameter.

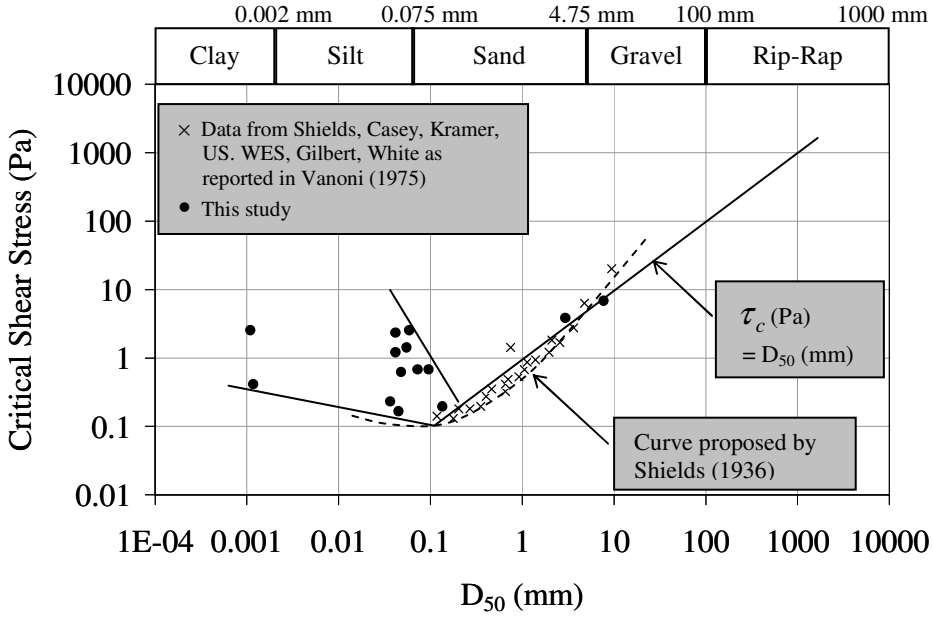

Figure 2.16 Critical shear stress versus mean particle diameter (After Briaud *et al.* 2001)

Based on the results from hole erosion and crack erosion tests, Wan and Fell (2004) reported that non-plastic soils showed a reduced erosion rate when compacted to a high dry density and to the dry side of optimum. However, Parker *et al.* (1995) did point out that the erosion rate increased with an increase in the bulk density of the soil.

2.5 Methods to Measure the Erosion Rate and the Critical Shear Stress

Various techniques were previously used to measure the erosion rate and critical shear stress; they are the hole and crack, flume, jet erosion, and rotating cylinder tests. All these methods were developed to simulate field conditions in order to study the erosion of cohesive and non-cohesive soils.

2.5.1 Hole Erosion and Crack Erosion Test

Christensen and Das (1973) performed a series of hole erosion tests on two remolded cohesive soils to study the effect of different factors such as the hydraulic shear stress and temperature of eroding fluid on the erosion rate. All the tests were performed by forcing eroding fluid through a 19 mm diameter by 3 mm thick clay lining. The friction factors were calculated by assuming that the flow was through a smooth pipe. The hydraulic shear stress was then determined using Equation 2.4.

$$\tau_a = \frac{f\rho_w v^2}{8} \tag{2.4}$$

where, τ_a (Pa) is the hydraulic shear stress; f is the friction factor; ρ_w (kg/m^3) is the density of eroding fluid; v (m/s) is the mean velocity of the flow through the hole. The critical shear stress of two different cohesive soils was approximately 1 Pa.

Wan and Fell (2004 and 2002) carried out a hole erosion test to study the internal erosion and piping of soils ranging from cohesive to non-cohesive at an unsaturated state. A hydraulic gradient was applied across a 6 mm diameter hole in the soil and then the flow rate through it was

measured at regular time intervals. The hydraulic gradient was calculated using the pressure heads measured with stand pipes located at the inlet and outlet of the hole (Figure 2.17).

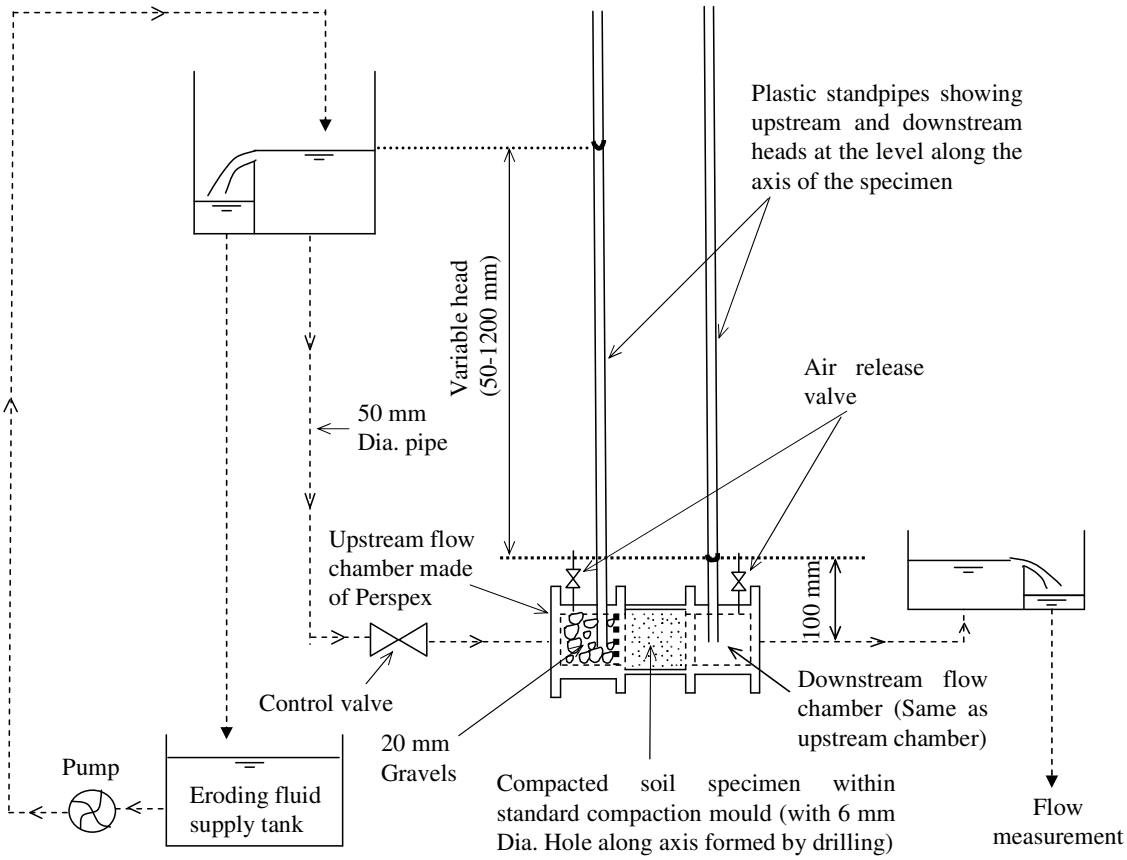

Figure 2.17 Schematic diagram of hole erosion apparatus (Wan and Fell 2004)

To determine any variation in the erosion rate and diameter of hole over time, it was assumed that the friction factor changed linearly with time between its initial and final values. They defined the friction factor for laminar and turbulent flow conditions as given in Equations 2.5 and 2.6, respectively.

$$\tau_a = f_L v \tag{2.5}$$

$$\tau_a = f_T v^2 \tag{2.6}$$

where, τ_a (Pa) is the hydraulic shear stress on the surface; v (m/s) is the mean flow velocity through the hole; and f_L (kg/m^2/s) and f_T (kg/m^3) are the friction factors for laminar and turbulent flow, respectively. They calculated the hole diameter at any time during erosion by Equations 2.7 and 2.8 for laminar and turbulent flow, respectively.

$$\phi_i = \left(\frac{16 Q f_L}{\pi \rho_w g s} \right)^{\frac{1}{3}} \qquad \text{For laminar flow conditions} \qquad (2.7)$$

$$\phi_i = \left(\frac{64 Q^2 f_T}{\pi^2 \rho_w g s} \right)^{\frac{1}{5}} \qquad \text{For turbulent flow conditions} \qquad (2.8)$$

where, ϕ_i (m) is the soil hole diameter at time t; Q (m^3/s) is the flow rate through the hole at time t; g (m/s^2) is gravitational acceleration; s is the hydraulic gradient across the hole at time t; and ρ_w (kg/m^3) is the density of eroding fluid. The erosion rate and hydraulic shear stress were then calculated using Equations 2.9 and 2.10, respectively.

$$\dot{\varepsilon} = \frac{\rho_d}{2} \left(\frac{d\phi_i}{dt} \right) \qquad (2.9)$$

$$\tau_a = \frac{\rho_w g s \phi_i}{4} \qquad (2.10)$$

where, $\dot{\varepsilon}$ (kg/s/m^2) is the erosion rate; ρ_d (kg/m^3) is the dry density of the soil. They reported that the erosion rate changed linearly with the hydraulic shear stress. It was also pointed out that the critical shear stress of cohesive soils could vary from 6-150 Pa. The following shortcomings with the experimental setup were identified.

- The reason for assuming that the friction factor changed linearly with time was not clearly explained.

- Entry loss in the applied head was not considered and therefore the calculated values of critical shear stress were overestimated.

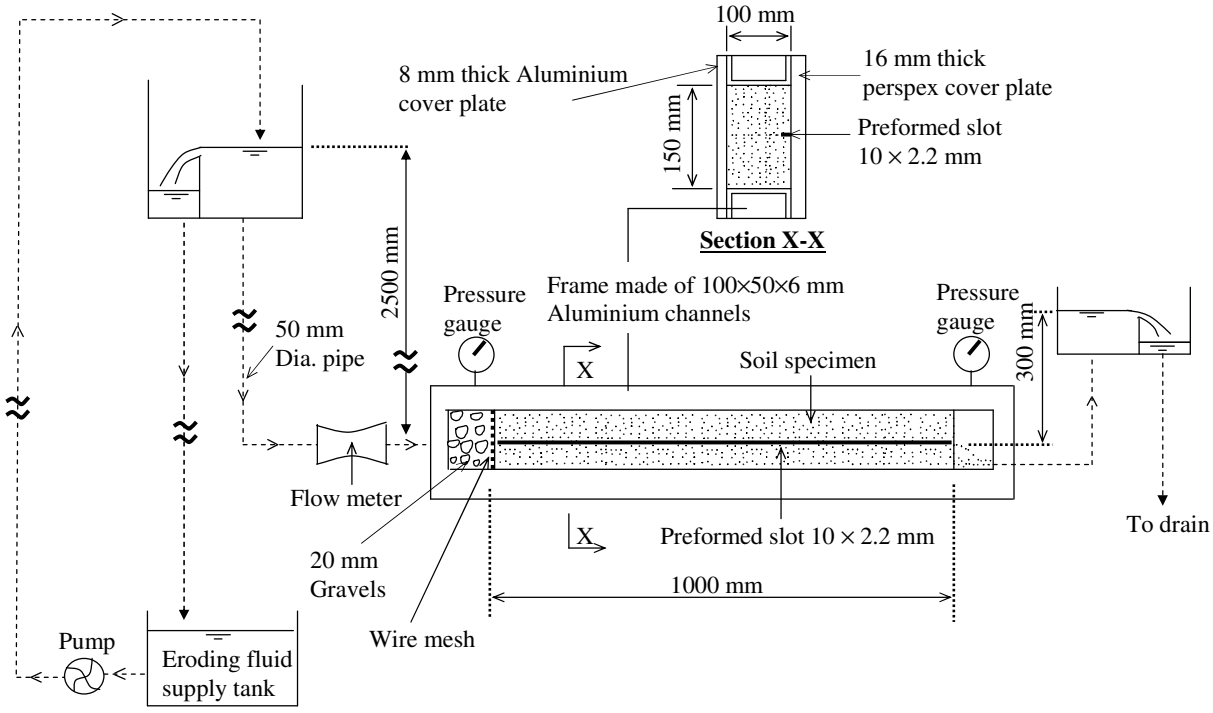

Figure 2.18 Crack erosion apparatus (Wan and Fell 2004)

Wan and Fell (2004) also conducted a series of slot erosion tests to study the erosion characteristics of soil in cracks in an embankment. An experimental setup with perspex glass face, through which the formed slot could be observed, was used for the investigation (Figure 2.18). The width of the slot (the side facing the Perspex) was measured continuously over time and then used to predict the erosion rate and hydraulic shear stress. The following assumptions were made to perform the calculations (Wan and Fell 2002).

- The slot was elliptical and remained uniform at every section of the sample.

- The depth of the preformed slot changed proportionally with time square. The reason for making the assumption was not given.

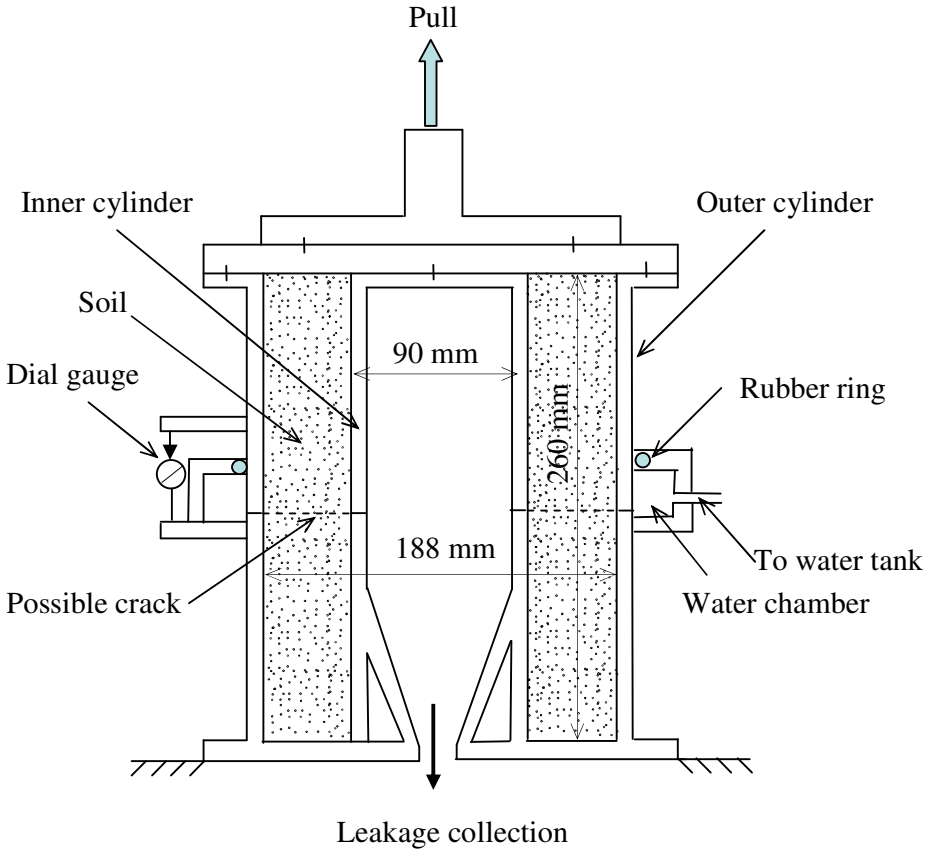

Figure 2.19 Schematic diagram of cracking, leakage and erosion apparatus (Hjeldnesa and Lavania 1980)

Hjeldnesa and Lavania (1980) performed a test with a single apparatus to study erosion, cracking, and leakage (Figure 2.19). While a crack was formed through a pre-defined fracture plane (by pulling), the eroding fluid was forced through under a certain hydraulic gradient to investigate how quickly erosion started, yielding to blow off (i.e. uncontrolled excessive flow through the slit formed because of the tensile deformation and erosion of the sample). They

concluded that well graded silty-gravely sand was much better material to use in an earth and rock filled dam than silty clayey fine sand because of its self healing properties. Failure or blow off occurred when the tensile deformation was equal to the maximum particle size of well graded silty-gravely sand.

2.5.2 Flume Test

This type of test was a common technique previously used to measure the soil erosion parameters of cohesive and non-cohesive soils (Lyle and Smerdon 1965; Kandiah and Arulananthan 1974; Kamphuis and Hall 1983; Shaikh *et al.* 1988; Parker *et al.* 1995). Erosion tests on seven different soils collected from Texas were performed by Lyle and Smerdon (1965) using a flume that was 22 m long, 0.75 m wide, 0.4 m deep, and had a 0.2% slope. The hydraulic shear stress was calculated by:

$$\tau_a = \rho_w g h S \tag{2.11}$$

where, h (m) is the depth of the flow and S is the slope of the flume. The erosion rate was calculated from a concentration of sediment and flow rate. It was concluded that the critical shear stress and erosion rate were controlled by the individual or combined effect of properties such as the plasticity index, void ratio, and vane shear strength. A similar approach was used by Kandiah and Arulananthan (1974) albeit with a smaller 2.5 m long, 0.15 m wide, and 0.3 m deep flume. They studied the erosion of saturated and unsaturated Yolo loam soil. The hydraulic shear stress was calculated using Equation 2.11, which was also used by Lyle and Smerdon (1965). The erosion test was performed under a given hydraulic shear stress, and the erosion rate was determined by weighing the sample before and after the test.

The erosion characteristics of consolidated cohesive soils (consolidated under 48 kPa – 350 kPa pressure) were tested by Kamphuis and Hall (1983) using a flume which could apply a hydraulic shear stress of up to 26 Pa onto the surface. A different approach was used to calculate the critical shear stress. The critical shear velocity at which erosion started was calculated using the critical velocity measured with a pitot tube at a certain depth of the flow. This critical shear velocity was then used with Equation 2.12 to calculate the critical shear stress.

$$\tau_c = \rho_w u_{*c}^2 \qquad (2.12)$$

where, u_{*c} (m/s) is the critical shear velocity. They concluded that the critical shear stress increased with the compressive strength, vane shear strength, plasticity index, clay content and consolidation pressure. Shaikh *et al.* (1988) used a flume with an adjustable slope to test the erodibility of unsaturated clayey soils influenced by pore water chemistry and slaking. The applied shear stress was changed to a range of 1.67-12.9 Pa. The velocity distribution was measured by pitot tubes and it was then used with the Prandtl-Von Karmen equation (applicable to a smooth channel) to predict the hydraulic shear stress.

All the flume tests described above were designed to study the erosion characteristics of disturbed soil samples. Briaud *et al.* (1999 and 2001) developed a piece of equipment called erosion function apparatus (similar to flume apparatus) to investigate the scour erosion of cohesive soil. A series of tests using the apparatus were conducted on undisturbed samples collected from near the piers of different bridges. They were set with a 1 mm high protrusion in water flowing through a 101.6 mm wide x 50.8 mm rectangular pipe (Figure 2.20). The hydraulic shear stress was calculated using Equation 2.4 and the friction factor was determined using the moody diagram, assuming that the average height of roughness element was the radius of a mean

particle. The erosion rate was calculated based on the time taken to erode a sample of a given height.

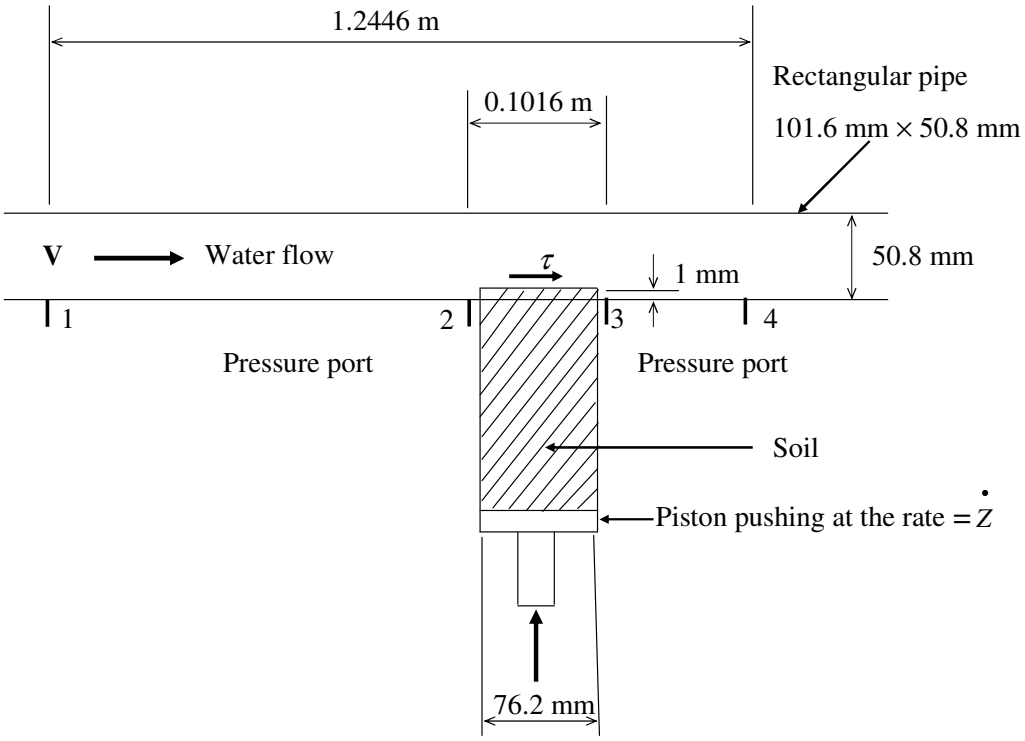

Figure 2.20 Schematic diagram of the erosion function apparatus (Briaud *et al.* 2001)

2.5.3 Jet Erosion Test

The scour erosion tests using submerged jet erosion apparatus were previously conducted by several researchers (e.g. Dunn 1959; Hanson 1991; Hanson and Robinson 1993). The objective of this test was to investigate the erodibility of soil under the direct impact of a water jet. In every experiment, a jet of water was impinged on the soil surface, but with different arrangements. Dunn (1959) made a setup to apply a submerged jet of water perpendicular to the soil surface, to replicate erosion in a typical channel. The maximum shear stress and starting point of erosion occurred a small distance away from the centre of the soil sample where the jet was directed. The magnitude of hydraulic shear stress was determined by replacing the soil surface with a steel

plate on which soil grains were attached. The plate contained a one inch square shear plate at the position of the maximum shear stress. The method adapted by Hanson (1991) was intended to predict the depth of scour over time rather than measuring the critical shear stress. A 13 mm diameter jet of water with a velocity ranging from 1.66 to 7.31 m/s was placed onto the surface of the soil under the water. The maximum depth of scour (D_s) was then measured at predetermined times during each test. Tests were performed on four soils and some conclusions were drawn based on the results.

- The depth of scour increased over time and the higher the water velocity the deeper the scour at a given time.

- The log-log plot of average scour over time $\left(\frac{D_s}{t}\right)$ against time (t) was straight line with negative slope and it had different intercepts at time axis according to the velocity of water; the higher the velocity, the greater the intercept.

- A coefficient called Jet index (J) was introduced to express the erodibility of the soil.

2.5.4 Rotating Cylinder Test

Rotating cylinder tests were performed by several researchers to study the erosion of saturated cohesive soils (e.g. Kandiah and Arulananthan 1974; Arulananthan *et al.* 1975; and Sargunan 1977). A typical device for a rotating cylinder test is illustrated in Figure 2.21. To transmit shear stress to soil surface from the outer rotating cylinder, the eroding fluid was filled in the annular space between the soil sample and outer rotating cylinder. The sample was stationary, but was mounted on bearings. The hydraulic shear stress was calculated by measuring the torque required

to keep the sample stationary against the rotating eroding fluid and cylinder. The erosion rate was calculated based on the difference in weight before and after the test.

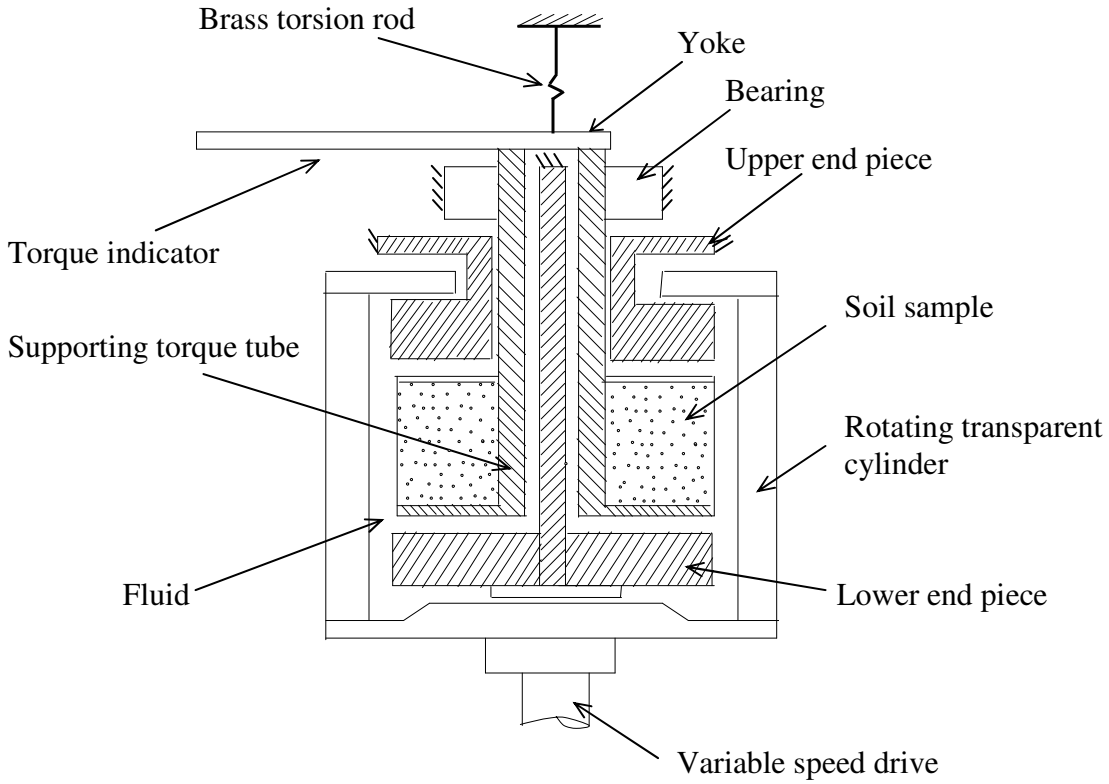

Figure 2.21 Rotating cylinder apparatus (Arulananthan *et al.* 1975)

Since the abovementioned test was only useful for testing saturated remolded soils, Chapuis and Gatien (1986) modified it for use on undisturbed and remoulded cohesive soils. This modified apparatus could collect the eroded soil, which was then used to directly calculate the erosion rate and therefore it was claimed to be more accurate than the previous apparatus. Most recently, Lim (2006) conducted a series of tests using a modified rotating cylinder apparatus to investigate erosion of saturated and unsaturated clay samples. He used a torque meter to continuously measure the torque independent of the rotating speed of the outer cylinder. He

stated that this method predicted the hydraulic shear stress more accurately than previous versions.

2.6 Erosion Control and Soil Stabilisation Techniques

Internal erosion and surface erosion cause severe problems, such as loss of life and properties, especially in dam failures, and loss of money in reconstruction and maintenance. It is therefore necessary to introduce suitable measures to control erosion, some of which, including their pros and cons, are explained in the following section in detail.

2.6.1 Native Vegetation

(a) (b)

Figure 2.22 Examples of (a) Protected face of a small dam with vegetation (b) Maintenance of embankment protected with vegetation

Native vegetation is a common practice that engineers follow to reduce the surface erosion of earth dams, highway embankments, and cut slopes etc. Figure 2.22 (a) and (b) show the established grass cover over a dam and the maintenance of plants on an embankment, respectively. Grass type plants will be planted on the slopes of an earth structure after construction and watered until they commence growing. A dense cover of low-growing grassy vegetation is recommended, because, it will provide protection from surface erosion, but its root structure does not penetrate the embankment so deeply as to create a potential path for internal erosion. The type of grass and its fertilisation should be appropriate for local conditions. Proper vegetation should be established and maintained over the entire embankment, outlet, and spillway. Though the vegetation is successful in controlling erosion, it will take some time to establish and may not prove to be a quick solution.

2.6.2 Chemical Stabilisation

Use of chemical admixtures is a popular method for reducing surface and internal erosion in earth dams and embankments. A number of studies were previously conducted to investigate the effectiveness of chemical admixtures such as lime, cement, pozzolanic fly ash (ASTM class C), milled slag and gypsum to control the erosion of unstable and erodible soils (e.g. Indraratna *et al.* 1991; Indraratna 1996; Perry 1977; Biggs and Mahony 2004; Machan *et al.* 1977; Kawamura and Diamond 1975). They all reported that chemical stabilisation significantly decreased erosion. Although chemical stabilisation is a promising control measure, economic considerations restricts its use to selective locations of dams and embankments. These locations are:

- The crest and slope of earth structures
- The foundation interface

- The periphery of conduits
- The vicinity of rigid (concrete) structures

A summary of different chemical additives and their stabilisation mechanisms are clearly explained in the following section.

2.6.2.1 Chemical stabilisation mechanism

The type of chemical admixtures used for stabilisation may be categorised as traditional and non-traditional. While lime, cement, gypsum, and pozzolanic fly ash (ASTM class C) are classified as traditional stabilisers, lignin additives and polymers are grouped into non-traditional stabilisers. The known chemical properties of traditional stabilisers are useful for defining their stabilisation mechanisms on problematic soils. However, the chemical composition of non-traditional stabilisers available on the market is not usually provided, and constituents of a certain type of stabiliser changes from one brand to another, depending on the manufacturer. Therefore, it is always a challenge to define what reaction mechanisms are involved in stabilisation.

Vast numbers of studies were conducted to investigate the applicability of traditional stabilisers on problematic soils such as soft clay and erodible soils (e.g. Indraratna *et al.* 1991; Uddin *et al.* 1997; Balasubramaniam *et al.* 1989; Perry 1977; McDaniel and Decker 1979; Biggs and Mahony 2004; Indraratna *et al.* 1995; Rajasesekaran *et al.* 1997, Chew *et al.* 2004). According to literature, the stabilisation mechanisms of traditional stabilisers on clayey soils are well established and are discussed below.

Hydration

This reaction happens immediately when quick lime (*CaO*) reacts with soil pore water to form $Ca(OH)_2$, as given in Equation 2.13.

$$CaO + H_2O \rightarrow Ca(OH)_2 + Heat \uparrow \quad (2.13)$$

Since a considerable amount of water is used for this reaction, the water content of treated soils decreases immediately after these stabilisers are added. This reduction in water will lead to an increase in the strength of the soil. In contrast, when cement is added to soft soils hydration occurs rapidly, but primary cementitious products such as hydrated calcium silicates and hydrated calcium aluminates are produced. These gels significantly increase the strength of soil treated with cement (Uddin 1995).

Ion exchange and flocculation

When lime or cement is added to clayey soils, monovalent cations such as sodium and potassium are replaced with multivalent cations such as Ca^{2+}, which leads to flocculation (Uddin 1995; Uddin and Buesuceso 2002). In general, the order in which cation replacement occurs in soils will be given by the Lyotropic series $Na^+<K^+<Mg^{2+}<Ca^{2+}<Al^{3+}$. As a result of the ion exchange, negative charges around the soil particles are reduced which decreases the inter-particle distance and hence, the inter-particle bond strength increases.

Pozzolanic reaction

Calcium hydroxide in the pore water from lime and cement treatment reacts with silicates and aluminates in the clay (pozzolans) to form a gel of calcium silicate hydrates and calcium aluminate hydrates, which bind the particles together (Equations 2.14 and 2.15). It is a time

dependent process and therefore, the strength of the treated soils will change with curing time (Uddin 1995; Uddin and Buesuceso 2002; Indraratna *et al*. 1991).

$$Ca^{2+} + 2(OH)^{-} + SiO_2 \rightarrow CSH \quad (2.14)$$

$$Ca^{2+} + 2(OH)^{-} + Al_2O_3 \rightarrow CAH \quad (2.15)$$

where, *CSH* and *CAH* are the calcium silicate hydrates and calcium aluminate hydrates, respectively.

One or a combination of the above mentioned stabilisation mechanisms are commonly involved in treating clayey soils with any traditional additives. With this description, studies conducted on the stabilisation of erodible soils with traditional additives are elaborated below.

2.6.2.2 Behavior of erodible soils stabilised with traditional additives

A number of investigations on the stabilisation of soft soil using traditional additives were previously conducted, but there is only limited literature available on chemically stabilised erodible soils. For instance, the effect of pozzolanic fly ash on the stress path response, shear strength, and compressibility of a dispersive soil collected from Thailand has been discussed in detail by Indraratna *et al.* (1991). Moreover, it was concluded from the study that the content of fly ash of 8-10% was sufficient to improve the shear strength of dispersive soils to reduce erosion (Figure 2.23 (a) and (b)). They reported that the changes in the characteristics of dispersive soil occurred as a result of flocculation by cation exchange and pozzolanic reaction.

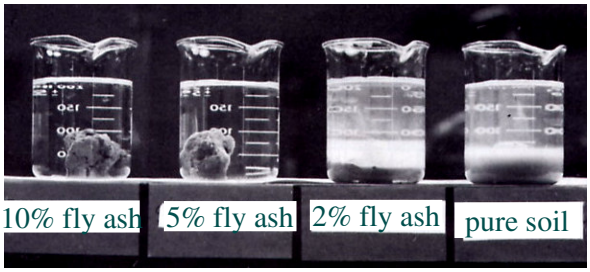

(a)

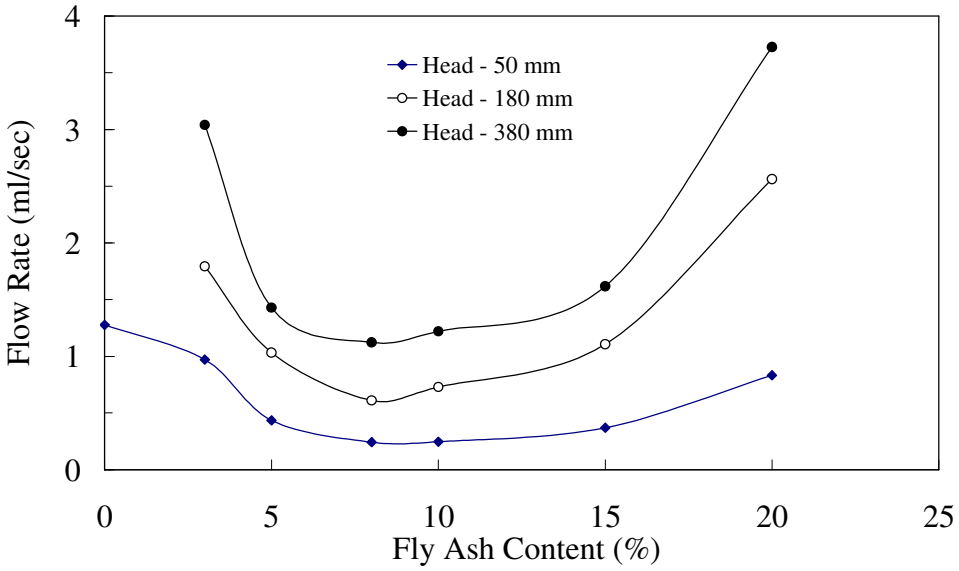

(b)

Figure 2.23 Behaviour of fly ash treated dispersive soil (a) Soil dispersivity test (b) Pinhole test results (Indraratna *et al.* 1991)

The engineering properties of an erosive colluvial soil in NSW (Indraratna 1996) were improved after being treated with milled slag. The milled slag stabilised the soil through its self hardening properties (cementation and flocculation). The erosion characteristics of four different soils ranging from heavy monmorillonite-bearing clay to a predominantly sandy soil were studied using controlled artificial rainstorm sequences (Machan *et al.* 1977). All the soils were treated with small amounts of general Portland cement and hydrated lime, and effects of treatment on erosion were investigated. They stated that about 1% of cement with curing period of 3 days

significantly decreased the erosion rate of all soils. A similar response was observed for the same amount of hydrated lime treatment on soils except for monmorillonite-bearing clay, but only after 7 days of curing. 3% of hydrated lime was required to achieve similar results for monmorillonite-bearing clayey soil. The use of Aluminium sulfate (Alum) and lime to reduce the erosion of dispersive soil was investigated by Ryker (1977). The amount of lime necessary to treat the surface of the dams was selected based on the appropriate shrinkage limit of treated soil, which reduced the risk of cracking. They pointed out that using 3% of $Ca(OH)_2$ was adequate to stabilise the different dispersive clays collected from Oklahoma, USA. It was also reported that alum treatment on dispersive clays with low application rate (0.3-1.6 %) produced favorable results. Because of its high solubility in water, the cost of using alum in the field was also less than lime, but the following shortcomings with using alum were identified.

- Alum costs five times more than lime.
- The chemical was strongly acidic, and therefore the neutralisation of chemicals such as agricultural lime was required to encourage vegetation growth.

In addition, lime was widely used around the world in the construction of earth structures such as dams and dykes. A summary of some important results is outlined in Table 2.1.

Table 2.1 Summary of lime treatment to control the erosion in different earth structures

Country	Amount of hydrated lime	Type of test	Curing	Problem	Structure type and location where treated soils placed	Remarks	Reference
New South Wales, Australia	0.5%	Small scale dam model investigation	Not provided	Tunneling failure due to dispersion	Upstream face of the embankment	Recommended to compact the soil to 80% of max. dry density	Rosewell 1977
Canada	1%	Pinhole test	Not provided	Erosion of sensitive marine clay	Dyke's foundation	Reported that lime acted as cementing agent	Dascal and Hurtubise 1977
New Mexico	4%	Pinhole test	Minimum of 4-day curing	Internal erosion of dispersive soils	Fractured sandstone foundation of Los Esteros dam	Recommended to cure soil-lime mix in loose state at near OMC* before the placement and compaction	McDaniel and Decker 1979
Mississippi, USA	2-3%	Laboratory dispersion test	Minimum of 2-day curing	Surface erosion	Slopes of dams	Recommended to cure soil-lime mix in loose state before the compaction	Perry 1977

OMC – Optimum Moisture Content

The application of gypsum for mitigating erosion was previously explored by some investigators (e.g. Biggs and Mahony 2004; Rosewell 1977). According to Biggs and Mahony (2004), gypsum (in liquid form) can be used in road construction to reduce the sodicity of soils. A reduction in sodicity helped to decrease the erosion of road materials. Rosewell (1977) built a small scale model dam to study the effect of gypsum on tunnelling failures. He reported that mixing 0.5% of gypsum to the upstream face of the dams stopped tunnelling failures, provided the soil was also uniformly compacted to 80% of its maximum dry density.

Chemical stabilisers used in the construction of earth dams and road embankments may cause some problems, such as (a) corrosion of steel structures (e.g. due to gypsum treatment), (b) problems with vegetation on treated soils because of an acidic or alkali environment created by the treatment and (c) the use of stabilisers such as milled slag requires stringent scrutiny from environmental bodies because of the presence of heavy metals and other impurities (Indraratna 1996; Perry 1977; Sherard *et al.* 1972; Ryker 1977; Biggs and Mahony 2004). Therefore, the need to identify an alternative chemical treatment to avoid some of these shortcomings is vital.

2.6.2.3 Characteristics of lignosulfonate as a soil stabiliser

Lignosulfonates were previously used to stabilize cohesive to non-cohesive soils. According to Karol (2003), these stabilisers are made from waste liquor by-products from wood processing industries such as paper mills. For stabilisation purposes, solutions of lignosulfonate were used as raw liquor or used with other additives to achieve desire soil properties.

Lignin based stabilisers such as ammonium persulfate-lignin and sodium dichromate-lignin were used as grout to bind particles together, especially fine granular soils (US Army Corps of Engineers 1995; Karol 2003). Reactants such as sodium bichromate, potassium bichromate, ferric chloride, sulphuric acid, aluminium sulphate (alum), aluminium chloride and ammonium

persulfate were used to make lignin grout form a gel after being injected into soils. It was reported that the strength of the gel depended on the type of reactants used in the grout system. For example, the strength of ammonium persulfate-lignin system gel was approximately 40% of a sodium bi-chromate-lignin system. Even though sodium dichromate-lignin improved the soil significantly, it disappeared from the market because of heavy metal constituents such as chrome in the stabiliser. Karol (2003) reported that the setting time of lignin grouts depends on the pH of the chemical grout, as shown in the Figure 2.24. As described in this figure, the higher the pH the longer the setting time.

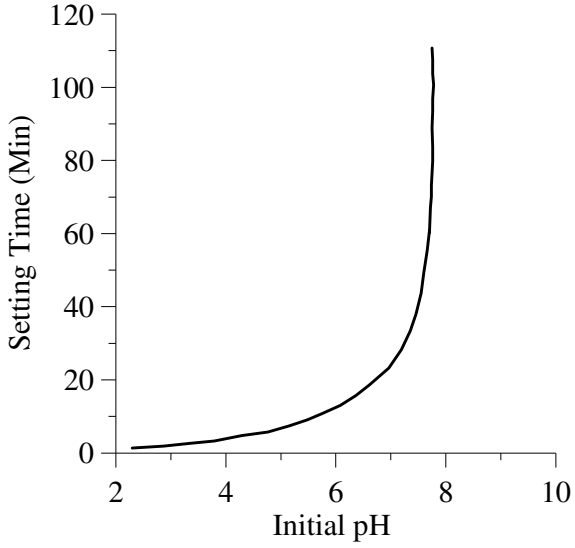

Figure 2.24 Setting time of lignin based grouts with pH (Karol 2003)

Lignosulfonate stabilisers were also used to improve the strength of cohesive soils (Puppala and Hanchanloet 1999; Pengelly *et al.* 1997; Tingle and Santori 2003). Puppala and Hanchanloet (1999) reported that clayey soils treated with a stabiliser consisting of lignosulfonate and sulphuric acid showed a significant increase in their shear strength and resilient modulus. They pointed out that lignosulfonate was like a binder while the sulphuric acid acted as a primary stabiliser to alter the structure of the clay through pozzolanic reactions. Tingle and Santori (2003)

investigated the effect of lignosulfonate on different clayey soils and found that lignosulfonate stabiliser significantly improved the strength of a low plasticity clayey soil. This increase in unconfined compressive strength of low plasticity clay due to 3.4% of lignosulfonate was comparable to 7.0% treatment with cement. A solution containing ammonium lignosulfonate and potassium chloride was injected into expansive soil and a significant reduction in the swell was observed (Pengelly *et al.* 1997).

In addition to the above mentioned studies, a number of researchers performed experiments to investigate whether this particular type of chemical in low volume road construction would improve the strength of sub-grade and control dust emission (e.g. Chemstab 2003; Tingle and Santori 2003; Sanders *et al.* 1997; Lohnes and Coree 2002). The results are summarised in Table 2.2.

Table 2.2 Summary of different lignosulfonate products used in low volume road construction

Brand Name	Purpose	Country	Fines content (%) (<75 μm)	Effectiveness	Reaction mechanism	Dosage	Reference
Lignosulfonate	Dust control	USA	<5	42-61% of less dust produced	Binder	2.3 L/m^2	Sanders *et al.* 1997
Chemstab	Improve the strength of subgrade	Australia	44	50 % increase in CBR	Not proposed	0.6 L/m^3	Chemstab 2003
Lignosulfonate and Sulfuric acid (SA-44/LS-40)	Improve the strength of subgrade	USA	70	70-120% increase in UCS	Binder (LS-40) and Pozzolanic (SA-44)	1:0.1:200 and 1:0.1:300 dilution[1]	Puppala and Hanchanloet 1999
Lignosulfonate	Improve the strength of subgrade	USA	100	150 % increase in UCS	Not proposed	3.5 % by dry weight (powder form)	Tingle and Santori 2003
Lignosulfonate	Dust control	USA	8 to 20	Dust controlled	Not proposed	2 shots @ 2.26 L/m^2	Lohnes and Coree 2002

[1] Ratio of SA-44: LS-40: Water

As discussed above, lignin based stabilisers successfully stabilised soils ranging from cohesive to non-cohesive, but it is clear that the properties of lignin based stabilisers vary significantly with the constituents which determine the stabilisation mechanisms of these additives. Accordingly, there is no standard stabilisation mechanism as defined for traditional admixtures such as cement, lime, and gypsum. Lignin based stabilisers with different properties are available on the market and therefore, it is necessary to examine their effects on related soil specimens before applying them in the field. According to the literature the advantages of using lignin based admixtures over traditional stabilisers are as follows:

- The pH of the soil does not change significantly after treatment. This will help most vegetation to thrive on top of the treated soils, especially on the slope of dams and highway embankments. Moreover, leachate through the treated soils does not affect the ground water, because, there are no heavy metals in the stabiliser (Chemstab 2003).

- The amount of chemical stabilisers necessary to improve the soil is less than traditional stabilisers (Tingle and Santori 2003).

2.7 Tensile Stress-Strain Behaviour of Soil and Its Influence on Erosion Related Problems

Tensile strength of soils is generally negligible compared to compressive strength and is not considered when analyzing the stability of engineering structures. However, the importance of tensile stress-strain behavior was understood by engineers after 1960, especially in construction of dams and multi-layer pavement subject to severe cracking from excessive tensile stress. Cracks existing in dams are dangerous and can cause serious consequences. For example, a

tensile crack, especially in homogeneous earth dams, will act as a channel to carry reservoir water which will erode soil particles from the crack wall and cause internal erosion and piping, especially if constructed with erodible soils. Consequently, a catastrophic failure may occur causing loss of life and environmental pollution. This is why many previous researchers investigated tensile stress-strain behaviour to select suitable soils for construction and identify appropriate placement conditions such as moisture content and dry density. Different tensile testing methods and factors affecting the tensile stress-strain behavior of soils are discussed in detail below.

2.7.1 Experimental Methods to Investigate the Tensile Stress-Strain Behaviour

Several investigations using different experimental methods were conducted to understand the tensile stress-strain characteristics of compacted soils. All of these studies may be classified as direct tensile tests, indirect tensile tests and flexural beam tests. They are explained in the following section.

2.7.1.1 Direct tensile tests

Direct tensile tests were conducted by applying a tensile force along the longitudinal axis of a soil sample until it failed. However, the experimental set up, loading method, and shape of the sample differed from study to study. Cracking, leakage, and erosion of earthdam materials were investigated by Hjeldnes and Lavania (1980) using a single experimental setup (Figure 2.19). The tensile stress-deformation characteristics of soil and its effect on the blow off (i.e. uncontrolled excessive flow through the slit formed because of the tensile deformation and erosion of the

sample) were studied. The lower half of the cylinder was fixed and the upper half was pulled at a rate of 0.1 mm/min for 2 min. If there was no leak after 5 min, then another increment was applied; this continued until the leakage discharge observed. The tensile load was measured by strain gauges and tensile-deformation at the fracture plane was measured by three dial gauges fixed to the outer cylinder. Well graded silty-gravelly sand with no clay size particles, and silty clayey fine sand were tested. Because of its self healing properties, well graded silty gravelly sand was selected as a suitable dam construction fill.

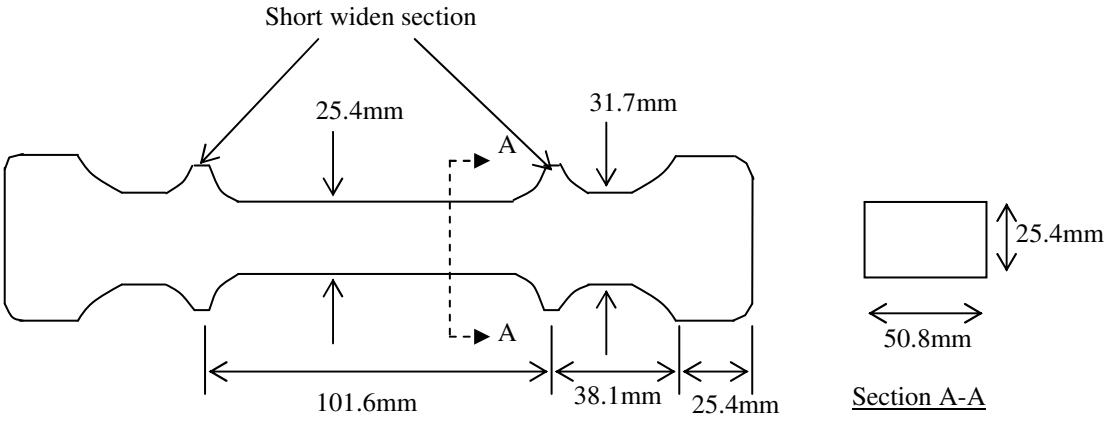

Figure 2.25 Sample shape and dimensions used by Ajaz and Parry (1974)

Ajaz and Parry (1974) conducted an unconfined direct tension test to compare the tensile stress-strain behaviour of compacted clays with compressive behaviour. The shape of the sample is given in Figure 2.25. A Displacement Measuring Optical Device method (DMOD) was used to observe two surface markers embedded in the centre of the short widened section at each end of the central portion of the sample and the readings were used to calculate tensile strain. In order to check the uniformity of strain along the specimen (center portion of the sample) during the load-controlled tension test, 0.9-1.0 mm diameter lead shot were embedded into one of the 50.8 mm wide faces and readings of any deformation were taken with the help of radiographic technique.

For a comparison, two pieces of lead shot were also spiked into the sample at the same place as the surface markers were embedded for DMOD observations. It was concluded that the strain between two lead shots embedded in the shoulders of the specimen was almost equal to the average of local strains obtained at the central portion of the sample, which had a constant cross sectional area.

2.7.1.2 Indirect tensile tests

Indirect tensile tests in the form of a Brazilian cylinder test or diametral compression test were previously conducted. A number of investigations were performed using this Brazilian cylinder test to study the tensile stress-strain characteristics of soils (e.g. Krishnayya *et al.* 1974; Narain and Rawat 1970; Dass *et al.* 1994). They all used the same concept to measure tensile strength as described in Figure 2.26, which illustrates the tensile stress distribution along the diameter of a cylindrical soil sample caused by a compressive load applied along the diameter.

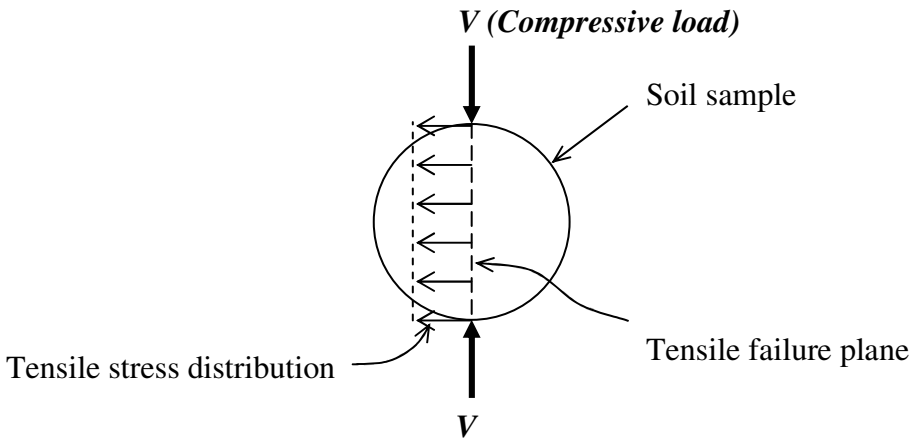

Figure 2.26 Theoretical tensile stress distribution in the indirect tensile test (Dass *et al.* 1994)

The tensile strength of the soil was determined by:

$$\sigma_{Tf} = \frac{2V}{\pi D_0 l} \tag{2.16}$$

where, σ_{Tf} (Pa) is the tensile strength; V (N) is the compressive load at failure; D_0 (m) is the diameter of the cylinder; and l(m) is the length of the sample.

Narain and Rawat (1970) performed a series of Brazilian tensile tests to investigate the effect of moisture content on tensile and compressive strength. A compressive load was distributed uniformly over the 101.6 mm diameter by 117 mm long sample by placing a narrow pad (a rubber strip 16 mm wide by 6 mm thick) between the loading plate and the sample.

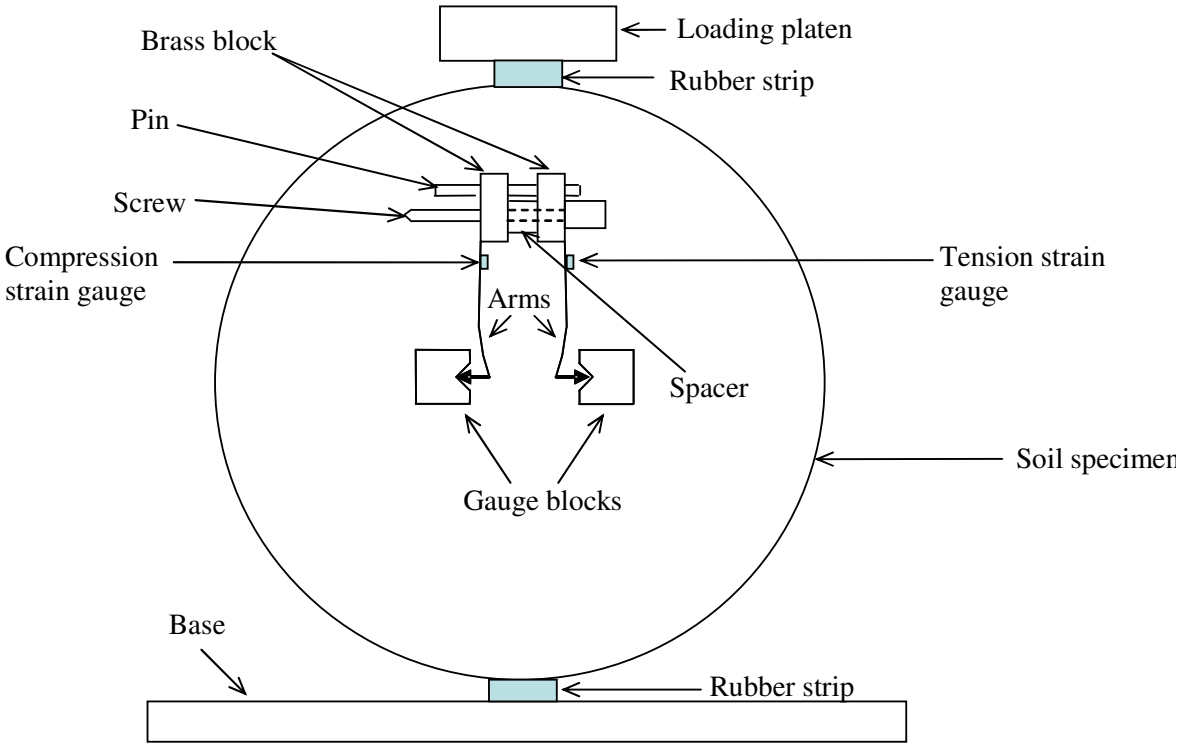

Figure 2.27 Measuring the tensile strain in Brazilian test (after Krishnayya *et al.* 1974)

Krishnayya *et al.* (1974) investigated how the loading rate, moisture content, compacted density, and the addition of bentonite affected the tensile stress-strain behaviour of soil. Diametral compression tests were performed with an arrangement to measure the tensile strain using a clip gauge, which measured the displacement between two gauge blocks fixed to the surface of the soil at both sides of the expected fracture plane (Figure 2.27). However, a different technique was used by Dass *et al.* (1994) to measure the tensile strain in Brazilian tensile testing. Black grid points were made at one end of the face of the sample. An image of the face and its optical characteristics were then taken with the help of a long distance microscope and photonic sensor of a video camera. The optical characteristics of the image were then transferred through the frame grabber into the computer monitor. It was then translated into an image file so that the strain could be calculated.

2.7.1.3 Bending tests

Bending tests were especially designed to determine the flexural strength of soil (Ajaz and Parry 1975; Leonards and Narain 1963). Ajaz and Parry (1975) performed tests by bending the beam with a simple two point loading system. A 51 mm x 51 mm x 254 mm long sealed sample was immersed in brine to counterbalance its own weight. Two equal loads were then applied to the beam using two perspex rods placed an equal distance from the centre so that the middle portion (152.4 mm) was under a constant bending moment (Figure 2.28). Loads were applied in increments until the soil failed. A number of lead shots were spiked into the sample at selected locations, as shown in Figure 2.28 and the tensile strain was then measured by a radiographic technique. Leonards and Narain (1963) adopted a different approach to measure tensile strain. They used soil samples of 76 mm wide x 70 mm deep x 562 mm long for testing. Two rows of 1 mm diameter x 50.8 mm long tungsten pins were embedded 44.5 mm into the soil beam through

a steel template. Pin displacements were measured with the aid of a cathetometer immediately after a load increment was added and immediately before the next load increment. The displacement values were then used to calculate the tensile strain.

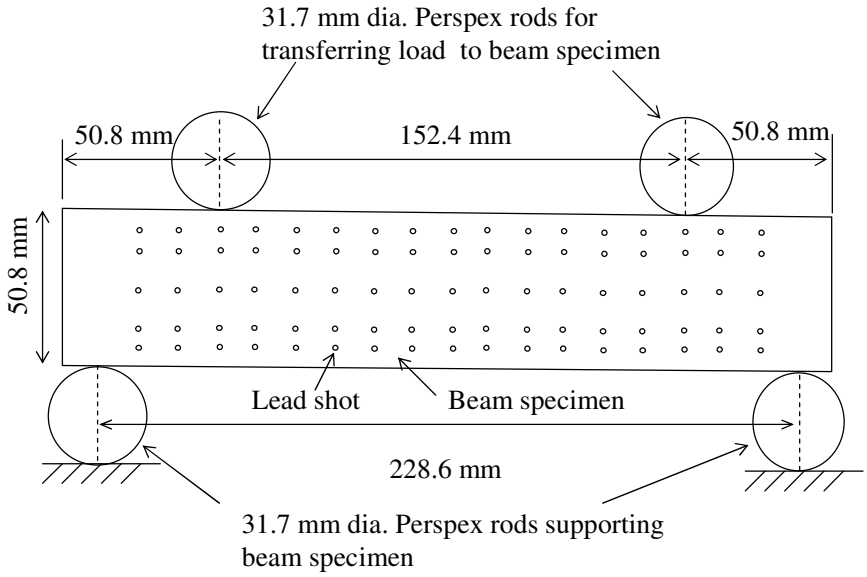

Figure 2.28 Specimen for the bending test (Ajaz and Parry 1975)

2.7.2 Factors Controlling the Tensile Stress-Strain Behavior

Several studies (Hjeldnes and Lavania 1980; Narain and Rawat 1970; Krishnayya *et al.* 1974; Ajaz and Parry 1975; Leonards and Narain 1963) were conducted to understand how factors such as placement water content, compacted density, loading rate, and plasticity, affect the tensile stress-strain behaviour of soil. They are clearly described in the next section.

Placement water content and compacted density

The placement moisture content and compacted density are the two main factors controlling the tensile stress-strain behaviour of compacted soils. According to most investigations, tensile

strength decreases and failure tensile strain increases (increase in flexibility) with an increase in the placement moisture content (Ajaz and Parry 1975; Leonards and Narain 1963; Krishnayya *et al.* 1974; Hjeldnes and Lavania 1980). Even though the general trend observed by all these researchers was similar, different observations were made on the tensile failure deformation in the region of wet of optimum. Leonards and Narain (1963) stated that an increase in the water content from 2-3% dry of optimum to nearly optimum significantly increased flexibility. However, little improvement in flexibility was observed when the water content increased to 3% wet side of optimum. Krishnayya *et al.* (1974) reported that increasing the water content above the optimum produced a significant increment in the tensile failure strain and a similar trend was observed by Ajaz and Parry (1975).

The effect of compactive effort on the tensile stress-strain characteristics was investigated by a few researchers (Krishnayya *et al.* 1974; Leonards and Narain 1963). Krishnayya *et al.* (1974) stated that the tensile strength increased with compactive effort below the optimum water content and decreased slightly above the optimum. They also pointed out that the stiffness of the soil increased with the degree of compaction for a water content well below optimum. Leonards and Narain (1963) reported that an increase in compactive effort from standard Proctor to modified American Association of State Highway Officials (AASHO) decreased the flexibility of the limestone residual soil by almost half.

Loading rate and type

The loading method and loading rate influence the behaviour of a soil under tensile stress to a certain extent (Ajaz and parry 1975; Krishnayya *et al.* 1974). As reported by Krishnayya *et al.* (1974), a minimum value for tensile strength and failure tensile strain was observed at a certain loading rate, depending on the placement moisture content, as shown in Figure 2.29.

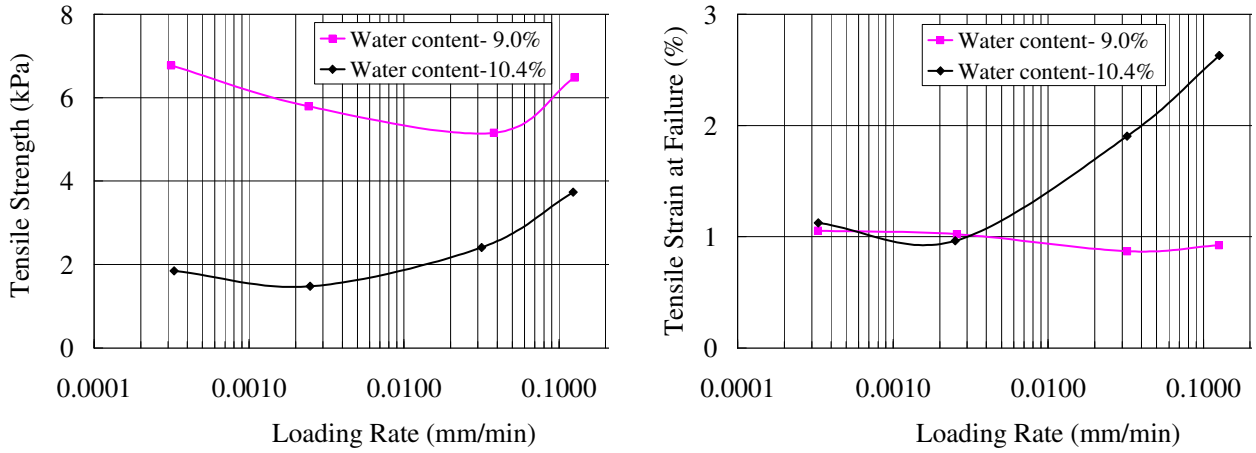

Figure 2.29 Effect of loading rate on tensile strength and failure tensile strain (Krishnayya *et al.* 1974)

Ajaz and Parry (1975) concluded from a series of tensile tests on clayey soils that the failure (peak) tensile stress obtained from the load controlled direct tension test was higher than that obtained from the strain controlled direct tension test for a given compacted soil. And they also reported that the tensile stress and strain at failure were less in a direct tensile test than a bending test for a given compacted soil.

Plasticity of the soil

In order to investigate the effect of plasticity on the tensile stress-strain behaviour, Krishnayya *et al.* (1974) performed a number of tests on mica till mixed with 6% bentonite. The addition of bentonite increased the plasticity index of the soil by 17.3%. It was concluded that flexibility could be increased without significantly reducing the tensile strength by just adding bentonite.

2.8 Summary

This chapter presented the outcomes of several studies relevant to the identification of erodible soils, to problems associated with erosion and remediation techniques, to different methods for predicting erosion parameters, and to factors controlling erodibility. The tensile stress-strain behaviour of compacted soils was also discussed. The conclusions drawn from these studies are summarised below.

General

- Non-cohesive soils such as silty sand, wind blown sand, flood deposits and man-made mounds can be classified as highly erodible soils, because, there are no bonds between the particles. Dispersive soils (cohesive soils) containing a preponderance of sodium cations are also highly erodible as they loose their cohesive strength upon contact with water (ICOLD 1990; Udomchoke 1991).

- Several methods namely the Emersion class test, the Soil Conservation Service (SCS) dispersion test, the standard pinhole test and the soil chemical test have been used to identify dispersive soils.

- According to a majority of investigations, the erosion rate changed linearly with the hydraulic shear stress. The minimum hydraulic shear stress necessary to initiate erosion was termed the critical shear stress (Arulananthan *et al.* 1975; Kandiah and Arulananthan 1974; Sargunan 1977; Shaikh *et al.* 1988; Wan and Fell 2004).

- The critical shear stress and erosion rate of saturated cohesive soils were mainly affected by pore water and eroding water characteristics. In general, the critical shear

stress decreased with the Sodium Absorption Ratio (SAR) for a given eroding fluid salt concentration and increased with eroding fluid salt concentration for a given SAR (Arulananthan *et al.* 1975; Sargunan 1977).

- The erodibility of compacted cohesive soils increased with the decrease in dry density, while it decreased with an increase in the water content. The flaking or slaking phenomenon governed the erodibility of soil compacted at the dry of optimum (Kandiah and Arulananthan 1974; Wan and Fell 2004).

- The hydraulic shear stress, size and weight of soil particles, dry density and moisture content, influenced the erosional behaviour of compacted non-cohesive soils (Wan and Fell 2004; Briaud *et al.* 2001; Parker *et al.* 1995).

- It was reported that a strong relationship existed between the tensile stress-strain behaviour of soils and cracking, which could explain serious consequences such as internal erosion and piping in embankment dams. According to the majority of investigations on the tensile behaviour of compacted soil, tensile strength decreases and failure tensile strain increases (increase in flexibility) with an increase in the placement moisture content (Ajaz and Parry 1975; Leonards and Narain 1963; Krishnayya *et al.* 1974; Hjeldnes and Lavania 1980). Also, the tensile strength and stiffness increased with compactive effort for a soil placed at dry of optimum water content.

Relevance to the current study

- Different experimental techniques have been used to simulate field conditions to determine the erosion rate and critical shear stress. The flume test and jet erosion test simulate soil eroding under a unidirectional flow and direct impact of a jet of water, respectively (e.g. Lyle and Smerdon 1965; Kandiah and Arulananthan 1974; Kamphuis and Hall 1983; Dunn 1959; Hanson 1991; Hanson and Robinson 1993). The current study concentrates on the erosion characteristics of soil in cracks in embankment dams. Only a limited number of studies such as hole erosion and crack erosion test to simulate erosion in a crack in embankment dams have been conducted in the past (Wan and Fell 2004). These studies measured the erosion rate based on various assumptions and generally overestimated the critical shear stress. A new apparatus designed by the writer was therefore used in the current investigation to study erosion characteristics of soil in cracks.

- The findings of several studies conducted on erodible soils treated with chemical additives such as lime, gypsum, cement, alum and pozzolanic fly ash demonstrated that chemical stabilisation is a promising method for controlling erosion (e.g. Indraratna *et al.* 1991; Indraratna 1996; Machan *et al.* 1977; Perry 1977; Biggs and Mahony 2004). However, some problems such as a considerable rise in soil pH, corrosion of steel structures, impact on environment, and occupational health and safety issues, raised the question of using traditional additives to control erosion (Indraratna 1996; Perry 1977; Sherard *et al.* 1972; Ryker 1977; Biggs and Mahony 2004). A need for identifying an alternative stabilisation to avoid some of these short

comings is therefore vital. This current study investigated the effectiveness of such a new stabiliser based on lignosulfonate for controlling erosion.

- Only a limited number of studies have been conducted to explore the relationship between the strength and erosion characteristics of soils (e.g. Dunn 1959; Kamphuis and Hall 1983). They all found that the critical shear stress changed linearly with the vane shear strength, however no comprehensive model correlating the erosion rate with strength properties of soil is available. The current study includes the development of a theoretical erosion model in terms of tensile stress-deformation characteristics, and it will be discussed in detail in the next chapter.

CHAPTER 3

THEORETICAL MODEL FOR EROSION RATE

3.1 Introduction

This chapter outlines the empirical and analytical models available for predicting critical shear stress in terms of the shear strength of soil, and uncertainties in developing a comprehensive erosion model that incorporates the shear strength properties. It also contains detailed procedures and assumptions used to develop a rigorous analytical model for the erosion rate, embracing the tensile stress-deformation characteristics of soil. The chapter concludes with a description of the different parameters in the model and details of appropriate methods used to predict these parameters.

3.2 Present Status of Erosion Modeling

Only a few researchers have attempted to correlate the critical shear stress with the shear strength or tensile strength of soil (e.g. Dunn 1959; Lyle and Smerdan 1965; Kamphuis and Hall 1983; Reddi and Bonala 1997; Hjeldnes and Lavinia 1980). Dunn (1959) performed a series of jet erosion tests on cohesive soils collected from canal beds and found that the critical shear stress varied linearly with the vane shear strength for a certain soil. He proposed the following empirical expression to calculate the critical shear stress.

$$\tau_c = 0.96 + \frac{S_v \tan\theta}{1000} + 8.66 \tan\theta \qquad (3.1)$$

where, τ_c (Pa) is the critical shear stress; S_v (Pa) is the vane shear strength; and θ is the angle related to either the amount of fines or plastic index. Lyle and Smerdan (1965) conducted flume tests on seven different soils and developed an empirical expression [Equation (3.2)] for the critical shear stress in terms of the void ratio and the vane shear strength.

$$\tau_c = \xi(S_v)^{\eta} \tag{3.2}$$

where, τ_c (Pa) is the critical shear stress; S_v (Pa) is the vane shear strength; and ξ and η are two empirical functions of the void ratio. Kamphuis and Hall (1983) performed a set of erosion experiments using a flume on two different soils collected from a landslide and the bed of the Mackenzie River in Canada. The clay content and pre-consolidation pressures were changed to study the influence of the shear strength on the critical shear stress. It was found that the critical shear stress of over-consolidated clayey soils changed linearly with the vane shear strength and unconfined compressive strength. However, they pointed out that the presence of expansive minerals such as monmorillonite in the soil could significantly alter the results obtained from the experiments and therefore, the developed empirical model could not be applied in these cases.

Reddi and Bonala (1997) developed an analytical model for the critical shear stress (under seepage erosion) in terms of true cohesion (C_t), as given in Equation (3.3). To develop this model, it was assumed that the tensile strength was equal to the true cohesion. The study was limited to a sand-kaolinite mixture only to avoid the effect of chemical properties such as the sodium adsorption ratio and total dissolved salts on the erosion rate. Therefore, the research only considered physically induced erosion so that the mathematical model could be developed easily. The shear strength (cohesion) of the soil was measured using the direct shear apparatus.

$$C_t = \left[\frac{k\delta}{4\pi(1+e)}\right]\left(\frac{R}{r}\right)\tau_c \qquad (3.3)$$

where, k is the mean coordination number; δ is the proportionality coefficient; e is the void ratio; R (m) is the mean particle radius; r (m) is the contact radius between particles; and τ_c (Pa) is the critical shear stress. According to this model, a linear relationship exists between the true cohesion and the critical shear stress.

An experimental investigation was performed by Hjeldnes and Lavinia (1980) on two different soils, well graded silty gravely sand and silty clayey fine sand, to understand how tensile stress-deformation could affect erosion (see Figure 2.19 for details). It was found that blow off (i.e. uncontrolled excessive flow through the slit formed because of the tensile deformation and erosion of the sample) occurred for well graded silty gravely sand when the tensile deformation approached maximum particle size. For silty clayey fine sand compacted on the wet side of optimum water content, the blow off occurred instantaneously and at a lower tensile deformation compared to soil compacted at the optimum and dry side of optimum water content.

3.3 Uncertainties with Erosion Modelling Considering Shear Strength Properties

Only a few studies have been performed to date to establish a comprehensive relationship between the shear strength and erosion parameters with limited success. The following sections clearly explain why it is difficult to link the shear strength properties with erosion.

3.3.1 Why is It Difficult to Correlate Shear Strength with Erosion?

From literature, the following limitations can be identified as hindrances to developing a comprehensive model of the erosion rate in terms of the shear strength, but they cannot be applied for soil eroded by flaking or slaking (unsaturated soils).

3.3.1.1 Measuring true cohesion

When water in a reservoir (eroding fluid) seeps through a crack in a dam core, the eroding fluid comes to equilibrium with pore water, and thereby the effective normal stress acting on the soil surface becomes zero (Atkinson *et al.* 1990). Under zero normal stress, the only strength in the soil will be from inter-particle bonds formed by cementation, and electrostatic and electromagnetic forces. This is called "true cohesion" (Mitchell 1976; Reddi and Bonala 1997), and only this component will resist erosion when soil is saturated. Measuring true cohesion is complicated, because, it should be done under very low normal stresses.

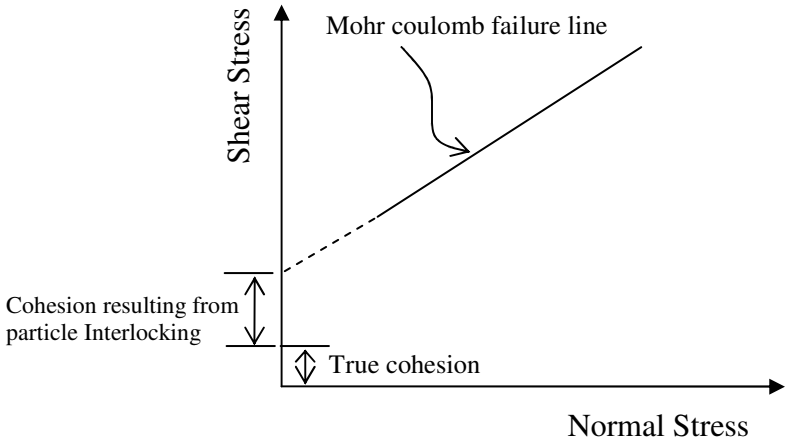

Figure 3.1 Components of cohesion determined by Mohr-Coulomb failure criterion

The conventional shear tests such as direct shear apparatus measure cohesion intercept that includes both true cohesion (if tests are conducted under normal stresses that do not destruct interparticle bonds) and cohesion resulting from particle interlocking as illustrated in Figure 3.1. Therefore, it is clear that measuring true cohesion with conventional shear apparatus is practically difficult.

A number of investigations have been conducted to measure the shear strength of soil at zero effective confining stress. Bishop and Garga (1969) reported the results of a triaxial drained compression test conducted at zero effective confining pressure on an apparently intact lump of blue London clay. Silty soil treated with cement-fly ash mixture was tested under zero effective confining stress to investigate the presence of bonds amongst the particles and their destruction with shearing (Lo and Wardani 2002). Even though these experimental studies were conducted at zero effective confining stress, the normal load on the failure plane was not zero, which meant that measuring the true cohesion of soil was still a challenge for researchers working on erosion modelling.

3.3.1.2 Difference in eroding fluid and pore fluid

The other difficulty of correlating the shear strength with the critical shear stress of saturated soil is the difference between the chemical characteristics of the eroding and pore fluids. As a result of an osmotic gradient formed by the difference between the concentrations of pore and eroding fluid salt, soil loses the strength, and erodes quickly. In conventional shear tests such as triaxial test, however, it is difficult to attain the same conditions existing in the erosion process.

3.3.2 How can Soil Strength Properties be used in Erosion Modelling?

Erosion can be better explained by the tensile stress-deformation characteristics rather than the shear strength. As described earlier, only inter-particle bonds will resist erosion under saturation and particles are dislodged during erosion because these inter-particle bonds break. Yielding and subsequent breakage of inter-particle bonds can be well demonstrated by the tensile rather than the shear behaviour of soil. It was previously assumed that tensile strength was a measure of strength from inter-particle bonds (Ingles 1962; Reddi and Bonala 1997). Hence, the tensile stress-deformation characteristics of soil will be the most appropriate property for modelling erosion. In addition, it is essential to maintain similar conditions during erosion and tensile tests, i.e. identical saturation procedures to bring pore and eroding fluids into equilibrium. Only under such conditions can the measured tensile strength represent the actual tensile strength of soil resisting erosion.

3.4 Theoretical Model Development

All available erosion models were developed based on experimental results, except the analytical model developed by Reddi and Bonala (1997), which can only be used to predict the critical shear stress for seepage erosion. Therefore, there is an imperative need to develop a mathematical model which could predict the erosion rate in terms of the strength of soil. An attempt is made here to formulate the erosion rate for chemically stabilised soil in terms of the characteristics of tensile stress-deformation, mean flow velocity, dry density of the soil, and mean diameter of the soil grains.

3.4.1 Assumptions

The mathematical model is intended to describe the erosion rate of chemically treated erodible soils due to water flow through internal cracks. In order to capture the erosion process with the above mentioned factors, some assumptions for developing the current model are made and briefly explained below.

1) Particles are assumed spherical in shape with the size of mean diameter representative of the soil particle size distribution. Similar spherical particle idealizations were also made for mathematical modelling by previous investigators (e.g. Briaud *et al*. 2001; Reddy and Bonala 1997). This assumption was used to calculate the number of inter-particle bonds in a soil mass that control the erosion and tensile strength.

2) Soil particles are transported during erosion as a suspended load moving at the same velocity as the stream. With the soils selected, the shear velocity (u_*) of the flow through the crack was high enough to keep eroded particles in suspension throughout their transportation period. If the shear velocity of the flow is higher than the settling velocity of the particles, then every detached particle will be in suspension while travelling (Barua 2004). The particle settling velocity, v_w, can be determined from Equation (3.4).

$$v_w = \frac{2gR^2(\rho_s - \rho_w)}{9\mu} \tag{3.4}$$

where, g (m/s^2) is the gravitational acceleration; R (m) is the particle radius; ρ_s (kg/m^3) is the density of the particle; ρ_w (kg/m^3) is the density of the eroding fluid; and μ (kgm^{-1}s^{-1}) is the dynamic viscosity of the eroding fluid. Silty sand with a mean particle diameter of 0.07mm

was tested during an experimental investigation in this study, and therefore, the corresponding settling velocity will be 0.0044 m/s. The required hydraulic shear stress (τ_a) to maintain detached particle in suspension can be calculated by:

$$\tau_a = \rho_w u_*^2 \tag{3.5}$$

Accordingly, if the hydraulic shear stress is higher than 0.02 Pa, then all particles will be in suspension. For dispersive clay, the maximum mean particle diameter was observed for cement treated samples with 0.04 mm with a settling velocity of 0.0014 m/s. The corresponding hydraulic shear stress is 0.002 Pa. The hydraulic shear stresses applied during whole erosion testing was far higher than these values and therefore, the assumption is justified for the current study.

3) The model is developed to examine erosion in a horizontal crack. The effect of gravity on flow through the crack is negligible.

4) Inter-particle bond strength is expressed by a mean value which is the same for all inter-particle bonds. A similar assumption was made by Ingles (1962) to develop a model for tensile strength in terms of inter-particle bond strength.

3.4.2 Model Concept

Soil particles can be detached by the eroding fluid and then transported as a suspended load, therefore, the energy required to complete the erosion is the sum of the energy used to detach the particles and the energy used for their transportation. According to the law of the conservation of energy, the sum of the energy used for the detachment and transportation should be equal to the

energy dissipated by the water for erosion. The formulation of these components is explained in the following sections.

3.4.3 Energy Dissipation by Water for Erosion

Excess hydraulic shear stress during erosion detaches and transports the soil. The energy dissipated by this excess hydraulic shear stress (ΔE) in δt time interval will be equal to the product of excess hydraulic force and distance traveled, as given in Equation (3.6).

$$\Delta E = Force \times Distance$$

$$\Delta E = (\tau_a - \tau_c)\pi\phi_i \, lv\delta t \qquad (3.6)$$

where, v (m/s) is the mean flow velocity through the crack; l (m) is the length of the crack; ϕ_i (m) is the diameter of the crack; τ_a (Pa) is the hydraulic shear stress; and τ_c (Pa) is the critical shear stress. However, only a certain fraction of energy dissipated by the flowing water is effectively used for the erosion process, because the flowing water loses part of its energy as heat and noise (Proffitt *et al.* 1993). Hence, the energy used for erosion $(\Delta E')$ can be expressed as:

$$\Delta E' = \omega(\tau_a - \tau_c)\pi\phi_i \, lv\delta t \qquad (3.7)$$

where, ω is the efficiency index which needs to be determined from the experimental results.

3.4.4 Determination of Energy Dissipation during Particle Detachment

An attempt is made here to estimate the amount of energy required to break a number of inter-particle bonds in δt time during erosion. The number of particles per unit volume (N) will be:

$$N = \frac{Dry\ density\ of\ the\ soil}{Weight\ of\ a\ soil\ particle}$$

$$N = \frac{6}{\pi(1+e)D^3} \tag{3.8}$$

where, e is the void ratio; and D (m) is the mean particle diameter. The diameter of the crack changes from ϕ_i to $\phi_i + \delta\phi_i$ in δt time interval as described in Figure 3.2.

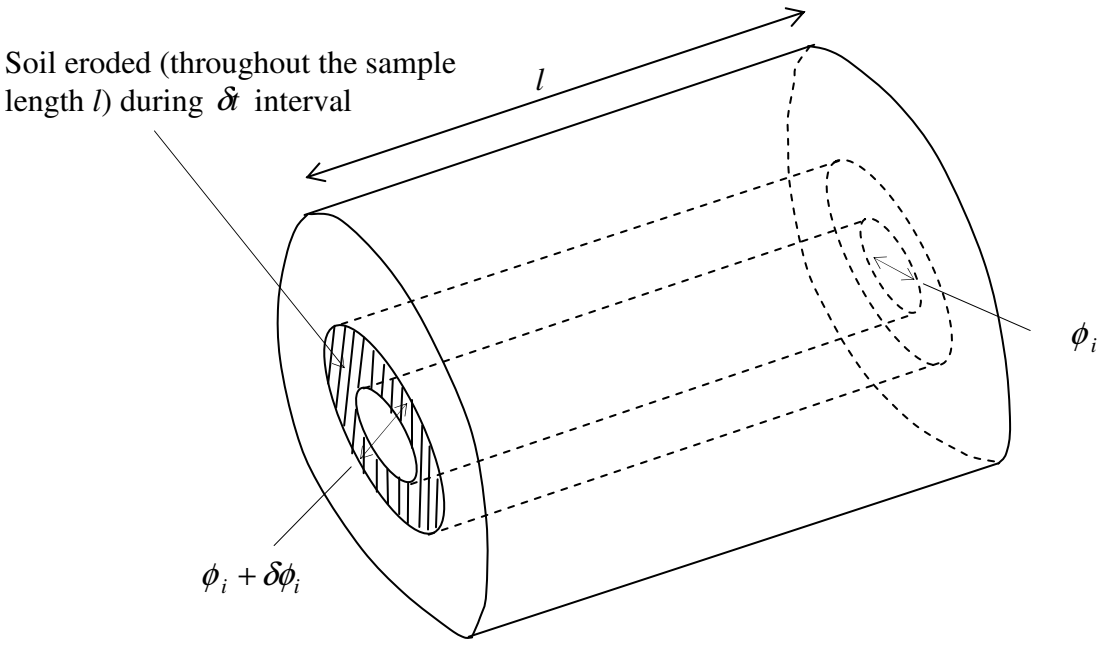

Figure 3.2 Change in crack diameter in δt interval

If the average number of common contacts (inter-particle bonds) per particle is k', then the total number of inter-particle bonds (N') broken during δt time interval can be expressed by:

$$N' = Nk' \times Volume\ of\ soil\ eroded\ in\ \delta t\ time$$

$$N' = Nk' \times \frac{\pi \phi_i l \delta \phi_i}{2}$$

$$N' = \frac{3k' \phi_i \, l \, \delta \phi_i}{(1+e)D^3} \tag{3.9}$$

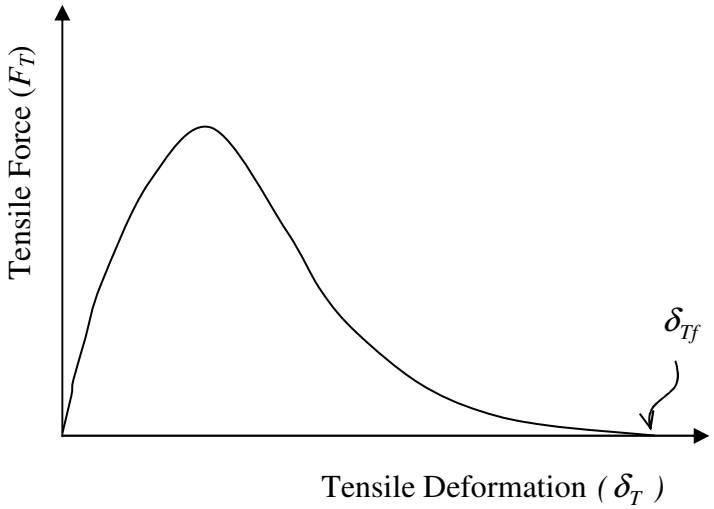

Figure 3.3 Typical tensile failure behaviour of a soil sample

Figure 3.3 shows a typical tensile force-deformation of a soil sample during a test conducted using a uniaxial tensile testing apparatus. Description of the apparatus, experimental procedure, and interpretation of observations are given in section 4.4.2.2 in Chapter 4. The energy required to break inter-particle bonds on the fracture plane to achieve tensile failure (E_T) will be:

$$E_T = \int_0^{\delta_{Tf}} F_T \times d\delta_T \tag{3.10}$$

where, F_T (N) is the tensile force; δ_{Tf} (m) is the failure tensile deformation; and δ_T (m) is tensile deformation. As proposed by Ingles (1962), the tensile strength of cemented soil with particles of size of *D* will be:

$$\sigma_{Tf} = F\left[\frac{k}{\pi D^2(1+e)}\right] \tag{3.11}$$

where, σ_{Tf} (Pa) is the tensile strength of the soil; *F* (N) is the inter-particle bond strength; and *k* is the mean coordination number. Hence, the number of inter-particle bonds on the unit surface of the fracture plane, *n*, can be expressed by:

$$n = \frac{k}{\pi D^2(1+e)} \tag{3.12}$$

The total number of inter-particle bonds (n') over the fracture surface having a cross-sectional area of A_s (cross-sectional area of the sample used for tensile testing) will be:

$$n' = \frac{kA_s}{\pi D^2(1+e)} \tag{3.13}$$

The energy required to break a single inter-particle bond can thus be determined by combining Equations (3.10) and (3.13), hence,

$$\Delta E_1 = \frac{\pi D^2(1+e)}{k}\int_0^{\delta_{Tf}} \sigma_T \times d\delta_T \tag{3.14}$$

where, ΔE_1 (J) is the energy required to break a single inter-particle bond; and σ_T (Pa) is the tensile stress. The total energy, ΔE_d, necessary for detaching N' number of inter-particle bonds

during erosion (in δt time interval) can now be formulated by combining Equations (3.9) and (3.14):

$$\Delta E_d = \frac{3}{D}\left[\frac{k'}{k}\right]\left[\pi\phi_i \, l\delta\phi_i\right]\times \int_0^{\delta_{Tf}} \sigma_T \times d\delta_T \qquad (3.15)$$

3.4.5 Determination of Energy Dissipation for Particle Transportation

As described under the assumptions stated earlier, every particle comes into suspension after detachment and subsequent movement in a stream with velocity *v*. Accordingly, the total energy used to transport all particles eroded in δt time will be equal to the kinetic energy gained by them, as given in Equation (3.16).

$$\Delta E_t = Kinetic\ energy\ gained\ by\ a\ particle \times N \times volume\ of\ soil\ eroded\ in\ \delta t\ time\ interval$$

$$\Delta E_t = \left[v^2 \times \frac{\pi D^3 \rho_w G_s}{12}\right] \times \frac{6}{\pi(1+e)D^3} \times \frac{\pi\phi_i \, l(\delta\phi_i)}{2}$$

$$\Delta E_t = \frac{v^2}{4}\rho_d(\pi\phi_i \, l\delta\phi_i) \qquad (3.16)$$

where, ρ_d (kg/s/m^2) is the dry density of the soil.

3.4.6 Formulation of the Model

According to the law of the conservation of energy, that fraction of energy used for erosion is equal to the energy used for the detachment and transportation of particles, i.e., the sum of Equation (3.15) and Equation (3.16) is equal to Equation (3.7).

$$\frac{3}{D}\left[\frac{k'}{k}\right]\left[\pi\phi_i\, l\delta\phi_i\right]\times\int_0^{\delta_{Tf}}\sigma_T\times d\delta_T+\frac{v^2}{4}\rho_d(\,\pi\phi_i\, l\delta\phi_i\,)=\omega(\,\tau_a-\tau_c\,)\pi\phi_i\, lv\delta t$$

$$\frac{\delta\phi_i}{\delta t}=\frac{\omega(\,\tau_a-\tau_c\,)v}{\left[\frac{3}{D}\left[\frac{k'}{k}\right]\times\int_0^{\delta_{Tf}}\sigma_T\times d\delta_T+\frac{v^2}{4}\rho_d\right]} \tag{3.17}$$

The relationship between the erosion rate, $\dot{\varepsilon}$, and the rate of change of crack diameter, $\left[\frac{\delta\phi_i}{\delta t}\right]$, now needs to be formulated. As illustrated in Figure 3.2, the total soil eroded (δm) during given time interval of δt will be:

$$\delta m=\frac{\pi\phi_i l\delta\phi_i\rho_d}{2} \tag{3.18}$$

In this study, the erosion rate is defined as the amount of soil eroded in unit time over a unit surface area and will be given by:

$$\dot{\varepsilon}=\frac{\rho_d}{2}\times\frac{\delta\phi_i}{\delta t} \tag{3.19}$$

Substituting Equation (3.17) into Equation (3.19) yields the erosion rate $\dot{\varepsilon}$ as:

$$\dot{\varepsilon}=\frac{\omega(\,\tau_a-\tau_c\,)v\rho_d}{\left[\frac{6}{D}\left[\frac{k'}{k}\right]\times\int_0^{\delta_{Tf}}\sigma_T\times d\delta_T+\frac{v^2}{2}\rho_d\right]} \tag{3.20}$$

Relationship between parameters k' and k

The mean coordination number (k) is equal to the number of contact points that each particle has. However, the amount of inter-particle bonds in a soil mass is not simply the product of the number of particles and the mean coordination number, because, every inter-particle bond (common contact) is shared by two adjacent spherical soil particles. This means that while determining the mean coordination number for two adjacent soil particles, this common contact is involved twice. Therefore, the number of inter-particle bonds in the soil mass should be half the product of particles in the soil mass and the mean coordination number, hence approaching the ratio $\left(\frac{k'}{k}\right)$ of 0.5. It is also clear from this analysis that determining exact value of mean coordination number is not required for modelling erosion.

The equation proposed for the erosion rate can now be simplified as:

$$\dot{\varepsilon} = \frac{\omega(\tau_a - \tau_c)v\rho_d}{\left[\frac{3}{D} \times \int_0^{\delta_{Tf}} \sigma_T \times d\delta_T + \frac{v^2}{2}\rho_d\right]} \tag{3.21}$$

where, $\dot{\varepsilon}$ (kg/s/m^2) is the erosion rate; ω is the efficiency index; τ_a (Pa) is the hydraulic shear stress; τ_c (Pa) is the critical shear stress; v (m/s) is the mean flow velocity; σ_T (Pa) is the tensile stress; δ_{Tf} (m) is the failure tensile deformation; δ_T (m) is the tensile deformation; ρ_d (kg/m^3) is the dry density of the soil; and D (m) is the mean particle diameter.

3.5 Comparison of the Current Model with the Existing Empirical Model

A universally accepted empirical model to predict the erosion rate is available in literature and is given by Equation (3.22).

$$\dot{\varepsilon} = \alpha(\tau_a - \tau_c) \tag{3.22}$$

A number of previous investigators used this empirical model to estimate the erosion rate (e.g. Arulananthan *et al.* 1975; Sargunan 1977). Figure 3.4 illustrates a typical erosional behaviour showing that the erosion rate is linearly proportional to the excess hydraulic shear stress $[\tau_a - \tau_c]$.

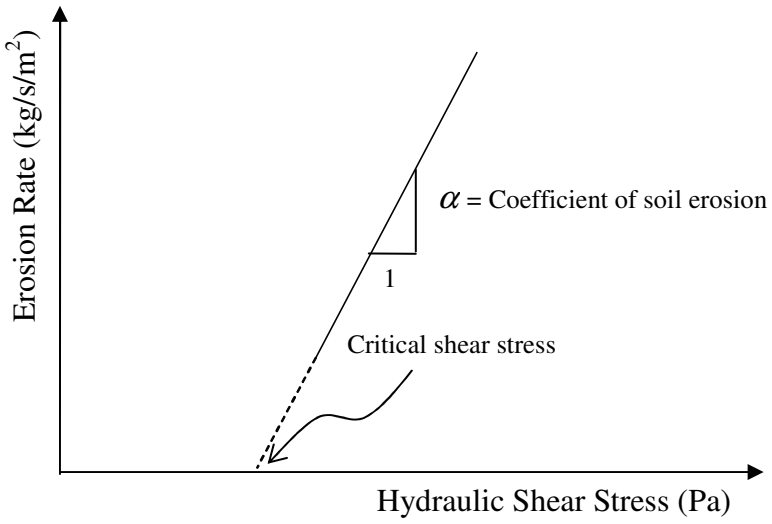

Figure 3.4 Typical curve for erosion rate vs. hydraulic shear stress

The model developed in this study is comparable with the typical empirical relationship given in Equation (3.22). By comparing Equations (3.21) and (3.22), the efficiency index, ω, which is constant, can be written as:

$$\omega = \frac{\alpha}{v\rho_d}\left(\frac{3}{D}\int_0^{\delta_{Tf}} \sigma_T d\delta_T + \frac{v^2}{2}\rho_d\right) \tag{3.23}$$

The coefficient of soil erosion determined from the experiment was substituted in Equation (3.23) to calculate the efficiency index. Since velocity through the crack changes during an erosion test, a set of efficiency indices must be obtained. It is obvious that the loss of flow energy due to noise and heat depends on the state of flow, and so too does the efficiency index. Therefore, it is necessary to develop an accurate formulation using the experimental results of the variation of efficiency index with a parameter which can represent the state of flow. The unit stream power and critical unit stream power were selected for this analysis, and the variation of efficiency index with these parameters was then developed using regression analysis. Unit stream power (P) is the power dissipated over unit surface area, while the critical unit stream power (P_c) is the minimum unit stream power necessary to initiate erosion. A generalised expression developed for the efficiency index in terms of the unit stream power and critical unit stream power will be discussed in detail in Chapter 6, under model validation. The efficiency index can then be expressed in terms of P and P_c {i.e. $\omega = F(P, P_c)$}and hence, the revised expression for the erosion rate will be:

$$\dot{\varepsilon} = \frac{F(P, P_c)(\tau_a - \tau_c)v\rho_d}{\left[\frac{3}{D}\times\int_0^{\delta_{Tf}} \sigma_T \times d\delta_T + \frac{v^2}{2}\rho_d\right]} \tag{3.24}$$

where, P (W/m^2) is the unit stream power; and P_c (W/m^2) is the critical unit stream power.

3.6 Parameter Identification

The erosion rate ($\dot{\varepsilon}$) of chemically stabilised soil experiencing a hydraulic shear stress (τ_a), can be predicted using Equation (3.24), if the critical shear stress (τ_c), mean flow velocity through the crack (v), unit stream power (P), critical unit stream power (P_c), mean particle diameter (D), area under the tensile stress-deformation curve $\left[\int_0^{\delta_{Tf}} \sigma_T \times d\delta_T\right]$, and dry density of soil (ρ_d) are known. Identification of these parameters and methods to measure them are discussed below in detail.

The unit stream power (P) can be calculated using Equation (3.25). It shows that the unit stream power is dependent of the hydraulic shear stress and the mean flow velocity.

$$P = \tau_a v \tag{3.25}$$

The critical unit stream power (P_c) will be given by:

$$P_c = \tau_c v_c \tag{3.26}$$

where, v_c is the critical flow velocity through the soil crack. The critical flow velocity will be calculated using Equation (3.27).

$$v_c = \left[\frac{8\tau_c}{f\rho_w}\right]^{0.5} \tag{3.27}$$

where, f is the friction factor; and ρ_w (kg/m^3) is the density of the eroding fluid. Therefore, the critical unit stream power is a function of the critical shear stress, and the friction factor.

The hydraulic shear stress, τ_a , on the crack surface will be estimated from:

$$\tau_a = \frac{f\rho_w v^2}{8} \tag{3.28}$$

The friction factor can be determined from the Moody diagram based on the relative roughness of soil surface and the Reynolds number.

The critical shear stress (τ_c) is the minimum hydraulic shear stress necessary to initiate erosion. An expression developed for τ_c in terms of the tensile strength of the soil will be discussed in detail under model validation in Chapter 6.

The standard Proctor compaction curve will be used to calculate the dry density (ρ_d) of the soil.

The value of $\int_0^{\delta_{Tf}} \sigma_T \times d\delta_T$ (area under tensile stress-deformation curve) will be determined using results obtained from the uniaxial tensile testing apparatus. Details of the apparatus and interpretation of observations are clearly described in Chapter 4.

3.7 Summary

This chapter described the development of a new erosion model that incorporates the tensile stress-deformation characteristics, mean flow velocity, dry density of the soil, mean particle diameter of the soil, excess hydraulic shear stress, unit stream power, and critical unit stream power. The problems associated with modelling erosion in terms of the shear strength were discussed in detail and the reasons for selecting the tensile stress-deformation behaviour for

modelling erosion were justified. The model was developed based on the law of the conservation of energy. The energy required for breaking inter-particle bonds, and the energy used to transport eroded particles were equated to the energy dissipated by water for erosion. This theoretical erosion model was compared with an empirical relationship previously proposed by several investigators (e.g. Arulananthan *et al.* 1975; Sargunan 1977). At the end of the chapter, methods for evaluating every model parameter were discussed.

CHAPTER 4

EXPERIMENTAL INVESTIGATION

4.1 Introduction

Two natural erodible soils, a dispersive clayey soil and a silty sand, collected from different sites in New South Wales (NSW), Australia were treated with a lignosulfonate mixture and general purpose Portland cement to investigate how effectively chemical stabilisation can reduce erosion. A series of erosion tests, tensile tests, *SCS* dispersion tests, Scanning Electron Microscopy (*SEM*) tests, pinhole tests, unconfined compression tests, and compaction tests were performed on chemically treated and untreated soils. This chapter describes the following:

- A preliminary investigation of chemically treated and untreated soils, including a procedure for performing a *SCS* dispersion test and a *SEM* test.
- Erosion testing on chemically treated and untreated soils using the Process Simulation Apparatus for Internal Crack Erosion (*PSAICE*). This includes a description of the apparatus, preparation of specimens, and interpretation of observations.
- Tensile testing using a newly built apparatus including a description of the apparatus, sample preparation, and interpretation of observations.

4.2 Types of Soils

Silty sand

A silty sand collected from Wombayen caves in NSW, Australia, was selected for this study because according to the standard pinhole test it is classified as an erodible soil consisting of a large volume of silt and fine sand. It is non-plastic and classified as silty sand (SM) according to the unified soil classification system (USCS). The particle size distribution is shown in Figure 4.1. The maximum dry density and optimum moisture content obtained from the standard Proctor compaction method were 1711 kg/m^3 and 10.3%, respectively.

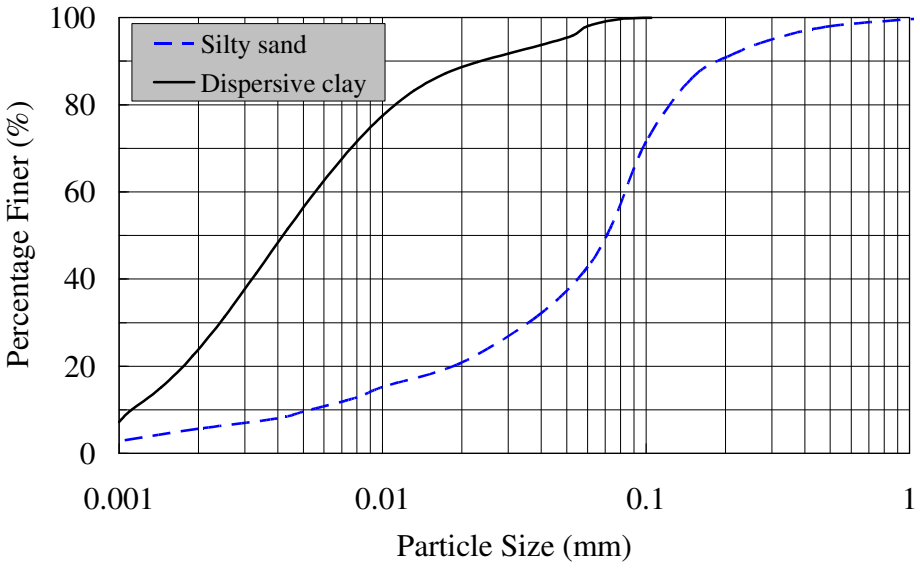

Figure 4.1 Particle size distribution of silty sand and dispersive clay

Dispersive clay

A dispersive clayey soil collected from Wakool, NSW, Australia was also chosen for this investigation. The particle size distribution is given in Figure 4.1. The liquid limit and plastic index of the soil were 47.6% and 29.4%, respectively. According to the standard pinhole test, it is

classified as a dispersive soil of *class D2*. The maximum dry density and optimum moisture content obtained from the standard compaction test were 1538 kg/m^3 and 22%, respectively. Mineralogical analysis showed that this dispersive clay contains a considerable amount of expansive minerals such as monmorillonite. The mineralogy of the soil is outlined in Table 4.1.

Table 4.1 Mineralogy of the dispersive clay

Mineral	Amount (%)
Kaolinite	4.4
Albite	2.6
Illite	13.9
Monmorillonite	9.1
Quartz	66.2
Mixed layer Illite-Smectite	3.2

4.3 Chemical Stabilisers Used

General purpose Portland cement manufactured in Australia and a lignosulfonate mixture were selected for the experimental investigation. The lignosulfonate mixture, a processed waste product from the paper manufacturing industry, is a dark brown liquid with a pH value of approximately 4. It is an inflammable stabiliser that does not corrode metals and is not classified as hazardous according to the National Occupational Health and Safety Commission (NOHSC) criteria (Chemstab 2003). However, it is important to read the Material Safety Data Sheet given

in Appendix C before using this chemical. For the sake of convenience, this mixture of lignosulfonate will hereafter be called lignosulfonate.

4.4 Experimental Investigation

4.4.1 Preliminary Investigation

A preliminary investigation includes the standard pinhole tests, standard Proctor compaction tests, unconfined compression tests, *SCS* dispersion tests, and *SEM* tests on both treated and untreated soil samples. To select the appropriate chemical dosages for detailed erosion testing, standard pinhole tests were conducted on chemically treated and untreated soils. Samples were prepared to their 95% of maximum dry density and optimum water content and cured for seven days in a humidity controlled chamber. A detailed test procedure is given in ASTM D 4647 (93).

Unconfined compression tests were performed to study the stress-strain behaviour of chemically treated and untreated soils. All of these tests were conducted on specimens of 38 mm in diameter and 76 mm in length compacted at their optimum water content and the maximum dry density. Specimens were wrapped in moisture proof bags and kept in the humidity controlled chamber to cure for 7 days. A strain rate of 0.5 mm/min was applied to carry out the tests.

Scanning Electron Microscopy (*SEM*) tests were performed on the chemically treated and untreated silty sand to investigate the stabilisation mechanism. Every sample was compacted to 95% of its maximum dry density at the optimum moisture content of 10.3%. Subsequently, an 18 mm diameter by 10 mm long sample was extruded using a specially made thin copper tube, and then kept in a humidity controlled chamber to cure for 7 days. They were dried in an oven before the *SEM* tests were carried out. To increase conductivity, the dried samples were then coated with

ultra thin layer of gold using a gold coater as shown in Figure 4.2. The gold coated samples are shown in Figure 4.3.

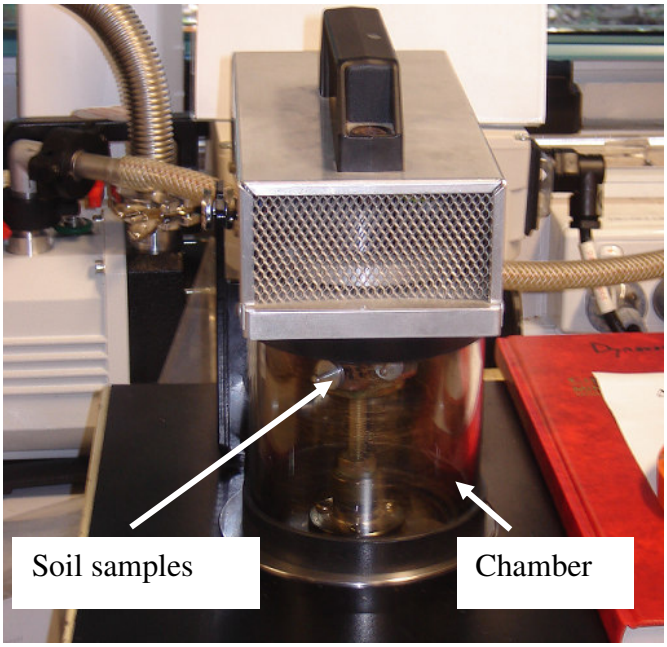

Figure 4.2 Ultra thin Gold coating setup

(a) (b) (c)

Figure 4.3 Gold coated soil surfaces of (a) Untreated (b) 0.4% lignosulfonate treated and (c) 2% cement treated silty sand

After the samples were coated with a thin layer of gold, they were placed in the SEM machine (Figure 4.4 (a) and (b)) for scanning. A number of digital images were captured to obtain a clear picture of the stabilisation mechanisms of both admixtures.

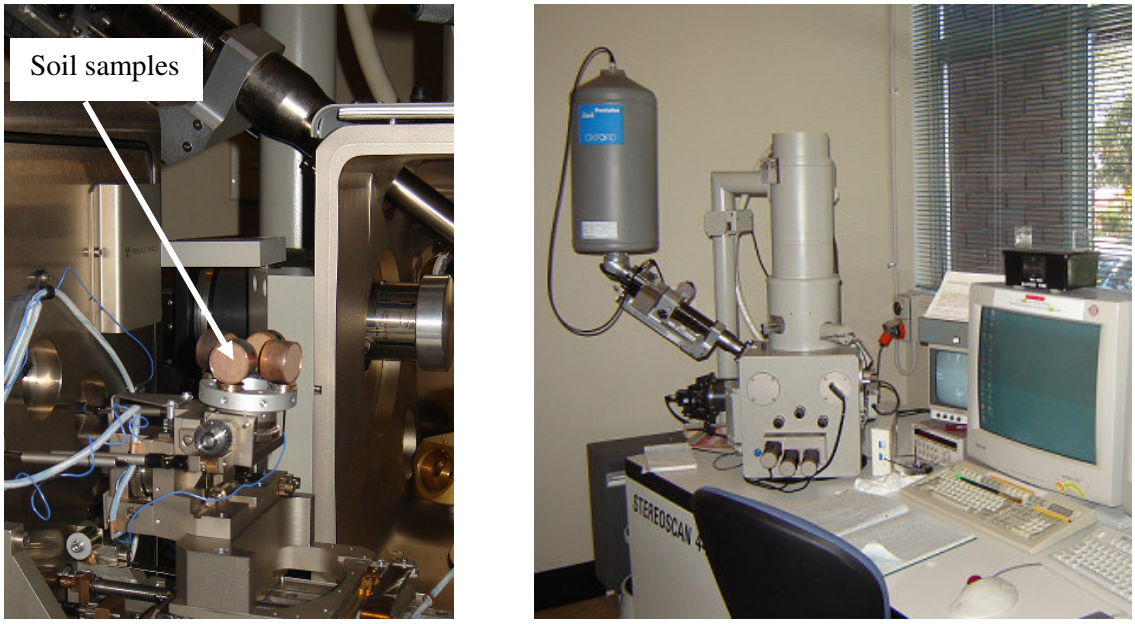

(a) (b)

Figure 4.4 SEM instrument (a) with samples set in the chamber and (b) ready for testing

A series of *SCS* dispersion tests were performed on cement treated and untreated dispersive clay samples to examine whether cement encourages flocculation through cation exchange. This test was used to calculate the amount of soil finer than 0.005 mm in soil-water suspension that was subjected to minimal mechanical agitation. Since the "percent dispersion" is a measure of dispersed clay in suspension (deflocculated clay particles), it will be a good indicator for expressing the degree of flocculation caused by chemical stabilisation. Tests were carried out according to the procedure developed by Sherard *et al.* (1972). The dispersive clay was mixed with 0.2%, 0.4% and 0.6% dosages of cement. All the samples were prepared at their optimum

water content, and tests were conducted within a few hours to avoid possible cementation, because, the objective was to investigate flocculation caused by cation exchange. A sub-sample (equivalent weight of 25 g dry soil) was put into a filtering flask with 125 ml of distilled water and then a suction was applied for 10 minutes to remove any entrapped air. The soil-water mix was then washed into a hydrometer jar to which distilled water was added up to the 1000 ml mark. The cylinder was then shaken end over end (approximately 30 times) for one minute. A hydrometer was placed into the suspension column to determine the percentage of soil finer than 0.005 mm in the soil-water suspension. A standard hydrometer test was also performed on the untreated soil to determine the percentage of soil finer than 0.005 mm. The "percent dispersion" of untreated and treated soil was then computed using Equation 4.1.

$$Percent\ dispersion = \frac{\%\ finer\ than\ 0.005\ mm\ \ in\ soil\ water\ suspension\ (untreated\ or\ treated)}{\%\ finer\ than\ 0.005\ mm\ \ from\ standard\ hydrometer\ analysis\ (untreated)}\ \% \qquad (4.1)$$

4.4.2 Detailed Investigation

4.4.2.1 Erosion tests using Process Simulation Apparatus for Internal Crack Erosion (*PSAICE*)

All erosion tests were performed with a newly built Process Simulation Apparatus for Internal Crack Erosion (*PSAICE*) designed and built at University of Wollongong. According to the objectives of this research, it was necessary to predict the erosion rate quantitatively to validate the erosion model. Around 70 tests were conducted on saturated samples of both types of soils under treated and untreated conditions. For each erosion test, an additional test was conducted on

an identical sample to determine the particle size distribution necessary for interpreting the observations, which will be described later in this chapter. A detailed procedure to find out the particle size distribution of eroded soil is given in Appendix A. A description of the experimental setup, sample preparation, and interpretation of observations are presented in the next section. A detailed drawing and safe operating procedure for the apparatus are given in the Appendix A.

Description of the apparatus

This equipment has an adjustable head tank capable of applying a hydraulic gradient of up to 40 across the sample. The eroding fluid is stored overnight in a 1000 litre tank under ambient conditions and pumped into the adjustable head tank during testing. A schematic diagram and photograph of the experimental set up are shown in Figure 4.5(a) and Figure 4.5(b), respectively. Two pressure transducers were connected to each end of the sample to measure any difference in the pressure across the crack. To continuously measure erosion, an inline process turbidity meter was installed next to the down stream side of the sample to constantly monitor effluent turbidity during the test. These values can then be used with the relationship developed between the concentration of solids (kg/m^3) and turbidity (NTU) to calculate the erosion rate. The procedure to develop the relationship between the concentration of solids and turbidity is explained later in this chapter. In order to continuously measure the flow rate, the effluent is weighed with an electronic balance. As shown in Figure 4.5(a), all pressure transducers, turbidity meter, and the electronic balance, have been connected to a data acquisition system.

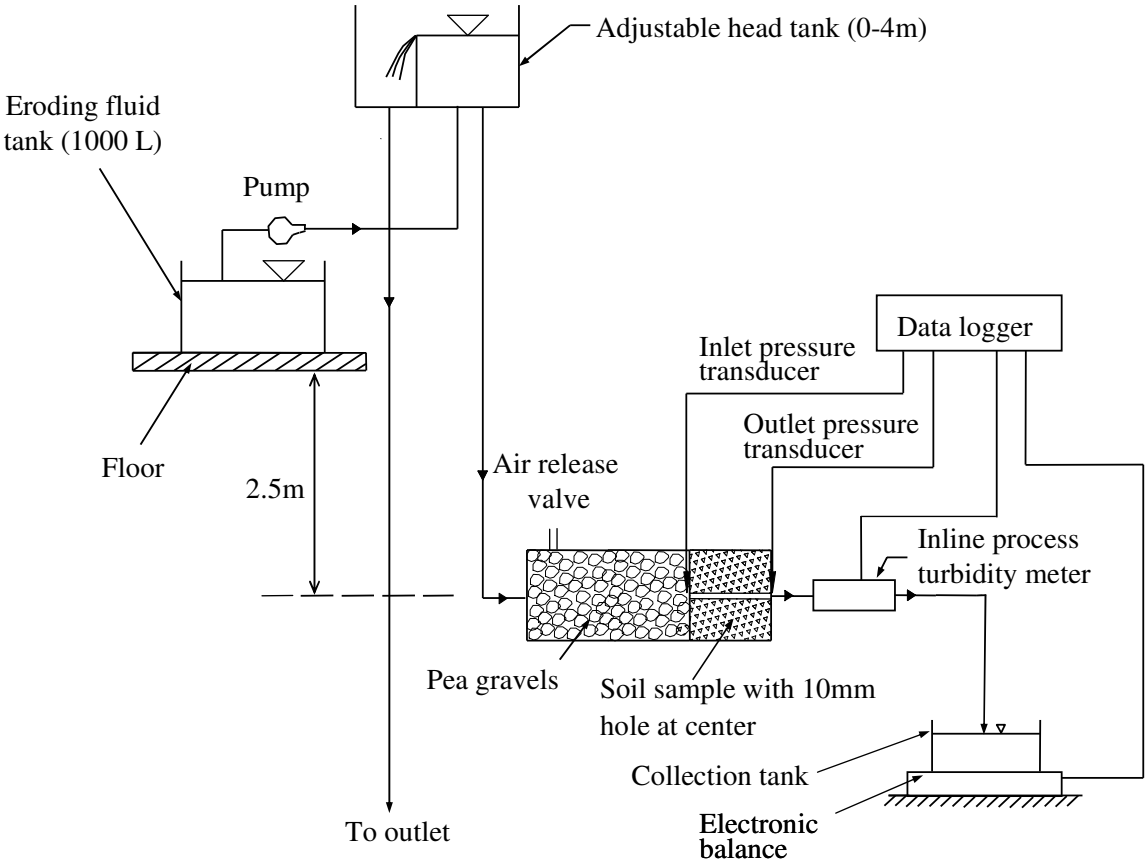

Figure 4.5(a) Schematic diagram of the Process simulation apparatus for internal crack erosion

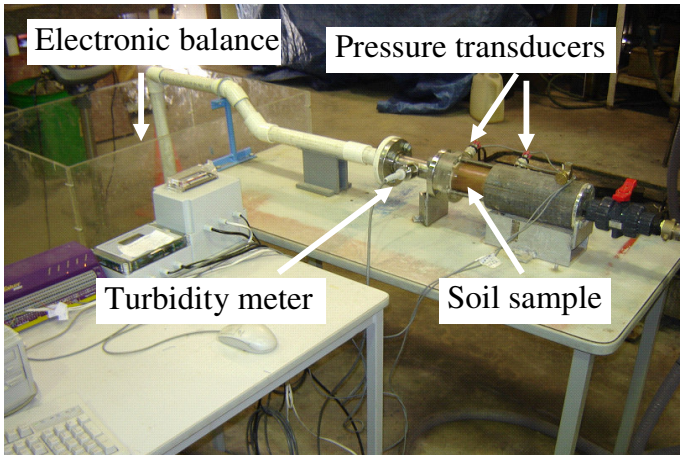

Figure 4.5(b) Photograph of the Process simulation apparatus for internal crack erosion

Sample preparation

Five dosages of cement, 0.5%, 1%, 1.5%, 2%, and 3%, and four dosages of lignosulfonate, 0.1%, 0.2%, 0.4%, and 0.6% by dry weight of soil were selected to stabilise the silty sand. Different mixing procedures were adopted, i.e., the soil was mixed with a predetermined amount of cement using a soil mixer and then water was added to achieve an optimum moisture content, but the predetermined amount of lignosulfonate was first mixed with the required amount of water to obtain an optimum water content, and then the mix was added to the soil. Once the soil was mixed with stabilisers, it was statically compacted inside a 72 mm diameter by 100 mm long copper tube using a compaction mould arrangement and AVERY machine, as illustrated in Figures 4.6(a) and (b), respectively.

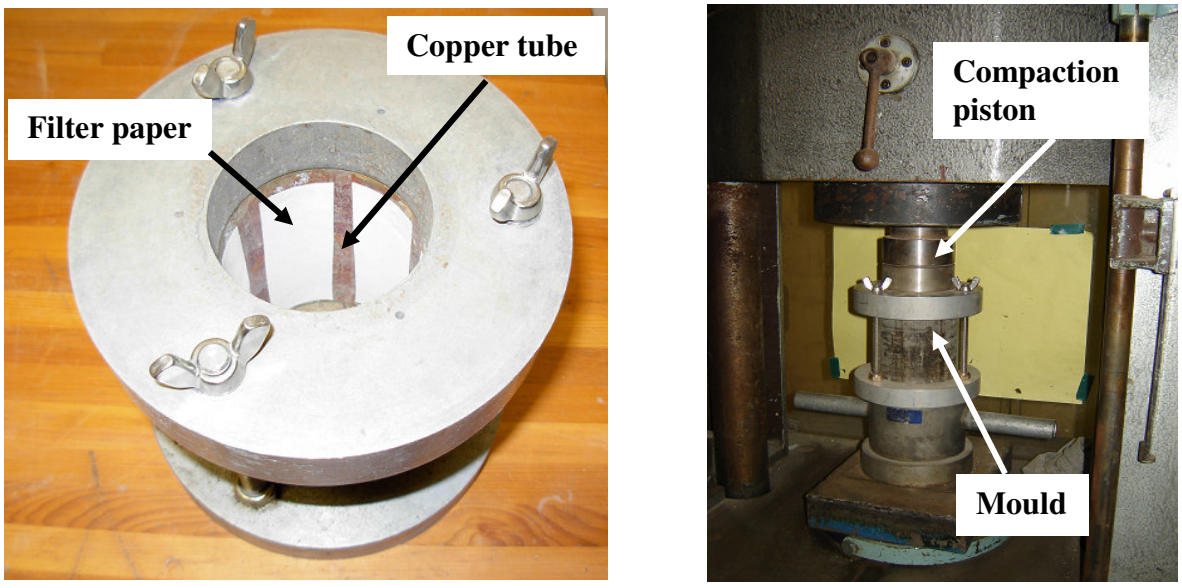

(a) (b)

Figure 4.6 (a) Copper tube sitting inside the compaction mould and (b) AVERY compression machine to statically compact the soil

A number of 6 mm holes were drilled around the surface of the copper tube so that the water could uniformly penetrate the soil sample. Every hole was covered internally with a filter paper, which would also facilitate water movement into the soil mass. To study the effect of compaction on erosion, all treated and untreated silty sand specimens were prepared at the optimum water content and at two compaction levels of 90% and 95% of the maximum dry density. As a comparison, a maximum dry density of 1711 kg/m^3 and an optimum water content of 10.3% of untreated soil were chosen as the maximum dry density and the optimum moisture content for all treated samples. A 10-mm crack was formed through the sample at the centre using an auger drill bit and a guiding block arrangement (Figure 4.7). All the treated and untreated specimens were wrapped in moisture proof bags and kept in a humidity controlled chamber to cure for 7 days. These compacted samples were then immersed in eroding fluid (tap water) until they were saturated.

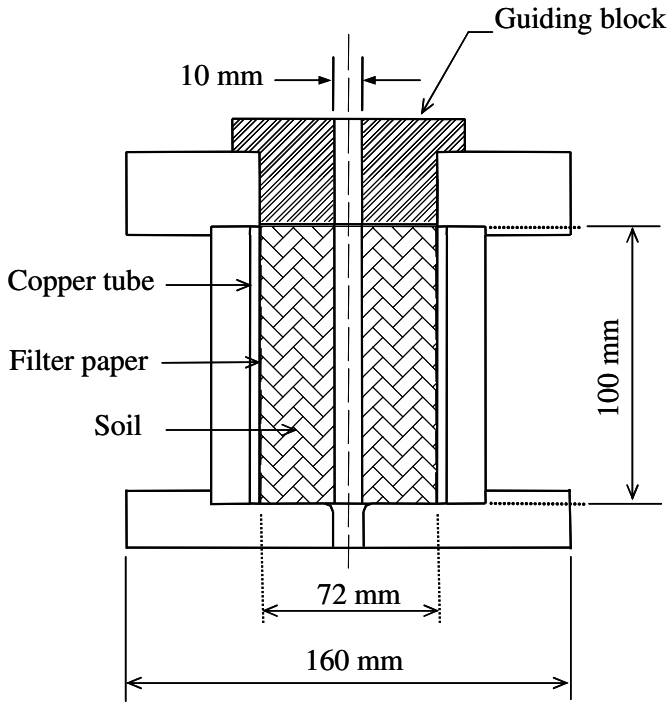

Figure 4.7 Crack forming arrangement

Three dosages of general purpose Portland cement, 0.2%, 0.4%, and 0.6%, and three dosages of lignosulfonate mixture, 0.2%, 0.4%, and 0.6% by dry weight of soil were selected to treat the dispersive clay. The mixing techniques and compaction method used to prepare samples of dispersive clay were similar to those used to prepare samples of silty sand. After preparation, the samples were wrapped in moisture proof bags and stored in the humidity controlled chamber to cure for 7 days. They were then soaked in eroding fluid (tap water), and both the swelling and weight of the sample were measured regularly. Every sample was soaked for 4 days based on these observations. A summary of the tests conducted on treated and untreated dispersive clay is given in Table 4.2.

Table 4.2 Summary of erosion tests conducted on dispersive clay

Chemical type	Amount of chemical	Degree of compaction	Moulding water content
Untreated	-	95% and 90%	Optimum, Dry of optimum, and Wet of optimum
Lignosulfonate treated	0.2%, 0.4%, 0.6%	95% and 90%	Optimum and Dry of optimum
Cement treated	0.2%, 0.4%, 0.6%	95% and 90%	Optimum and Dry of optimum

Interpretation of observations

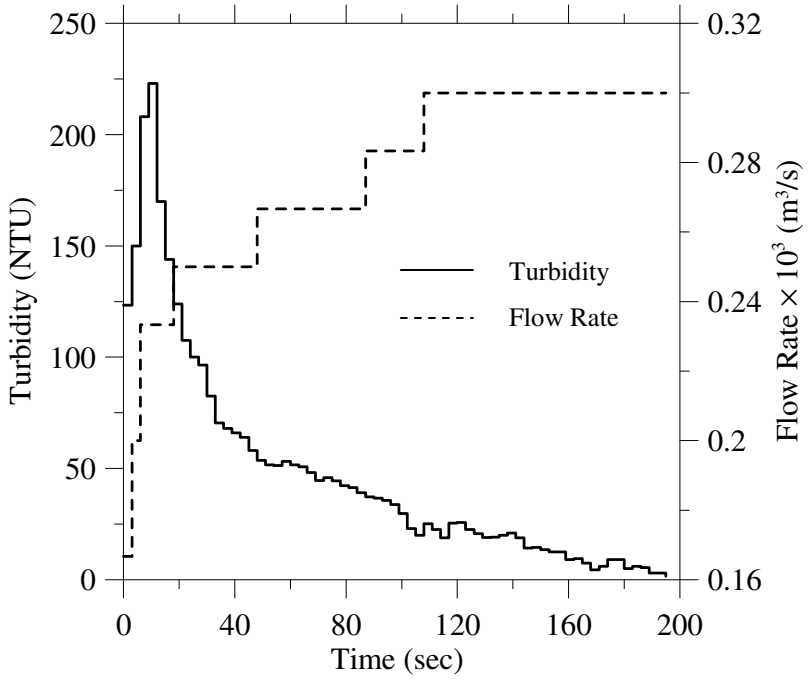

Figure 4.8 The effluent turbidity and flow rate with time for untreated dispersive clay (95% maximum dry density and wet of optimum)

The typical variation of effluent turbidity and flow rate over time during an erosion test is shown in Figure 4.8. It shows that the effluent turbidity increased for sometime and then decreased continuously as erosion progressed, but the flow rate through the crack increased with elapsed time. An interpretation of these observations to predict the erosion rate and soil crack diameter is described next. Observations were divided into n_1 segments with a time step of δt . If the flow rate and turbidity of i^{th} segment are Q_i (m^3/s) and T_i (NTU), respectively, the amount of soil eroded in a selected time step δt will be given by:

$$\delta m_i = k_c Q_i T_i \times \delta t \qquad (4.2)$$

where, δm_i (kg) is the eroded soil during the δt time interval; and k_c (kg/m^3/NTU) is an empirical factor relating turbidity to the soil solids concentrated in the flow. The relationship between turbidity and concentration was developed as follows.

Two steps are involved here. In the first, the relationship between turbidity and concentration was developed only for selected samples by directly measuring the turbidity and concentration. In the second, a simplified method was proposed to predict k_c based on the results obtained from the first step.

Step 1

A certain hydraulic gradient across the soil crack was applied for a period of time and the effluent was collected without losing sediment into the drain. Generally, 3 to 4 litres of effluent was collected and condensed (evaporation) to get a sufficient concentration for testing. The effluent was then put into a beaker and stirred with a magnetic stirrer. While stirring, a 150 ml sub-sample was then extracted for testing. It was mixed thoroughly and poured into the turbidity adaptor, and the turbidity reading was then logged (Figure 4.9).

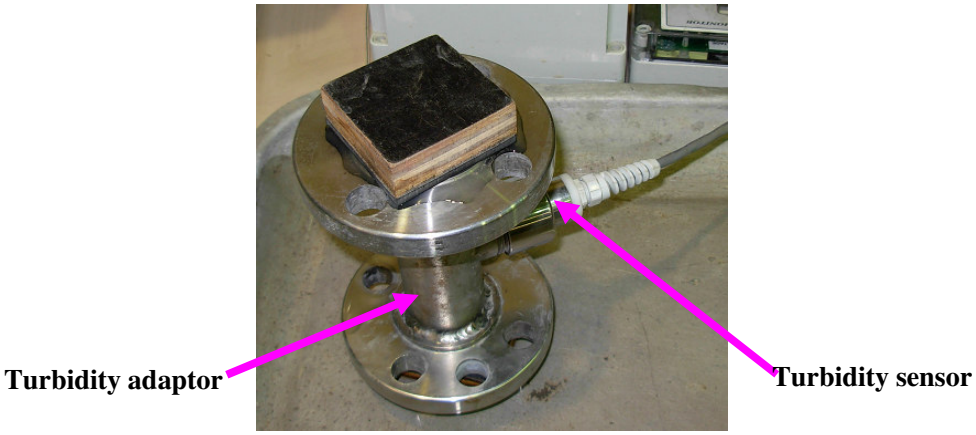

Figure 4.9 Arrangement to determine the relationship between turbidity and concentration

A similar procedure was repeated by diluting the sample to get a set of concentrations, which yielded a set of turbidity values. The weight of the sediment in the effluent was calculated by drying in the oven, and then the concentration was determined. The concentrations and corresponding turbidity values were plotted to explore the variation.

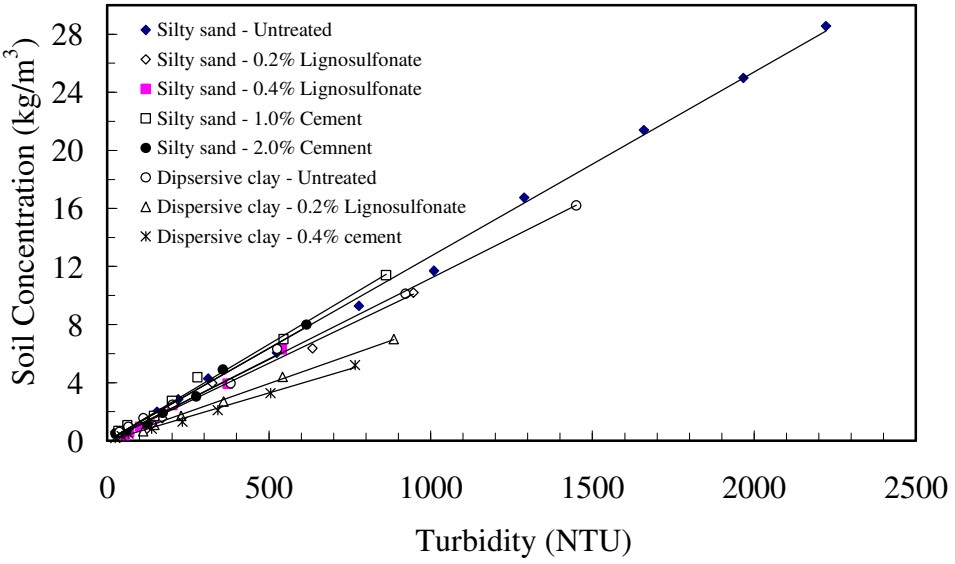

Figure 4.10 The relationship between the concentration of solids and turbidity for selected soil samples (prepared at 95% of their maximum density and the optimum water content)

As illustrated in Figure 4.10, the relationship between turbidity and concentration is linear, irrespective of the type of soil and the method of treatment, and the gradient of these lines gives a k_c value for the soil samples tested. However, this was a tedious method for predicting k_c. So to make it easier, an alternative method was used that assumed that the relationship between concentration and turbidity was linear. It is reasonable to make this assumption, because, relationships are linear for a range of turbidity values and different untreated and chemically treated conditions as shown in Figure 4.10. The derivation of this alternative method is given below.

Step 2 (Alternative method)

Total soil eroded during the test is given by:

$$M = m_1 - m_2 - m_3 \tag{4.3}$$

where, M (kg) is the total amount of soil eroded during the test; m_1 (kg) is the dry weight of the sample; m_2 (kg) is the dry weight of the soil removed while forming the crack; and m_3 (kg) is the dry weight of sample at the end of the test.

Based on the amount of soil eroded in each segment as given Equation 4.2, the total amount of soil eroded during the test will then be:

$$M = k_c \times \sum_{i=1}^{i=n_1} (Q_i T_i) \times \delta t \tag{4.4}$$

where, n_1 is the number of segments.

Combining Equations 4.3 and 4.4 yields:

$$k_c = \frac{(m_1 - m_2 - m_3)}{\sum_{i=1}^{i=n_1} (Q_i T_i) \times \delta t} \tag{4.5}$$

Using Equation 4.5 to predict the k_c value is quick and simple. The values of k_c obtained from the direct correlation of concentration with turbidity on selected samples (Figure 4.10) were compared with that calculated from Equation 4.5 for identical soil samples. It was found that they were very close, hence, k_c was predicted using Equation 4.5 for the rest of the testing program. The value of k_c for untreated and cement treated silty sand was 0.013 kg/m^3/NTU. A slightly

smaller value of k_c (0.011 kg/m^3/NTU) was obtained for lignosulfonate treated soils. A range of k_c values were observed for treated and untreated dispersive clay, as summarised in Table 4.3.

Table 4.3 Calculated k_c values for untreated and treated dispersive clay

Chemical type	Amount of chemical	Water content	K_c value	
			95% Compaction	90% compaction
Untreated	-	Wet of optimum	0.011	0.011
		Optimum	0.011	0.011
		Dry of optimum	0.011	0.012
Cement treated	0.2%	Optimum	0.011	0.011
	0.4%		0.007	0.008
	0.6%		0.008	0.008
	0.2%	Dry of optimum	0.011	0.013
	0.4%		0.009	0.010
	0.6%		0.007	0.008
Lignosulfonate treated	0.2%	Optimum	0.008	0.008
	0.4%		0.007	0.008
	0.6%		0.008	0.008
	0.2%	Dry of optimum	0.008	0.010
	0.4%		0.010	0.009
	0.6%		0.009	0.010

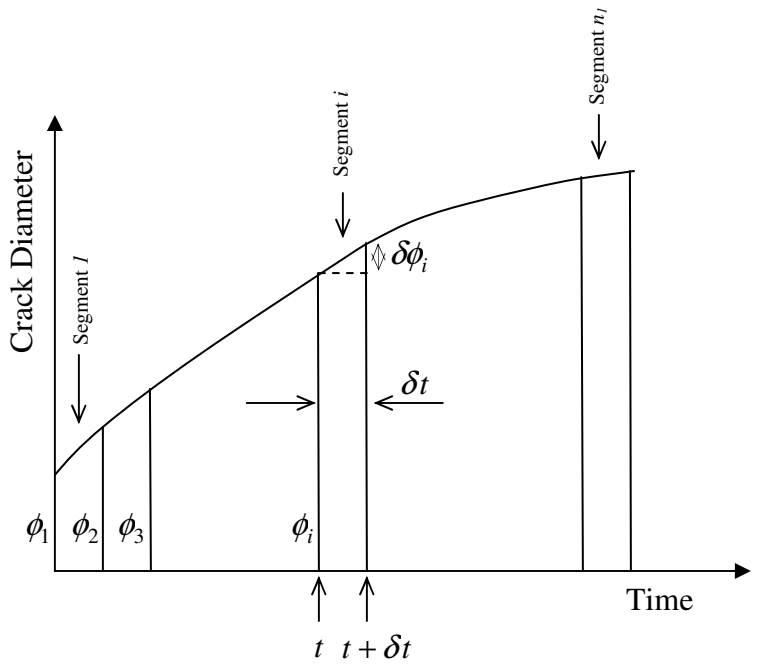

Figure 4.11 Variation of crack diameter during an erosion test

When the diameter of the crack changes by $\delta\phi_i$ in a time interval δt, as illustrated in Figure 4.11 (see Figure 3.2 in Chapter 3 for more details), the amount of soil eroded during this time is:

$$\delta m_i = \frac{\pi \phi_i l \rho_d}{2} \times \delta\phi_i \tag{4.6}$$

where, δm_i (kg) is the amount of soil eroded during a selected time interval δt; ρ_d (kg/m^3) is the dry density of compacted soil; l (m) is the length of the crack; and ϕ_i (m) is the diameter of the crack at time t. The erosion rate is defined as the amount of soil eroded in unit time over a unit surface area. Hence, Equation 4.6 yields the erosion rate as:

$$\dot{\varepsilon} = \frac{\rho_d}{2} \times \frac{\delta\phi_i}{\delta t} \tag{4.7}$$

where, $\dot{\varepsilon}$ (kg/s/m^2) is the erosion rate.

Combining Equations (4.6) and (4.2) gives:

$$\delta\phi_i = \frac{2k_c Q_i T_i}{\pi\phi_i l\rho_d} \times \delta t \tag{4.8}$$

Equation (4.8) can be used to calculate the change in diameter of the crack during erosion for each time step using the flow rate, turbidity of effluent, and initial diameter of the crack. Once the diameter of the crack is determined, the erosion rate can then be calculated using Equation (4.9), which is obtained by combining Equations (4.7) and (4.8).

$$\dot{\varepsilon} = \frac{k_c Q_i T_i}{\pi\phi_i l} \tag{4.9}$$

Two different approaches were used to predict the hydraulic shear stress, τ_a, applied to the surface of the crack. These methods are discussed in detail below.

a) Friction factor method

The hydraulic shear stress on the surface of the crack can be determined using:

$$\tau_a = \frac{f\rho_w v^2}{8} \tag{4.10}$$

where, f is the friction factor, ρ_w (kg/m^3) is the density of the eroding fluid; and v (m/s) is the mean velocity of the flow through the crack at time t, which can be calculated using the flow rate and diameter of the crack. The friction factor was calculated from the Moody diagram (Figure 4.12) based on the relative roughness and Reynolds number.

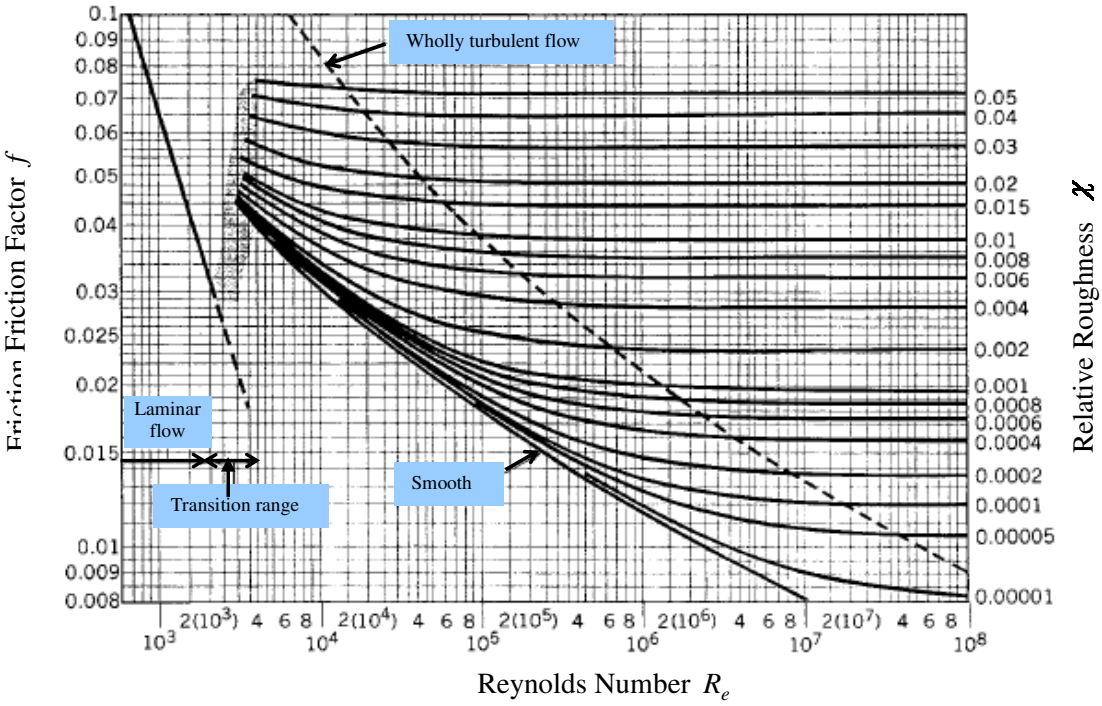

Figure 4.12 Moody diagram used for the friction factor calculation

Relative roughness (χ) can be calculated from:

$$\chi = \frac{D}{2\phi_i} \tag{4.11}$$

where, D (m) is the mean particle diameter. The height of the roughness element was taken as the radius of the mean particle. A similar approach was used by Briaud *et al.* (2001) to calculate the hydraulic shear stress. The change in mean particle size for specimens of silty sand (untreated and treated) was negligible, but it changed for dispersive clayey specimens (untreated and treated). A summary of the mean particle size of untreated and chemically treated dispersive clay is given in Table 4.4.

Table 4.4 Mean particle diameter of treated and untreated dispersive clay

Chemical type	Amount of chemical	Water content	Mean particle diameter (Micron)	
			95% Compaction	90% Compaction
Untreated	-	Wet of optimum	7	6
		Optimum	8	7
		Dry of optimum	8	8
Cement treated	0.2%	Optimum	18	18
	0.4%		28	30
	0.6%		32	38
	0.2%	Dry of optimum	18	20
	0.4%		32	35
	0.6%		40	42
Lignosulfonate treated	0.2%	Optimum	19	18
	0.4%		22	22
	0.6%		25	27
	0.2%	Dry of optimum	20	15
	0.4%		24	20
	0.6%		28	25

The mean particle diameter was determined based on the particle size distribution of the eroded particles obtained from the Malvern Mastersizer. Particle size analysis was performed without applying any dispersion agent in order to keep all the eroded particles at their original size. A detailed procedure for determining particle size distribution is given in Appendix A.

The Reynolds number can be calculated using Equation (4.12):

$$R_e = \frac{\rho_w v \phi_i}{\mu} \tag{4.12}$$

where, μ (kgm^{-1}s^{-1}) is the dynamic viscosity of the eroding fluid (tap water).

b) Hydraulic gradient method

This method is based on the hydraulic gradient measured across the crack. A similar approach was adopted by previous investigators (Wan and Fell 2004). The development of an expression for the hydraulic shear stress applied to the surface of the crack in terms of applied hydraulic gradient is described below.

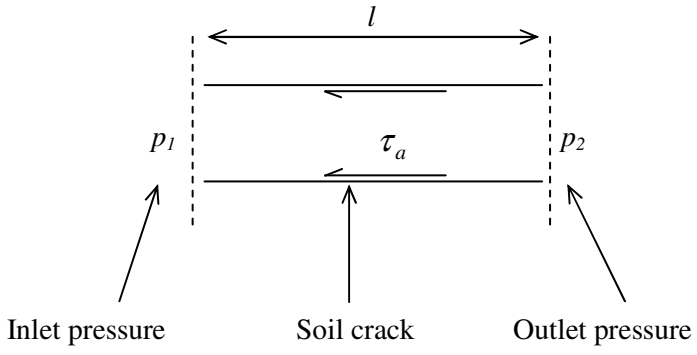

Figure 4.13 Boundary stresses acting on the soil crack

Figure 4.13 shows the boundary stresses acting on the crack. The hydraulic gradient (s) across the crack using the head balance equation is given by:

$$s = \frac{p_1 - p_2}{\rho_w g l} \tag{4.13}$$

where, $[p_1 - p_2]$ is the pressure drop across the crack.

Equating forces acting on the wall of the crack gives:

$$\tau_a \times \pi \phi_i l = [p_1 - p_2] \times \frac{\pi \phi_i^{\,2}}{4} \tag{4.14}$$

Combining equations (4.13) and (4.14) gives:

$$\tau_a = \frac{\rho_w g s \phi_i}{4} \tag{4.15}$$

It was found that both methods outlined above produced different results. Possible reasons for this discrepancy and the accuracy of these methods in predicting the critical shear stress will be discussed under Section 5.3 in Chapter 5.

4.4.2.2 Tensile tests

The tensile stress-deformation characteristics of soils were necessary to validate the erosion model developed in Chapter 3. Hence, a series of tests were performed using a uniaxial tensile testing apparatus designed and built at University of Wollongong. A summary of the tests conducted is given in Table 4.5.

Table 4.5 Summary of tensile tests conducted

Soil type	Type of stabiliser	Amount of stabiliser
Silty sand	Lignosulfonate	0.1%, 0.2%, 0.4%, and 0.6%
	Cement	0.5%, 1.0%, 1.5%, 2.0%, and 3.0%
Dispersive clay	Lignosulfonate	0.2%, 0.4%, and 0.6%
	Cement	0.2%, 0.4%, and 0.6%

Note: Every sample was prepared at 95% of their maximum dry density and optimum water content, and tests were conducted under saturated conditions.

Description of the apparatus

The uniaxial tensile testing apparatus is similar to the one developed by Hjeldnes and Lavinia (1980), but with alterations to the dimensions and the method of gripping the soil. This particular set up was selected for the current study, because, it measures the tensile stress-deformation of the soil resulting from inter-particle bonds existing on a pre-defined fracture plane. A schematic diagram and photograph of the tensile testing apparatus is given in Figures 4.14 (a) and (b), respectively. A detailed drawing of the apparatus and the safe operating procedure are given in Appendix A.

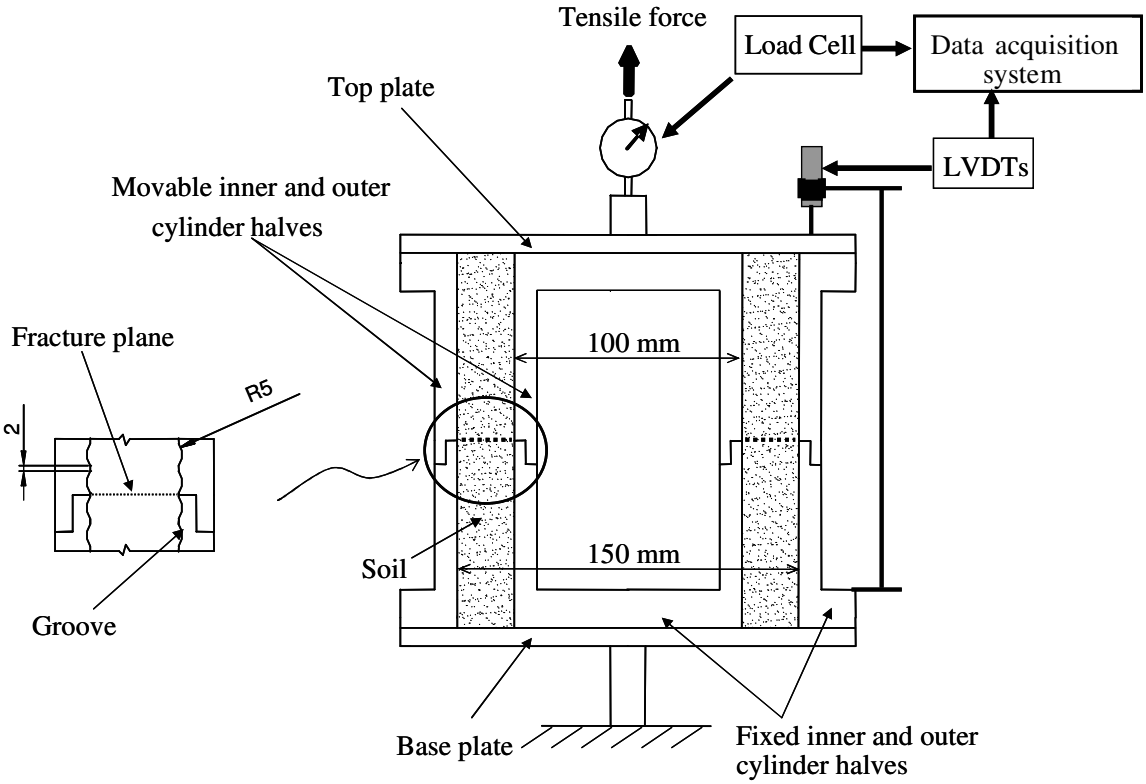

Figure 4.14(a) A schematic diagram of the uniaxial tensile testing apparatus

As can be seen from Figure 4.14(a), the uniaxial tensile testing device consists of two co-axial rigid plastic cylinders which have been cut through the middle. The inner and outer diameters of the soil annulus are 100 mm and 150 mm, respectively. Hence, the samples of soil are a hollow cylinder 150 mm long by 25 mm thick, with a cross sectional area of 9821.4 mm^2. Grooves were made inside the outer cylinder and outside the inner cylinder, as shown in Figure 4.14(a), to grip the soil firmly and transfer the tensile load to the sample. The upper and lower halves of each cylinder are aligned at the joint with a step guide. A number of 2 mm holes were drilled into the inner and outer cylinders close to the fracture plane to facilitate water penetration during soaking. The inner and outer cylinder halves in the lower part of the apparatus were connected to a base plate to make them a single unit. When the sample is ready for testing, both

cylinder halves in the top part of the apparatus were connected to a top plate in order to assemble them as a single unit. The base plate was then fixed to the bottom of the INSTRON universal testing machine to stop the lower part of the apparatus from moving. The upper part of the apparatus was connected to the INSTRON universal testing machine through the top plate (Fig. 7(b)). A load cell was used to measure the tensile load, while tensile deformation at the fracture plane was measured using three LVDTs. The LVDTs and the load cell were connected to a data acquisition system, and then strain controlled tensile tests at a rate of 0.01 mm/min were conducted.

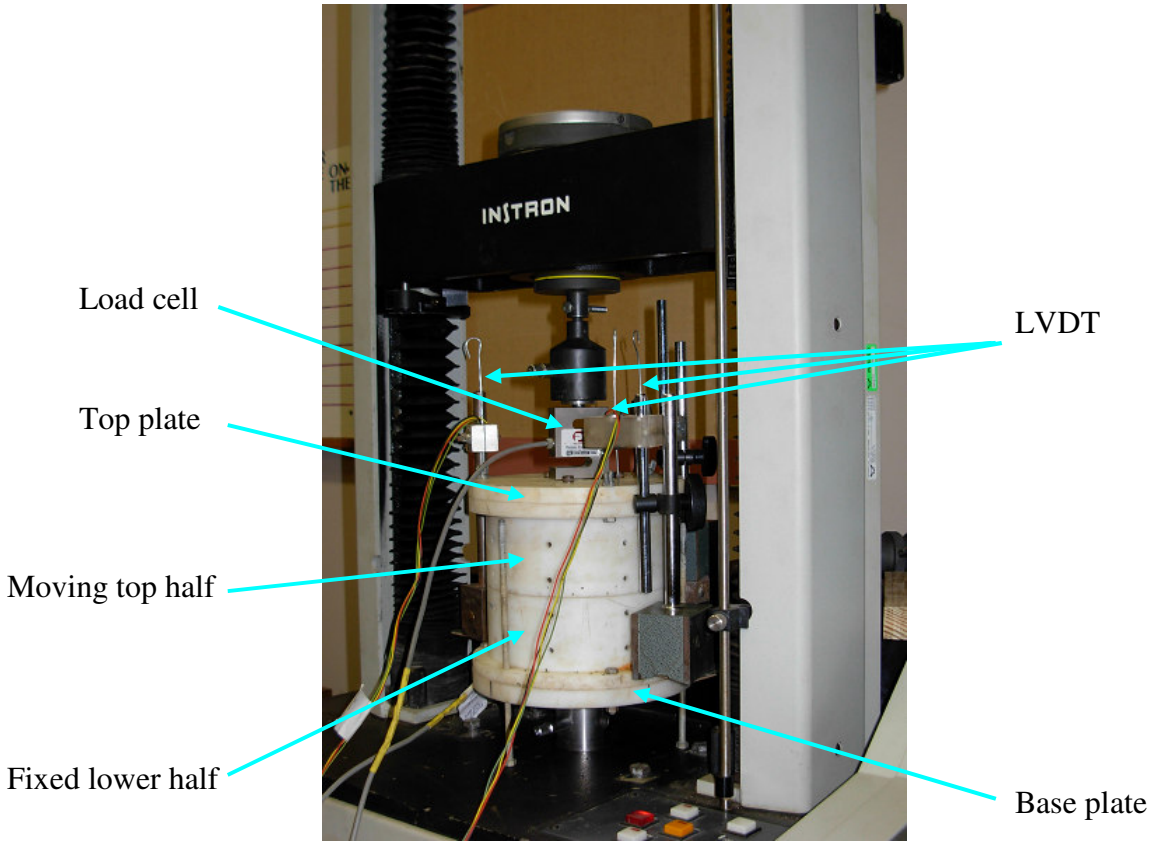

Fig. 4.14(b) Photograph of the uniaxial tensile testing apparatus

Sample preparation

Soil was mixed with chemical stabilisers exactly the same as those described under sample preparation for erosion testing. Once the soil was mixed, a specially made piston was used to statically compact it into five equal layers between the cylinders to the required dry density. Figures 4.15 (a) and (b) show the compaction mould with collar and compaction of the soil with an AVERY compression machine, respectively. The lower part of the mould was kept as a single unit, while the upper part was set up with a collar for compaction. After the soil was compacted to the required height, the top plate was attached to the inner and outer cylinder halves. The specimen was covered with moisture proof bag and kept in a humidity controlled chamber to cure for 7 days. It was then placed in water (the eroding fluid) for saturation. It can be noted that the saturation time was kept the same for both tensile and erosion tests to ensure identical conditions for testing.

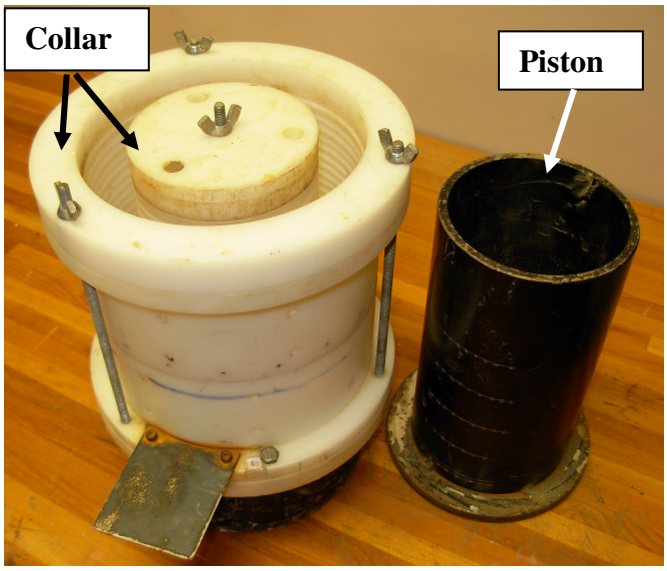

Figure 4.15(a) Compaction mould and piston

Figure 4.15(b) Compaction of soil with AVERY compression machine

Interpretation of observations

The tensile force was calculated based on the force balance of the upper part of the setup. The forces acting on the upper part of the apparatus are described in Figure 4.16.

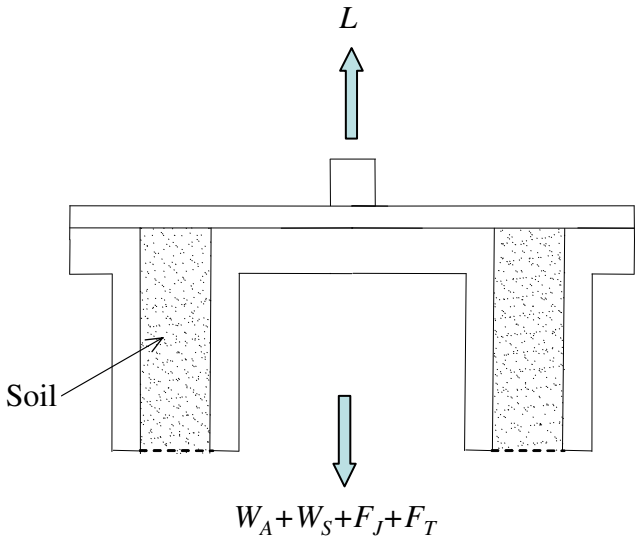

Figure 4.16 Forces acting on the upper half of the apparatus

If the equilibrium of the top part of the apparatus is considered, the tensile force (F_T) acting on the fracture plane can be calculated using Equation 4.16.

$$F_T = L - (W_A + W_S + F_J)$$

$$F_T = L - F_d \qquad (4.16)$$

where, L is the tensile load applied; W_A is the weight of the upper part of the apparatus; W_S is the weight of the soil in the upper part of the apparatus; and F_J is the friction between the surfaces of the cylinder at the joint. For convenience, the sum of forces W_A, W_S and F_J are denoted by F_d. The magnitude of F_d was measured by bringing the upper part of the apparatus and the soil (after failure) to its initial position and then lifting it at the same rate of strain as was applied during tensile testing. Once (F_d) is known, Equation 4.16 can then be used to calculate F_T. Since the objective of the tensile test was to calculate the area under the tensile stress-deformation curve (to validate the erosion model), the tensile stress was plotted against tensile deformation, as described in Figure 4.17. The parameter representing the integral $\int_0^{\delta_{Tf}} \sigma_T \times d\delta_T$ in Equation 3.21 of the erosion model can be determined by calculating the shaded area (Figure 4.17). This area represents the energy required to break inter-particle bonds on a unit surface area of the fracture plane.

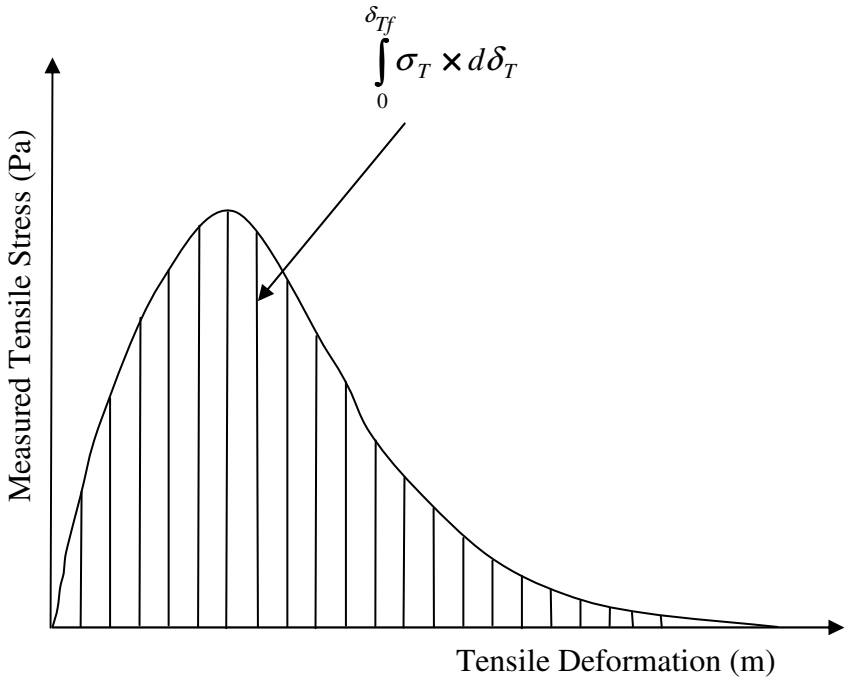

Figure 4.17 Calculation of area under the tensile stress-deformation curve

4.5 Summary

This chapter focused on a detailed experimental program conducted to investigate the erosion and tensile stress-deformation characteristics of chemically treated and untreated erodible soils. The contents of this chapter are summarised below.

- Details of preliminary experimental investigation including the standard compaction tests, pinhole tests, unconfined compression tests, *SCS* dispersion tests and *SEM* tests were outlined.

- A description of the Process Simulation Apparatus for Internal Crack Erosion (*PSAICE*), sample preparation for erosion test, and interpretation of observations were reported.

- A description of the uniaxial tensile testing apparatus, sample preparation for tensile test, and interpretation of observations were then explained.

The results of the experimental investigation will be discussed in the next chapter.

CHAPTER 5

EXPERIMENTAL RESULTS AND DISCUSSION

5.1 Introduction

This chapter primarily discusses the results of an experimental investigation into two different soils treated with lignosulfonate and cement. A brief description of the structure of this chapter is outlined below.

- The results of the preliminary investigation, including standard pinhole tests, standard Proctor compaction tests, unconfined compression tests, Soil Conservation Service (*SCS*) dispersion tests, and Scanning Electron Microscopy tests are discussed, and proved beneficial in the understanding of the stabilisation mechanism, erosional behaviour, and the stress-strain characteristics of treated and untreated erodible soils.

- The results of erosion tests performed using a Process Simulation Apparatus for Internal Crack Erosion (*PSAICE*) on chemically treated and untreated erodible soils are elaborated. An empirical expression for the coefficient of soil erosion was formulated in terms of critical shear stress, and the effects of two different approaches used to calculate the hydraulic shear stress was also discussed.

- The results of tensile tests conducted on chemically treated samples are reported at the end of this chapter.

5.2 Results of Preliminary Investigation

5.2.1 Compaction Characteristics of Erodible Soils

Compaction tests were performed to determine the optimum water content and the maximum dry density of chemically treated and untreated soils. A summary of the test results for silty sand and dispersive clay are given in Tables 5.1 and 5.2, respectively. They show that the effect of lignosulfonate treatment on maximum dry density and optimum water content is negligible, irrespective of the soil type. A similar response was observed for silty sand treated with cement, but the maximum dry density of dispersive clay treated with cement decreases slightly and the optimum water content increases from 22% to 23.3%.

Table 5.1 Maximum dry density and optimum water content for treated and untreated silty sand

Soil (Silty sand)	Amount of chemical (%)	Maximum dry density (kg/m^3)	Optimum water content (%)
Untreated	0.0	1711	10.3
Lignosulfonate treated	0.2	1712	10.4
	0.4	1705	10.2
	0.6	1716	10.4
Cement treated	1.0	1712	10.3
	2.0	1715	10.6
	3.0	1711	10.4

Table 5.2 Maximum dry density and optimum water content for treated and untreated dispersive clay

Soil (Dispersive clay)	Amount of chemical (%)	Maximum dry density (kg/m^3)	Optimum water content (%)
Untreated	0.0	1538	22.0
Lignosulfonate treated	0.2	1536	21.8
	0.4	1536	21.8
	0.6	1534	22.3
Cement treated	0.2	1538	22.0
	0.4	1532	23.0
	0.6	1524	23.3

5.2.2 Stabilisation Mechanism and Its Effect on Stress-Strain Behaviour of Treated Silty Sand

Stress-strain behaviour of treated silty sand

A set of unconfined compression tests and tensile tests were carried out to investigate the mechanical behaviour of treated soils. Figures 5.1(a) and 5.1(b) show the stress-strain behaviour of silty sand treated with lignosulfonate and cement, respectively, under uniaxial compression. An unconfined compression test was not conducted on untreated silty sand because of its low strength.

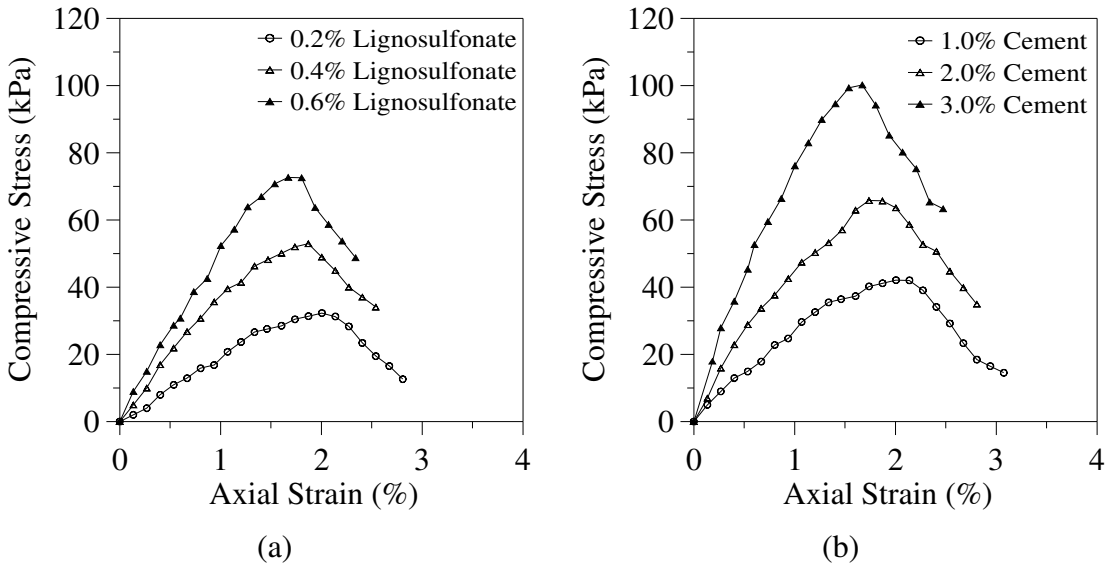

Figure 5.1 Variation of compressive stress with axial strain for (a) lignosulfonate treated (b) cement treated silty sand

Figure 5.1 illustrates that the compressive strength of treated soil increases while the failure strain decreases with the dosage of stabiliser. Since untreated soil is non-cohesive and all treated soils were compacted to the same dry density and kept under the same curing conditions, it could be argued that the only possible cause for an increase in the strength of treated soil with stabiliser dosage was the enhancement of cohesion attributed to cementation.

While complete set of tensile test data will be presented later in this chapter, selected test results are discussed here to endorse the existence of true cohesion (Figure 5.2). As can be seen from Figure 5.2, the tensile strength of treated soil increases with increasing amounts of lignosulfonate and cement, but the displacement at which the maximum tensile stress occurs decreases with the increasing amounts of cement and lignosulfonate. Since treated silty sand samples were prepared under the same dry density and curing condition, the increase in tensile strength was because of improvement in true cohesion through cementation.

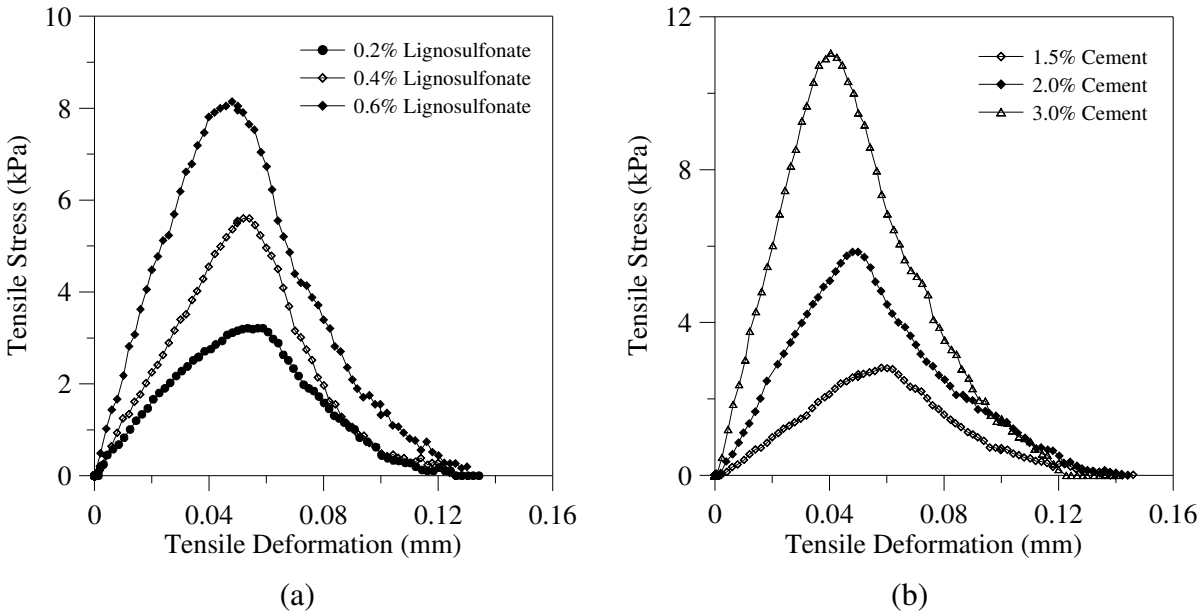

Figure 5.2 Tensile stress-deformation characteristics of (a) lignosulfonate treated (b) cement treated silty sand

To make this point clear, *SEM* tests were conducted on treated and untreated silty sand, and results are discussed below.

SEM tests

A number of digital images were captured using the Scanning Electron Microscopy (*SEM*) to obtain a clear picture of the stabilisation mechanisms of both stabilisers. Figures 5.3, 5.4, and 5.5 show the morphology of untreated, 2% cement treated, and 0.4% lignosulfonate treated soil samples, respectively.

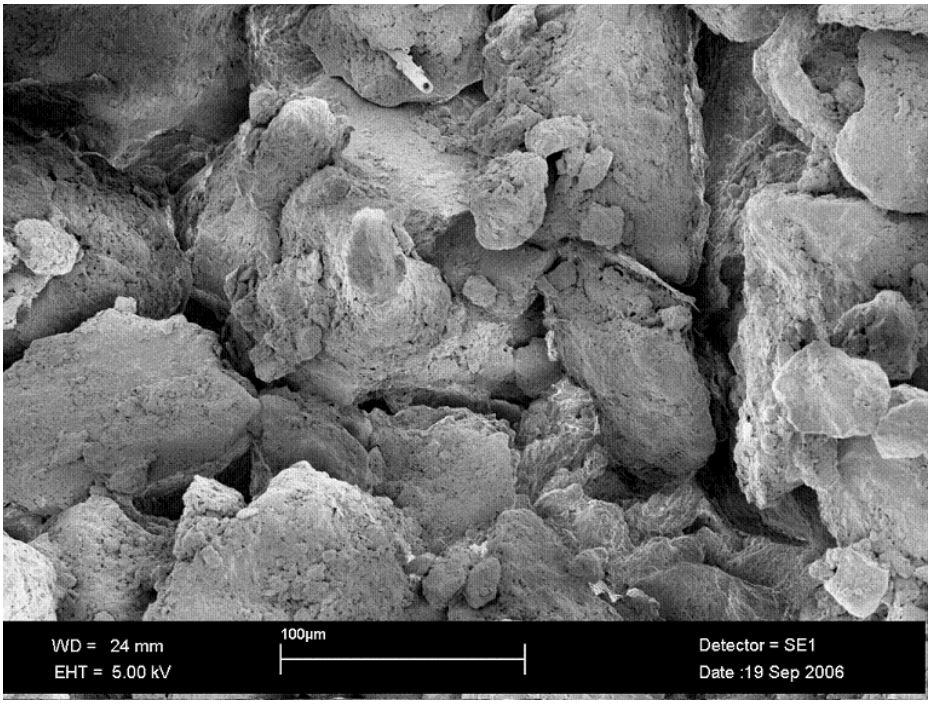

Figure 5.3 Micro features of untreated silty sand

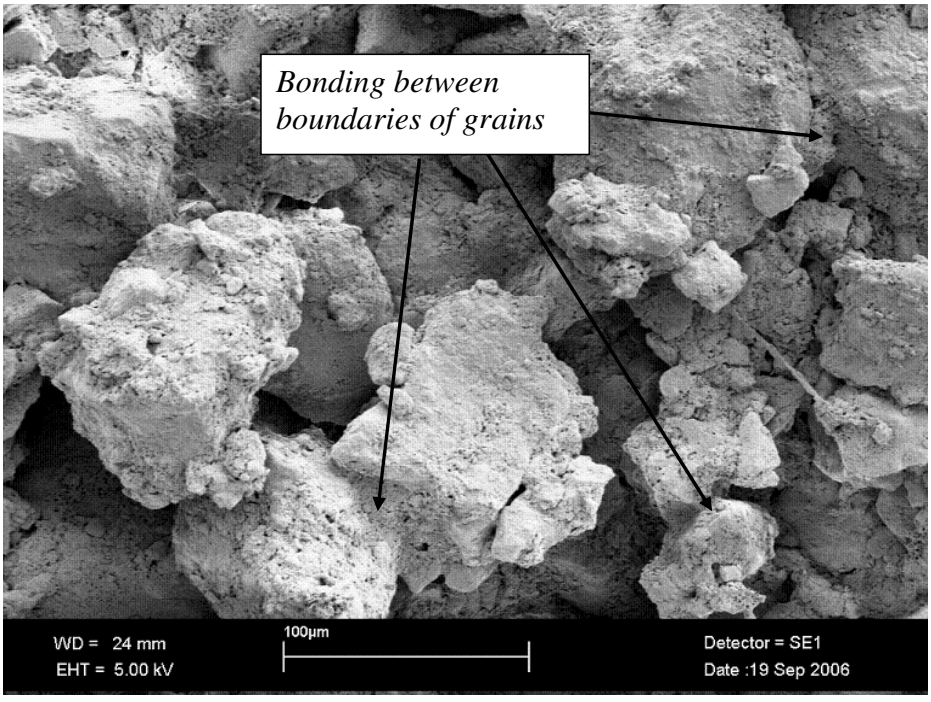

Figure 5.4 Micro features of 2% cement treated silty sand

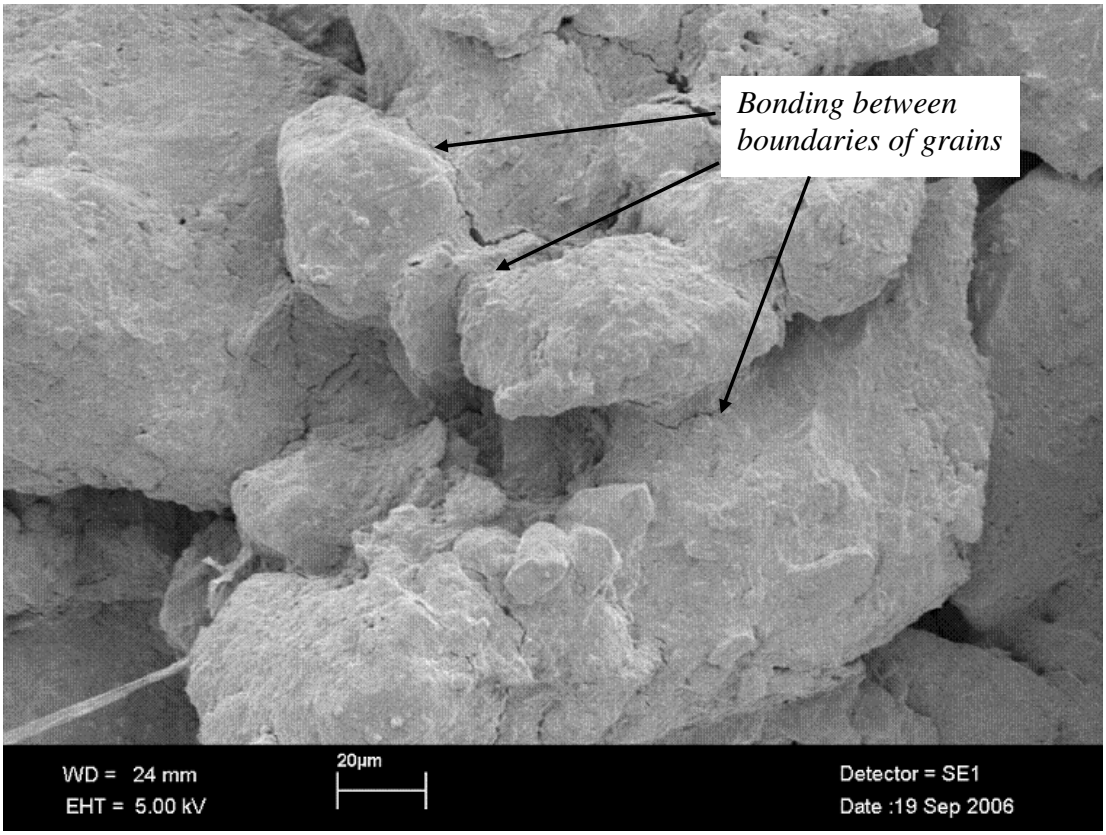

Figure 5.5 Micro features of 0.4% lignosulfonate treated silty sand

As can be seen in Figure 5.3, untreated soil grains are distinctly separate with clear boundaries between them. However, it is evident from Figure 5.4 that particles are bonded with precipitated cementing (bonding) materials. In the case of treatment with lignosulfonate (Figure 5.5), the particles are bonded closely together to produce a stronger soil structure. Based on these observations from the *SEM* photographs, it may be concluded that both stabilisers act as cementing agents to bind the particles together to form erosion resistant surface.

5.2.3 Stabilisation Mechanism and Its Effect on Stress-Strain Behaviour of Treated Dispersive Clay

Stress-strain behaviour of treated and untreated dispersive clay

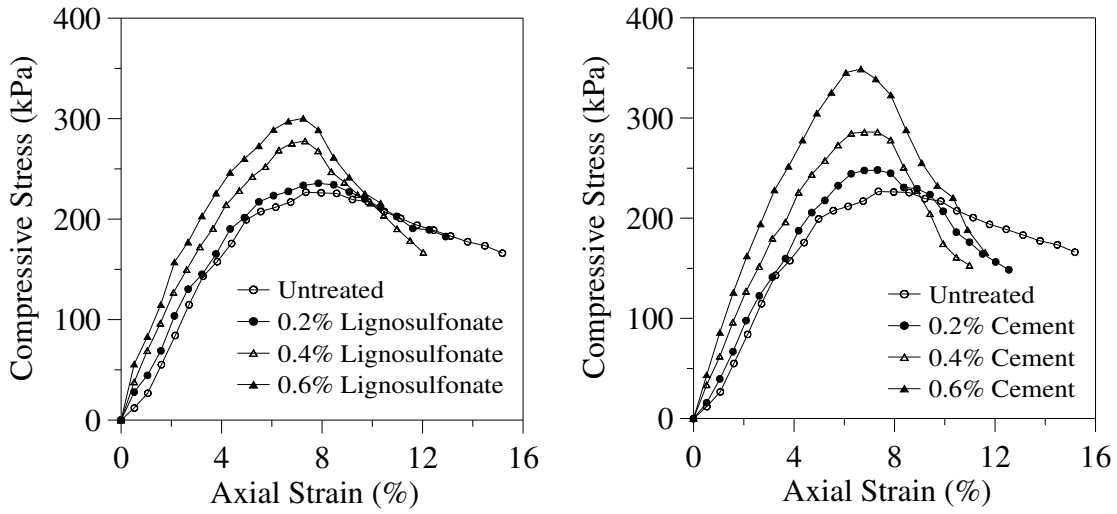

Figure 5.6 Variation of compressive stress with axial strain for (a) lignosulfonate treated and untreated (b) cement treated and untreated dispersive clay

The stress-strain behaviour of chemically treated and untreated dispersive clay is presented in Figure 5.6. As observed for the silty sand, the unconfined compressive strength of dispersive clay increases with dosages of cement and lignosulfonate. An increase in the strength of dispersive clay with 0.6% cement is higher than with 0.6% of lignosulfonate. On the other hand, an addition of 0.6% lignosulfonate to silty sand increases its strength more than the addition of 2% of cement, as discussed earlier (Figure 5.1). If the cement acts as a binder, like lignosulfonate, an increase in the strength of dispersive clay due to an addition of 0.6% cement would be less than

an addition of 0.6% of lignosulfonate. It is obvious that the stabilisation mechanisms of cement on dispersive clay and silty sand are not the same. The cement is known for its cation exchange property which may be responsible for the observed increase in the strength of dispersive clay. To ensure that the stabilisation mechanism of cement on dispersive clay is cation exchange, a set of *SCS* dispersion tests were conducted on cement treated and untreated dispersive clay.

SCS dispersion tests

The test results are given in Table 5.3 and show that the "percent dispersion" dropped significantly with the addition of 0.6% cement. Since the "percent dispersion" is a measure of de-flocculated clays in suspension, its reduction with cement treatment indicates the flocculation and settlement of clay. The dispersed clay particles in suspension settled because of flocculation through cation exchange induced by the cement.

Table 5.3 Percent dispersion of cement treated and untreated dispersive clay

Amount of cement (%)	Percent dispersion (%)
0.0	64
0.2	51
0.4	19
0.6	8

It can now be concluded that adding cement increases the strength of dispersive clay through cation exchange, leading to an increase in the strength of the inter-particle bond which subsequently enhances the unconfined compressive strength. However, lignosulfonate improves the strength of the dispersive clay with its binding capacity. It is therefore clear that altering the

clay structure through cation exchange is more effective than binding the clay particles with lignosulfonate.

5.2.4 The Results of Standard Pinhole Tests

The effect of chemical stabilisation on the erosion characteristics of soil was studied using the Standard Pinhole Apparatus. Tests were performed on samples compacted to 95% of the maximum dry density and the optimum water content (after 7 days of curing). Distilled water was used for testing. Although a quantitative prediction of erosion rate was not possible, this test was useful for identifying suitable chemical dosages for further testing in the *PSAICE*. A summary of the test results of silty sand and dispersive clay are given in Tables 5.4 and 5.5, respectively.

Table 5.4 Effect of chemical treatment on the erosion characteristics of silty sand

Soil	Amount of chemical (%)	Classification
Untreated	0.0	D1
Lignosulfonate treated	0.2	ND3
	0.4	ND2
	0.6	ND1
Cement treated	1.0	ND3
	2.0	ND2
	3.0	ND1

Scale: *D1* — *D2* | *ND4* — *ND3* | *ND2* — *ND1*

Dispersive | *Intermediate* | *Non Dispersive*

Table 5.5 Effect of chemical treatment on the erosion characteristics of dispersive clay

Soil	Amount of chemical (%)	Classification
Untreated	0.0	D2
Lignosulfonate treated	0.2	ND4
	0.4	ND3
	0.6	ND2
	0.8	ND2
Cement treated	0.2	ND4
	0.4	ND2
	0.6	ND1

Scale: *D1* — *D2* | *ND4* — *ND3* | *ND2* — *ND1*
Dispersive | *Intermediate* | *Non Dispersive*

Table 5.4 shows that the erosion resistance of silty sand increases with the amount of lignosulfonate and cement stabilisers. The amount of lignosulfonate and cement required to make silty sand non-erodible are 0.6% and 3.0%, respectively. As shown in Table 5.5, dispersive clay became non-erodible with the addition of 0.6% cement, however, lignosulfonate does not make it completely non-erodible. The Table 5.5 also shows that increasing the amount of lignosulfonate beyond 0.6% makes no significant difference to the erosional behaviour of this dispersive clay.

5.3 Results of Erosion Tests

Using the *PSAICE* to conduct the tests, the objective was to investigate the erosion of soil in an internal crack, such as those in earth dams. Predicted erosion rate and hydraulic shear stress were

used to calculate the erosion parameters, namely, the critical shear stress and the coefficient of soil erosion. The definitions of some important terms used in this study are outlined below.

The critical shear stress, τ_c, is the minimum hydraulic shear stress necessary to initiate erosion. The variation of the erosion rate with the hydraulic shear stress is linear, as illustrated in Figure 3.4 in Chapter 3. The critical shear stress will therefore be determined by extrapolating the straight line to the zero erosion rate. The slope of this straight line is presumed to be the coefficient of soil erosion. Moreover, the difference between the hydraulic shear stress (τ_a) and the critical shear stress is defined as excess hydraulic shear stress ($\Delta\tau = \tau_a - \tau_c$), the magnitude of which is of major importance for causing erosion.

5.3.1 Erosional Behaviour of Chemically Treated and Untreated Silty Sand

A number of rapid erosion tests under high excess hydraulic shear stress over a short period of time have been performed on samples of chemically stabilised and untreated silty sand. All the tests were conducted on samples compacted at the optimum water content and compaction ratios of 95% and 90% of the maximum dry density. For comparison, a series of tests with a smaller excess hydraulic shear stress were also conducted over a longer period of time. As discussed in Chapter 4, the friction factor method and hydraulic gradient method were used to calculate the hydraulic shear stress, and their accuracy was then compared. It is important to note that the predicted erosion rate was independent of these two approaches.

5.3.1.1 Friction factor method

Figure 5.7 shows the crack after an erosion test on 0.2% lignosulfonate treated soil compacted to 95% of the maximum dry density to be approximately circular.

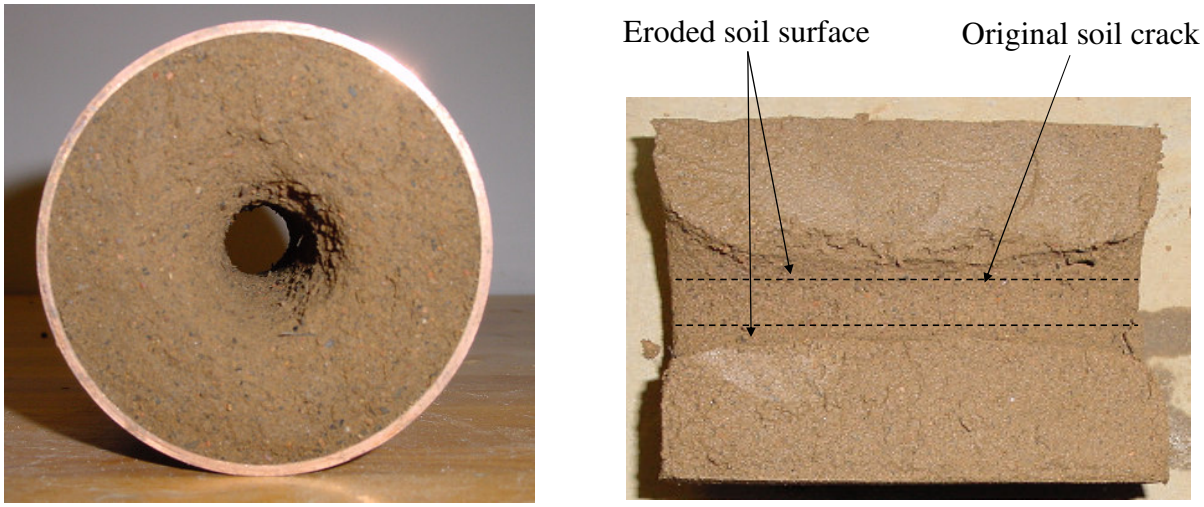

Figure 5.7 Eroded soil crack after a test on 0.2% lignosulfonate treated silty sand compacted at 95% maximum dry density (a) Cross section (b) Longitudinal section

As described in Chapter 4, the observations were analysed to calculate the erosion rate and the hydraulic shear stress applied on the surface of the crack. Figure 5.8 (a) and (b) illustrate the variation of hydraulic shear stress and erosion rate with time, for a rapid erosion test on a sample treated with 0.2% lignosulfonate and compacted to 95% of its maximum dry density.

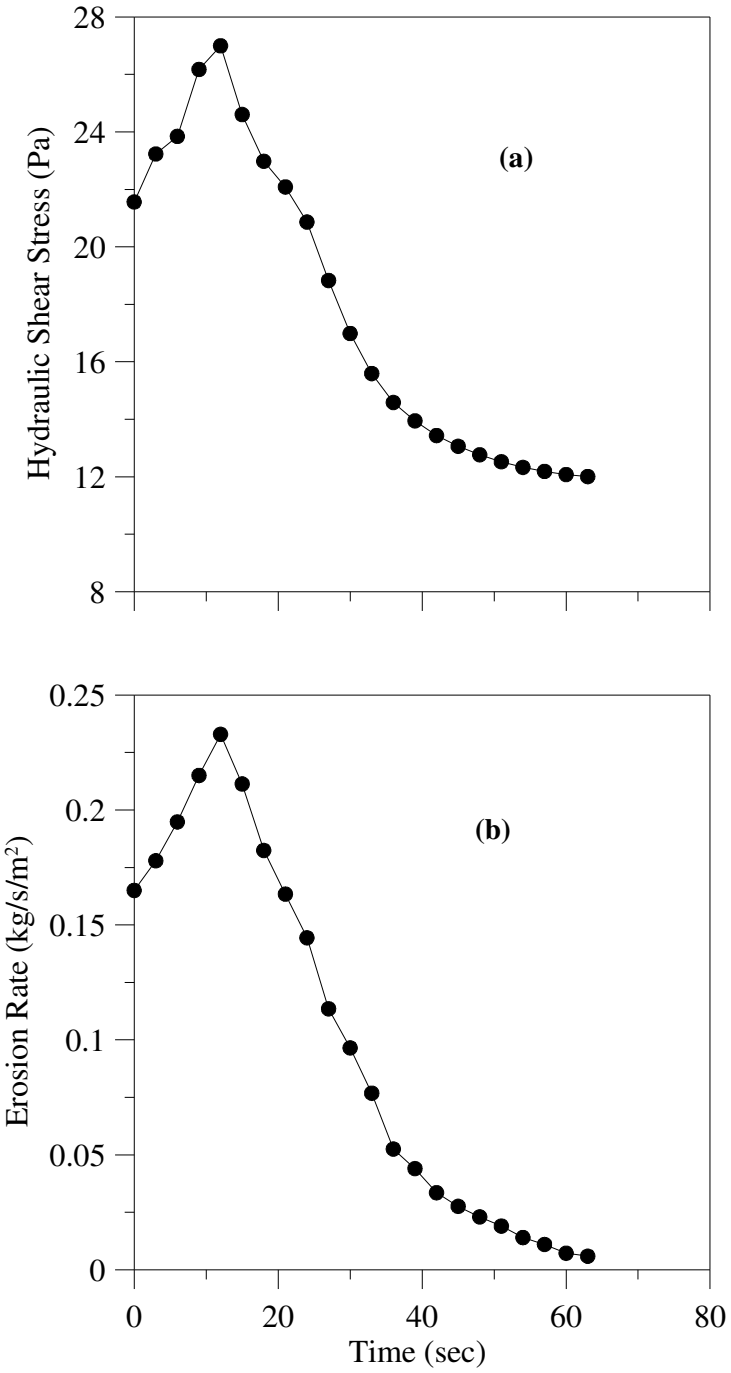

Figure 5.8 Variation of (a) hydraulic shear stress, and (b) erosion rate with time for silty sand treated with 0.2% lignosulfonate at 95% relative compaction (Rapid erosion)

As shown in Figure 5.8(a), the hydraulic shear stress increases for sometime and then decreases as erosion progresses. This variation in the hydraulic shear stress reflects on the erosion rate, as illustrated in Figure 5.8(b). To calculate the soil erosion parameters, the erosion rates and hydraulic shear stresses are plotted against each other as shown in Figure 5.9, where the erosion rate increases almost linearly with the hydraulic shear stress. A similar behaviour has also been reported by other researchers (Arulananthan *et al.* 1975; Sargunan 1977; Shaikh *et al.* 1988). The predicted critical shear stress and coefficient of soil erosion were 11.0 Pa and 0.0148 sm^{-1}, respectively.

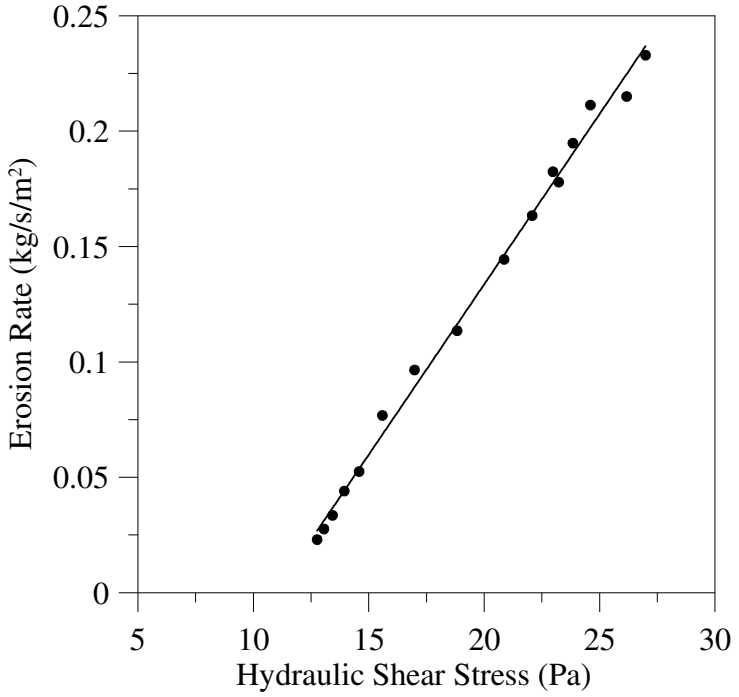

Figure 5.9 Erosion rate versus hydraulic shear stress for silty sand treated with 0.2% lignosulfonate at 95% relative compaction (Rapid erosion)

As illustrated in Figure 5.9, the excess hydraulic shear stress ($\Delta\tau$) applied to the surface of the crack is very high, and therefore a test at low excess hydraulic shear stress over a longer

period (Gradual erosion) was also conducted, and its effect on the prediction of erosion parameters was examined. For comparison, the variation of erosion rate and hydraulic shear stress with time, predicted from the gradual erosion, is plotted alongside that from the rapid erosion, as shown in Figure 5.10.

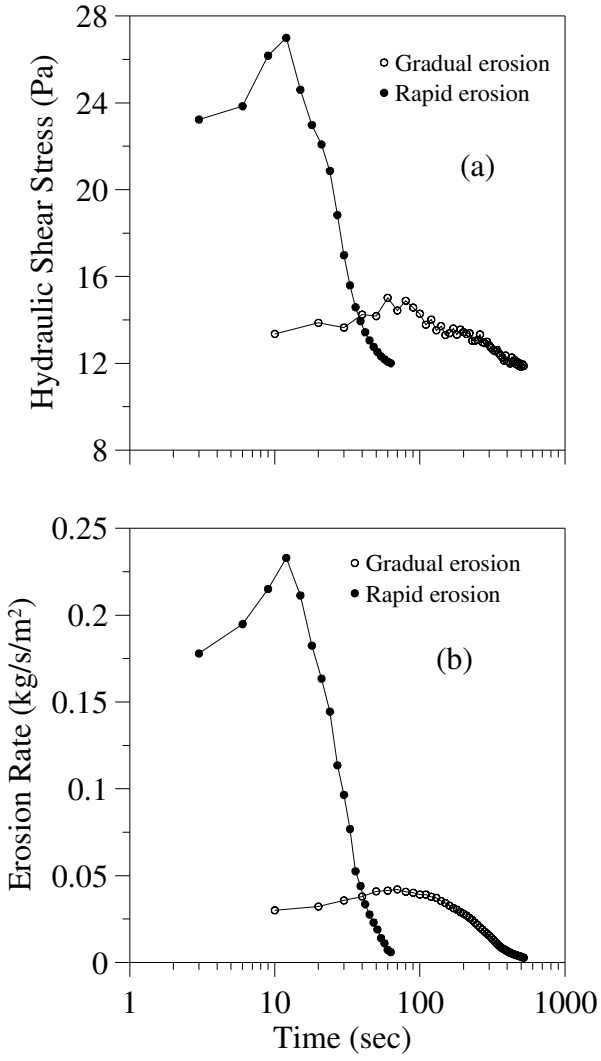

Figure 5.10 Variation of (a) hydraulic shear stress, and (b) erosion rate with time for silty sand treated with 0.2% lignosulfonate at 95% relative compaction (Gradual and Rapid erosion)

Figure 5.10 shows that the erosion rate predicted from the rapid erosion test is higher than that from the gradual erosion test. It shows that the greater the magnitude of $\Delta\tau$, the higher the erosion rate, and vice versa. For both types of tests, the erosion rate was plotted against the hydraulic shear stress, as shown in Figure 5.11, which shows that the gradients of the best fit lines for both sets of erosion data are almost similar. This indicates that the coefficient of soil erosion remains relatively constant irrespective of the magnitude of excess hydraulic shear stress.

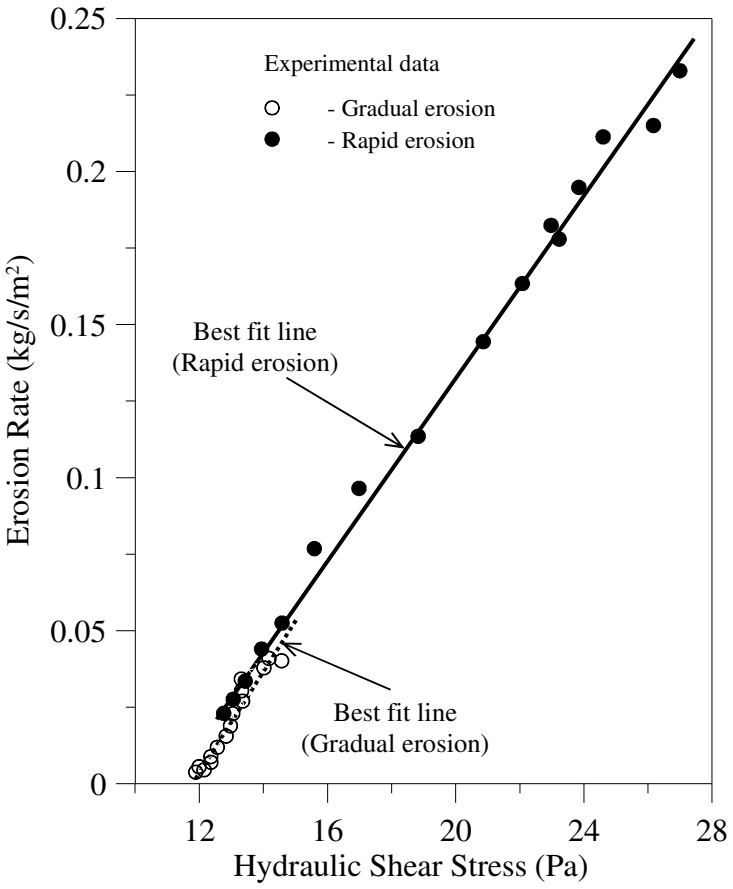

Figure 5.11 Erosion rate versus hydraulic shear stress for silty sand treated with 0.2% lignosulfonate at 95% relative compaction (Gradual and Rapid erosion)

The critical shear stress and coefficient of soil erosion calculated from the rapid erosion test were 11.0 Pa and 0.0148 sm^{-1}, respectively, while the gradual erosion test produced almost the same values of 11.7 Pa and 0.0152 sm^{-1}, respectively. Accordingly, this comparison proves that short term erosion under a high $\Delta\tau$ can be related to a longer period of erosion by a reduced $\Delta\tau$ via the constant coefficient of soil erosion. The erosion parameters obtained from the gradual and rapid erosion tests on selected soil samples are summarised in Table 5.6 for comparison.

Table 5.6 Calculated erosion parameters based on gradual and rapid erosion tests

Amount of Lignosulfonate (%)	Critical shear stress (Pa)		Coefficient of soil erosion (sm^{-1})	
	Rapid	Gradual	Rapid	Gradual
0.2	11.0	11.7	0.0148	0.0152
0.4	25.3	23.6	0.0064	0.0052
0.6	35.0	34.9	0.0031	0.0028

It is clear from the values given in Table 5.6 that the predicted erosion parameters are almost the same irrespective of the type of test. In the light of this observation, it was decided to conduct the rest of the testing program under rapid erosion conditions, because the volume of eroding fluid necessary for gradual erosion test was very high compared to the rapid erosion test. Hereafter, this chapter discusses only the results of the rapid erosion test.

Effect of chemical treatment

To illustrate the effect of lignosulfonate and cement stabilisation on the critical shear stress and the coefficient of soil erosion, the erosion rate against the hydraulic shear stress for all treated and untreated specimens are plotted on the same graph. Figures 5.12 and 5.13 indicate the variation of

the erosion rate with the hydraulic shear stress for two chemical stabilisers (compacted at 95% relative density).

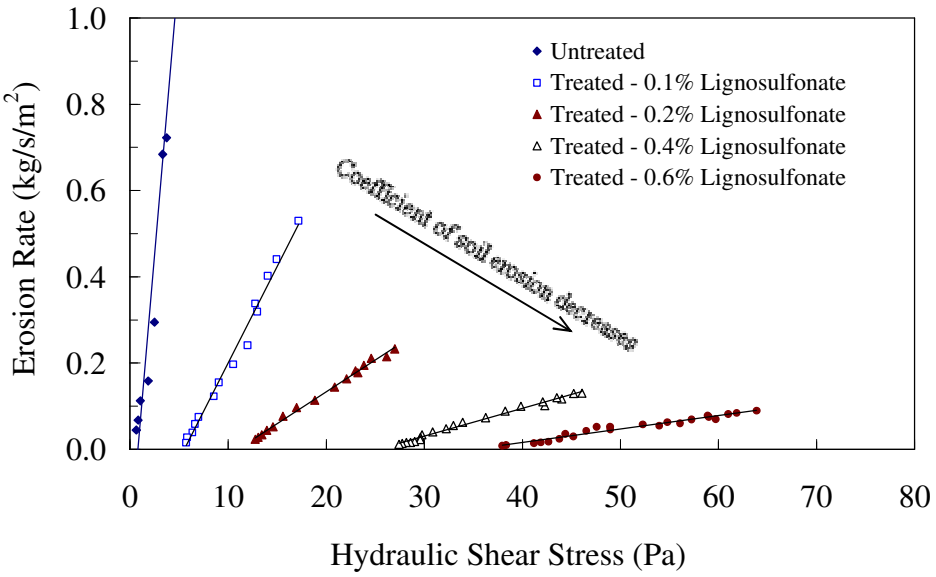

Figure 5.12 Erosion rate against hydraulic shear stress for lignosulfonate treated and untreated silty sand compacted at 95% of the maximum dry density (Friction factor method)

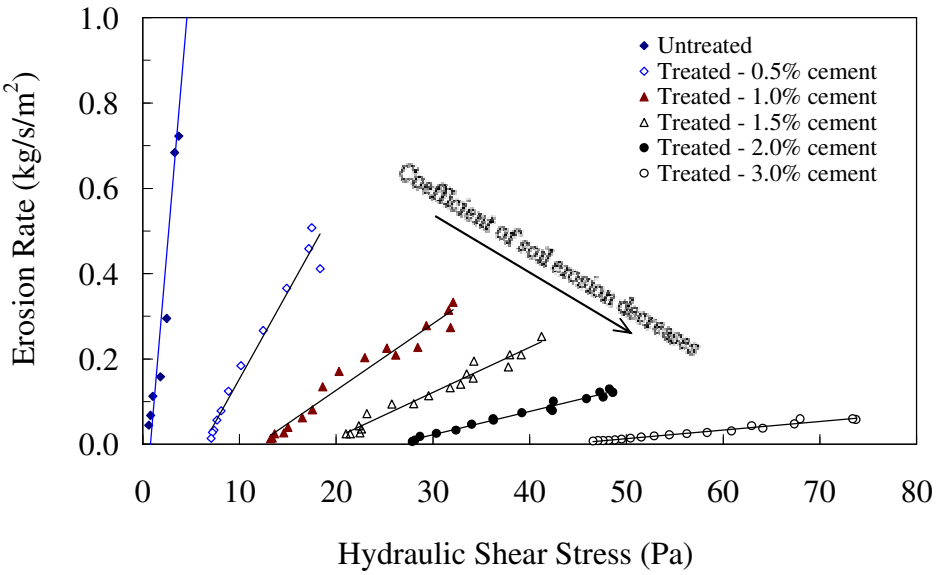

Figure 5.13 Erosion rate against hydraulic shear stress for cement treated and untreated silty sand compacted at 95% of the maximum dry density (Friction factor method)

It is evident from Figures 5.12 and 5.13 that the relationship between the erosion rate and hydraulic shear stress is linear, and the slope of the lines represents the coefficient of soil erosion. With increased levels of chemical additives, the coefficient of soil erosion decreases, as expected. It is noted that the critical shear stress also increases with the amount of chemical additives. Since untreated silty sand is non-cohesive and all treated and untreated soils were compacted to the same dry density and kept under the same curing conditions, it could be argued that the only possible cause for an increase in the erosion resistance of treated soil compared to untreated soil was the enhancement of cohesion attributed to cementation, as described earlier in this chapter.

When the dosage of cement is increased to 3%, the critical shear stress increases from 0.8 Pa to 43.4 Pa, and the coefficient of soil erosion decreases by 130 times that of the untreated soil. A similar response was observed for samples treated with lignosulfonate, but it is interesting to note that the coefficient of soil erosion drops from 0.265 sm^{-1} to 0.003 sm^{-1} even with the addition of 0.6% lignosulfonate. Moreover, the increment in the critical shear stress with 0.6% lignosulfonate treatment is equivalent to that with around 2.5% cement treatment. Hence, it can be concluded that significantly less lignosulfonate than cement is sufficient to achieve a given increase in erosion resistance.

Effect of degree of compaction

To investigate the effect of degree of compaction on the erosion characteristics of silty sand, the erosion rate was plotted against the hydraulic shear stress for lignosulfonate treated and cement treated soil samples compacted at 90% as shown in Figures 5.14 and 5.15, respectively.

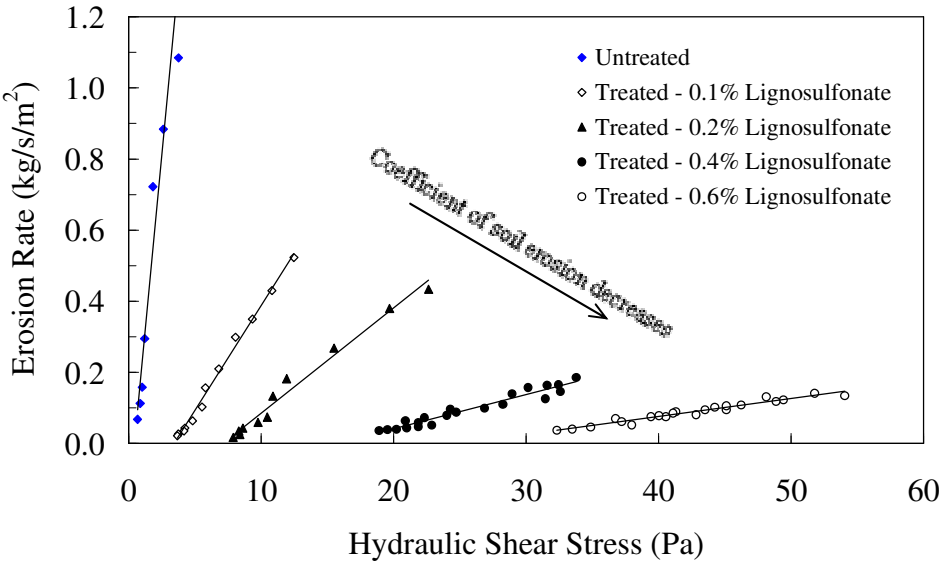

Figure 5.14 Erosion rate against hydraulic shear stress for lignosulfonate treated and untreated silty sand compacted at 90% of the maximum dry density (Friction factor method)

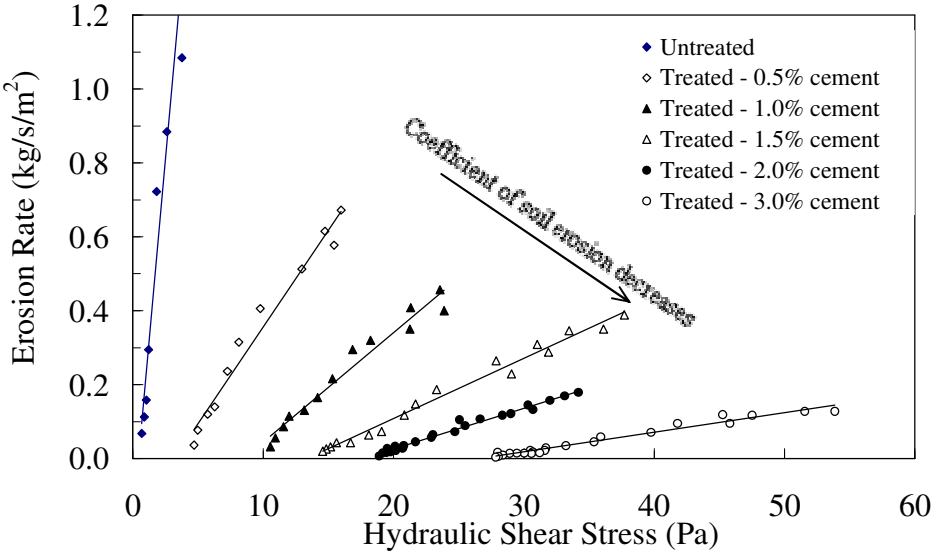

Figure 5.15 Erosion rate against hydraulic shear stress for cement treated and untreated silty sand compacted at 90% of the maximum dry density (Friction factor method)

For 90% compacted samples, the critical shear stress increases with the amount of stabilisers, while coefficient of soil erosion decreases, as illustrated in Figures 5.14 and 5.15. This is similar to the trend observed for 95% compacted samples. Moreover, for a given chemical dosage, the coefficient of soil erosion of a soil compacted to 90% is higher than a soil compacted to 95%, while the critical shear stress for the former is smaller than the latter. To clarify this point further, the variation of the critical shear stress with the amount of stabilisers for soils compacted to 90% and 95% are shown in Figures 5.16 and 5.17 for both chemicals.

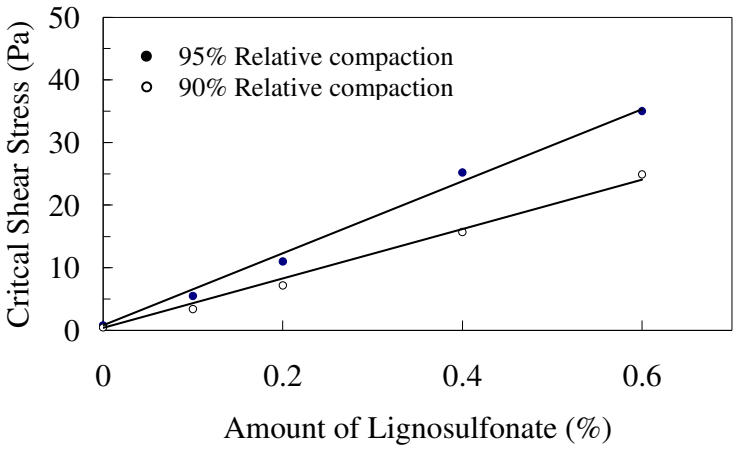

Figure 5.16 Variation of critical shear stress with quantity of lignosulfonate

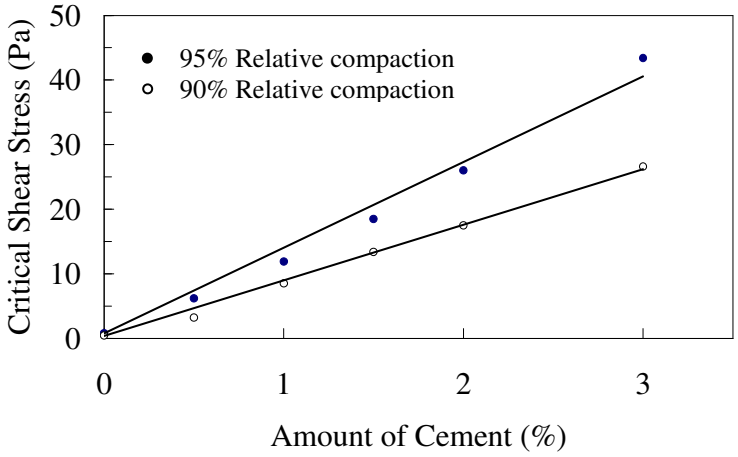

Figure 5.17 Variation of critical shear stress with quantity of cement

As shown in Figure 5.16 and 5.17, the critical shear stress changes linearly with the stabiliser dosage of both lignosulfonate and cement. It is also clear that significantly less lignosulfonate than cement is sufficient to attain a certain increase in the critical shear stress. In addition, the difference between the critical shear stress of soil compacted to 95% and 90% shows a continuously increasing trend as the amounts of lignosulfonate and cement increase. As expected, the degree of inter-particle bonds in a 90% compacted state is less than in a 95% compacted state because of the closer packing of the latter.

5.3.1.2 Hydraulic gradient method

This method predicts the hydraulic shear stress based on the difference in pressure measured across the crack. A similar approach was used by other investigators (Wan and Fell 2004; Lim 2006) to calculate the hydraulic shear stress. This method does not make any difference in the prediction of erosion rate, which was carried out by a unique approach adopted in this study, as discussed in Chapter 4.

For comparison, the hydraulic shear stress calculated from the gradient method was used to predict the critical shear stress for soil treated with 0.2% lignosulfonate and compacted at 95% of the maximum dry density (Figure 5.18). It was found that the critical shear stress predicted using the hydraulic gradient method was around 53.2 Pa, but it was 11.0 Pa using the friction factor method, which means the hydraulic gradient method overestimates the critical shear stress. The hydraulic gradient method determines the hydraulic shear stress based on the drop in pressure across the crack, which includes entry losses in the applied head. Consequently, the predicted critical shear stress is higher. However, the friction factor method is based solely on the velocity

of the flow through the crack, which can be measured accurately, and is therefore more accurate than the hydraulic gradient method.

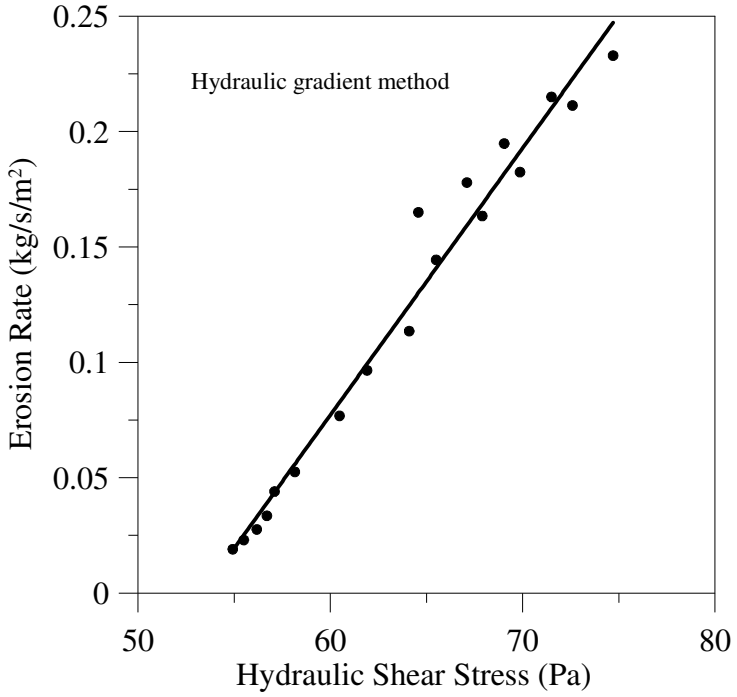

Figure 5.18 Erosion rate versus hydraulic shear stress for silty sand treated with 0.2% lignosulfonate (Hydraulic gradient method)

To understand the application of hydraulic gradient method for comparing the erosion characteristics of treated and untreated silty sand, the variation of the erosion rate with the hydraulic shear stress is plotted in Figures 5.19 and 5.20 for both stabilisers. As illustrated in these figures, the critical shear stress increases with the chemical dosage, while the coefficient of soil erosion decreases. It is therefore clear that even though the hydraulic gradient method predicts the erosion parameters with less accuracy, it still yields the same trend observed using the friction factor method. This method is quick and simple compared to the friction factor method, because the latter requires the particle size distribution of eroded soil, which must be determined through an additional test, as described in Chapter 4 and Appendix A. Hence, it can

still be used for a comparison between the erosion characteristics of treated and untreated soil, but not for obtaining an accurate prediction of the values of erosion parameters.

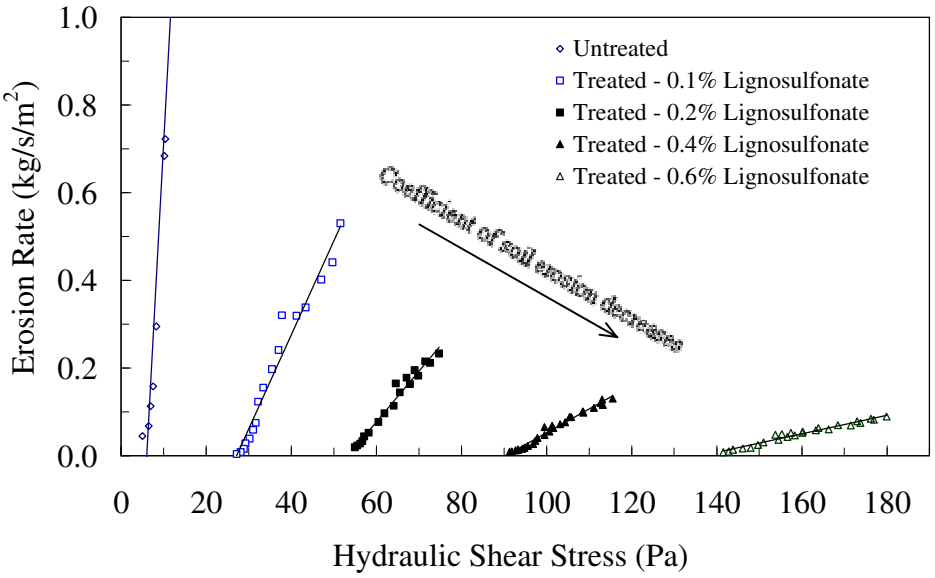

Figure 5.19 Erosion rate versus hydraulic shear stress for lignosulfonate treated and untreated silty sand compacted at 95% of the maximum dry density (Hydraulic gradient method)

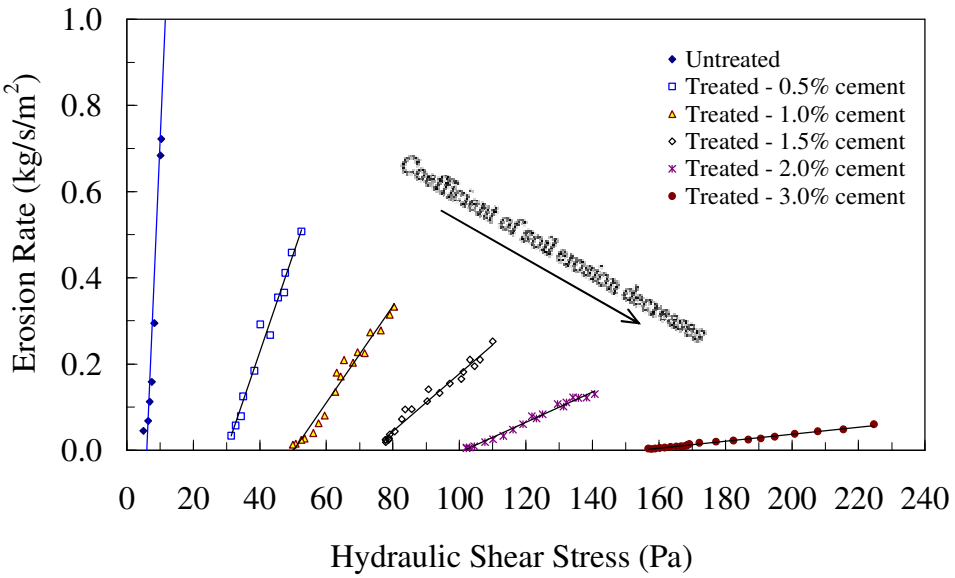

Figure 5.20 Erosion rate versus hydraulic shear stress for cement treated and untreated silty sand compacted at 95% of the maximum dry density (Hydraulic gradient method)

5.3.1.3 Development of an empirical model to predict the erosion rate of treated silty sand

To determine a simple expression for estimating the erosion rate of stabilised soils, an attempt was made to develop an empirical relationship between the critical shear stress and the coefficient of soil erosion. It was found that all data points for treated soils fall on a best fit line following a power function as shown in Figure 5.21, and the corresponding empirical expression for the erosion rate of chemically treated soils was determined by:

$$\dot{\varepsilon} = \frac{a}{\tau_c^b}[\tau_a - \tau_c] \tag{5.1}$$

where, $\dot{\varepsilon}$ (kg/s/m^2) is the erosion rate; τ_a (Pa) is the hydraulic shear stress; and τ_c (Pa) is the critical shear stress; *a* and *b* are constants. Values of *a* and *b* are given in Table 5.7.

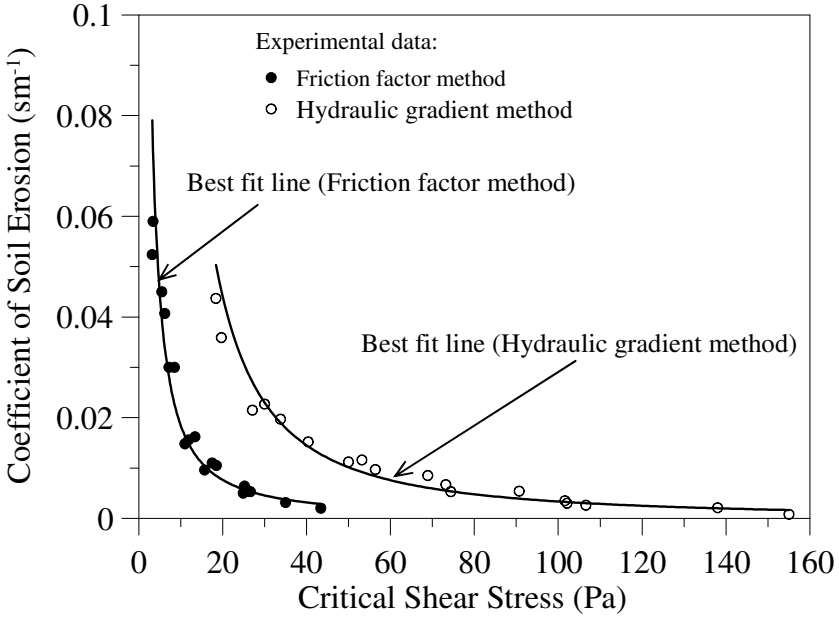

Figure 5.21 Variation of coefficient of soil erosion with critical shear stress for treated silty sand compacted at 95% and 90% of the maximum dry density

Table 5.7 Values of constants *a* and *b* to predict the erosion rate of treated silty sand

Method of analysis	*a*	*b*
Friction factor method	0.35	1.28
Hydraulic gradient method	5.6	1.61

To derive an expression for the critical shear stress of treated soils, the variation of the critical shear stress with the amount of lignosulfonate and cement is plotted in Figures 5.22 and 5.23 for both methods of analyses. Since the critical shear stress (τ_c) changes linearly with the amount of stabiliser, τ_c can be expressed by:

$$\tau_c = \tau_{c0} + m(CP) \tag{5.2}$$

where, τ_{c0} (Pa) is the critical shear stress of untreated soil; m is the proportionality coefficient as tabulated in Table 5.8; and *CP* (%) is the amount of chemical additives.

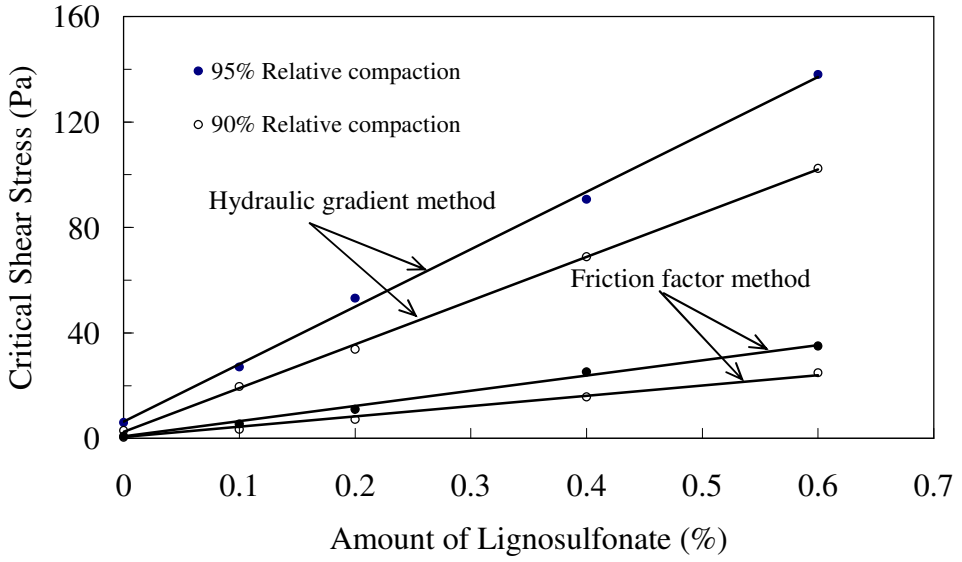

Figure 5.22 Variation of the critical shear stress with the amount of lignosulfonate

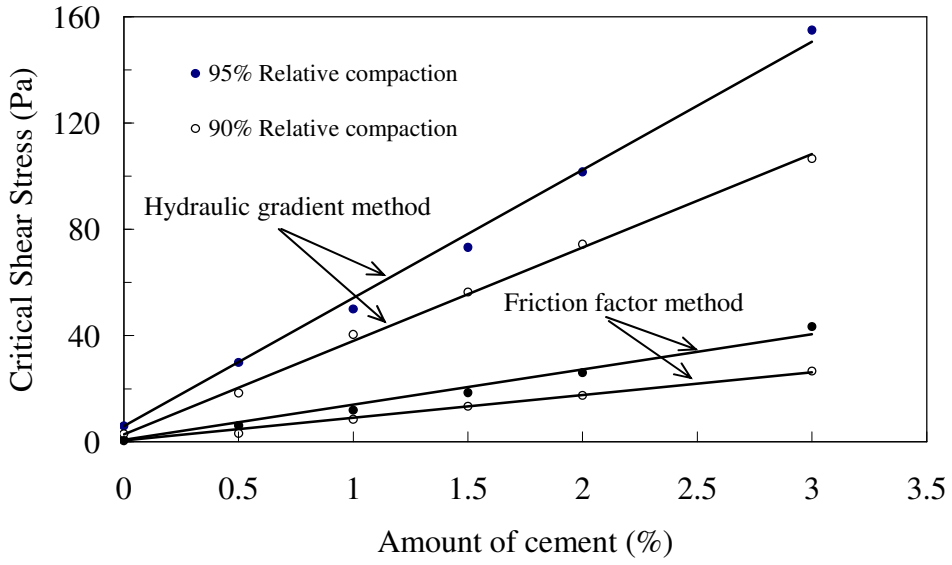

Figure 5.23 Variation of the critical shear stress with the amount of cement

Table 5.8 Proportionality coefficient (m) to determine the erosion rate of treated silty sand

Type of stabiliser	Degree of compaction (%)	Friction factor method		Hydraulic gradient method	
		(m)	(τ_{c0})	(m)	(τ_{c0})
Lignosulfonate	95	57.5	0.8	217.8	6.0
	90	39.2	0.5	166.0	2.8
Cement	95	13.2	0.8	48.2	6.0
	90	8.5	0.5	35.2	2.8

5.3.2 Erosional Behaviour of Chemically Treated and Untreated Dispersive Clay

A series of erosion tests on treated and untreated dispersive clay were performed to examine the effect of chemical stabilisation on erodibility. In addition, the effect of moulding water content

and degree of compaction on the erosion characteristics of the soil was also investigated. It is found from the results that the variation of erosion rate with the hydraulic shear stress for all treated and untreated samples of dispersive clay is linear as observed for this silty sand. The results are discussed in detail below.

5.3.2.1 Friction factor method

Effect of moulding water content and degree of compaction on the erodibility of untreated dispersive clay

In general, the moulding water content and the degree of compaction affect the erosional behaviour of compacted clayey soil significantly (e.g. Arulananthan *et al.* 1974, Wan and Fell 2004). In this study, their influence on the erosion characteristics of compacted untreated dispersive clay under saturated conditions was explored. Tests were performed on three different moulding water contents, wet of optimum (optimum + 2.5%), optimum, and dry of optimum (optimum - 2.5%), and two different compacted densities (95% and 90% of the maximum dry density).

As described in Figures 5.24 (a) and (b), the critical shear stress increases while the coefficient of soil erosion decreases with an increase in the moulding water content for a given degree of compaction. For soil compacted at 95% of the maximum dry density, the critical shear stress increases from 1.3 Pa to 4.1 Pa and the coefficient of soil erosion decreases from 0.093 to 0.013, when the water content changes from dry of optimum to wet of optimum. It can also be observed that a change in the erosion parameters is significant when the water content changes from dry of optimum to the optimum moisture content. However, there was no significant difference when the water content changes from the optimum to the wet of optimum. The

difference in the erosion resistance of untreated dispersive clay prepared at different moulding water contents can be explained based on the swelling characteristics. Dispersive clay compacted at dry of optimum swelled significantly during saturation and lost its strength drastically, leading to a decrease in the erosion resistance. On the other hand, the swelling was less for soil compacted at the optimum and wet of optimum, and so the reduction in the erosion resistance was less. When considering the effect of degree of compaction on erosion, the critical shear stress decreases as the degree of compaction changes from 95% to 90% of the maximum dry density for a given water content. It can therefore be concluded that both the moulding water content and degree of compaction affect the erodibility of untreated dispersive clay. Since erodibility of the soil changed significantly when the water content changed from dry of optimum to the optimum, only these two were selected for further study on treated soil samples.

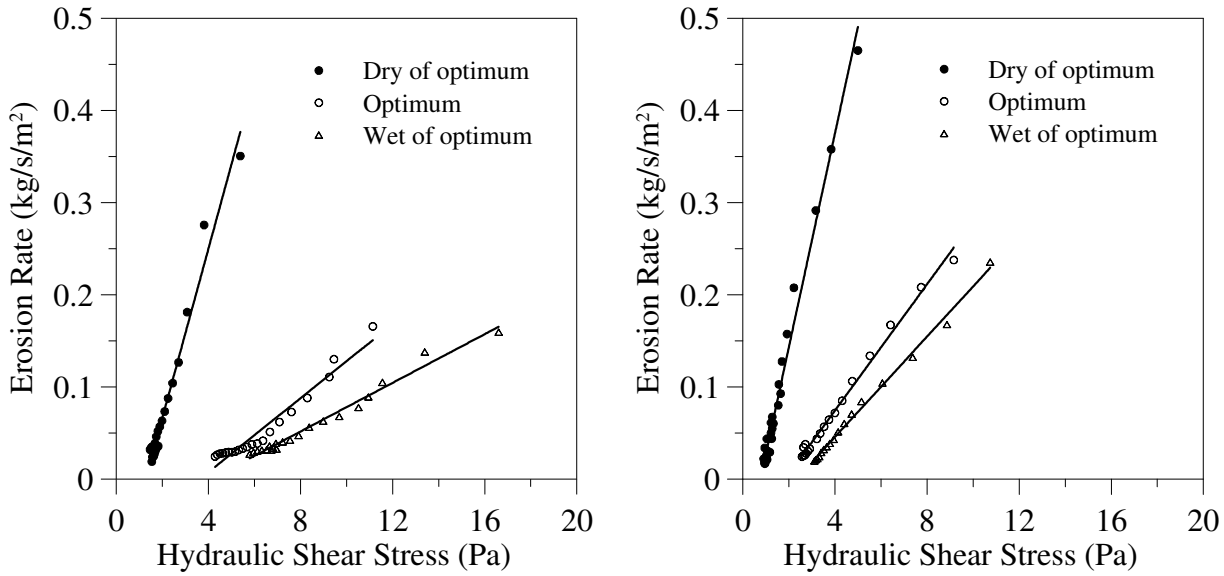

Figure 5.24 Erosion rate versus hydraulic shear stress for untreated dispersive clay compacted at (a) 95% and (b) 90% of the maximum dry density (at different moulding water contents)

Effect of chemical treatment, degree of compaction and water content on the erodibility of treated dispersive clay

To demonstrate the effect of chemical treatment, the erosion rate against the hydraulic shear stress is plotted for lignosulfonate and cement treated dispersive clay (compacted at 95% of the maximum dry density and the optimum water content) as shown in Figures 5.25 (a) and (b), respectively. There were similar responses for all samples compacted to 90% of the maximum dry density at the optimum water content, and 95% & 90% of the maximum dry density on the dry side of the optimum.

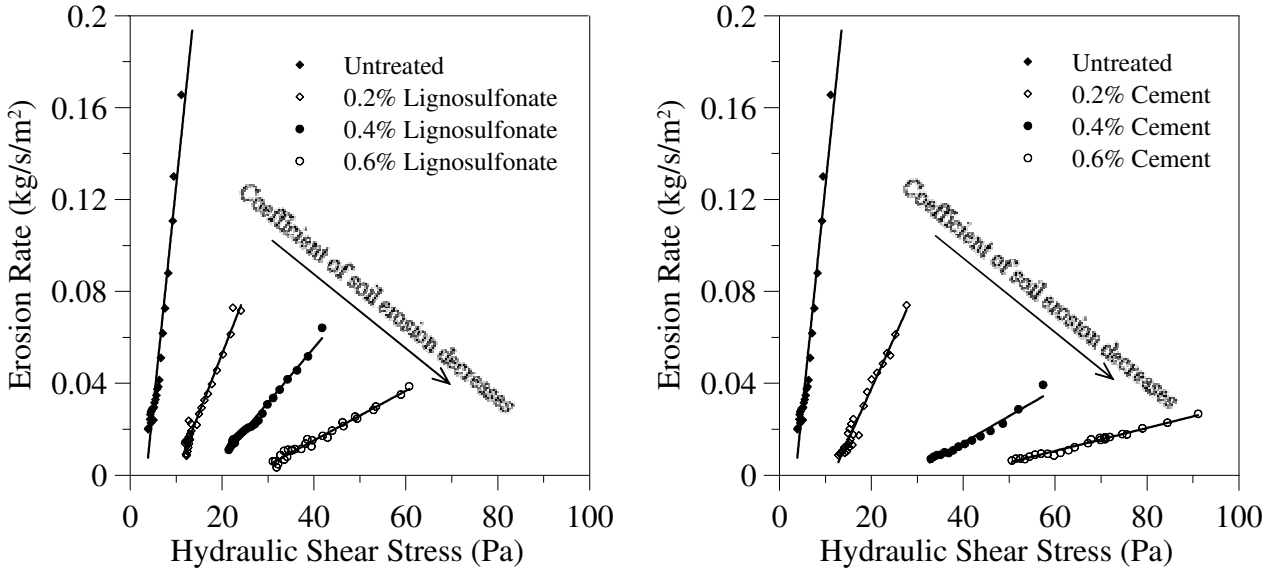

Figure 5.25 Erosion rate against hydraulic shear stress for (a) lignosulfonate treated and untreated (b) cement treated and untreated dispersive clay prepared at the optimum and 95% of the max. dry density (Friction factor method)

The results demonstrate that the erosion resistance increases with the amount of stabilisers, as observed for this silty sand. However, it is important to note that the critical shear stress increases from 3.6 Pa to 39.5 Pa with the addition of 0.6% cement, while the same amount of lignosulfonate treatment only increases the critical shear stress to 26.9 Pa. This shows that an increase in the critical shear stress of dispersive clay with 0.6% cement added is higher than with 0.6% of lignosulfonate. As discussed earlier in this chapter, cement alters the mineralogy of the dispersive clay through cation exchange, while the lignosulfonate acts as a binder. It may be concluded that altering the mineralogy of the dispersive clay is more effective in controlling erosion than just binding the clay particles with lignosulfonate. To illustrate the effect of chemical dosage, water content, and degree of compaction, variation of the critical shear stress is plotted against the chemical dosage for soil compacted at the optimum and dry of optimum, as shown in Figures 5.26 and 5.27, respectively.

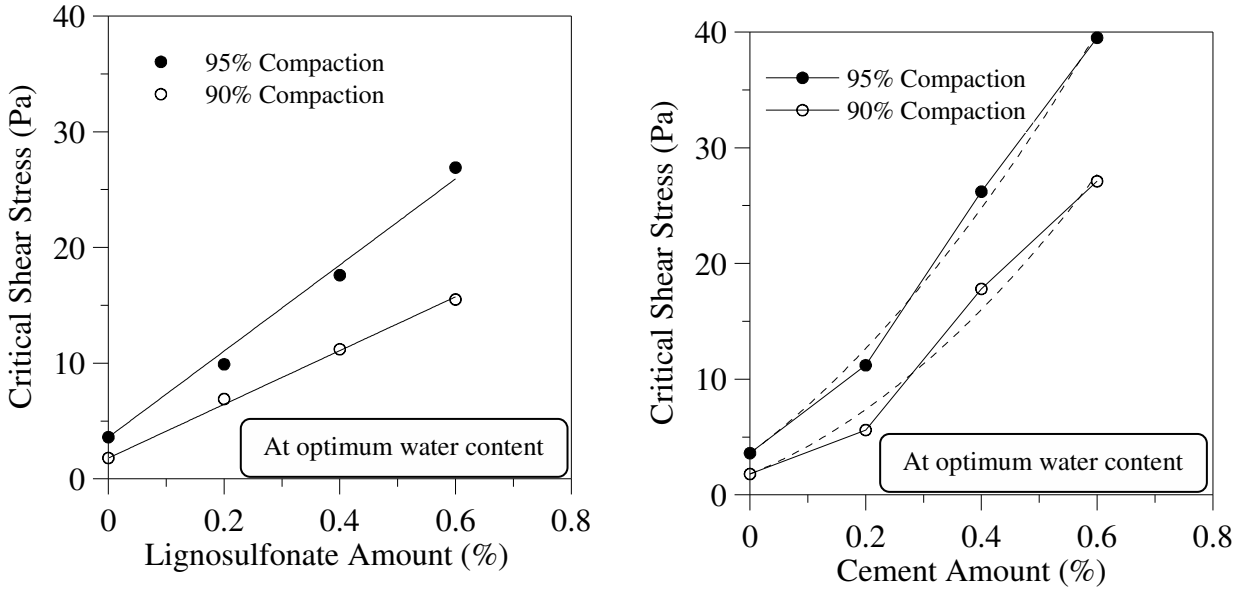

(a) (b)

Figure 5.26 Variation of critical shear stress with the amount of (a) lignosulfonate and (b) cement for dispersive clay prepared at the optimum water content (Friction factor method)

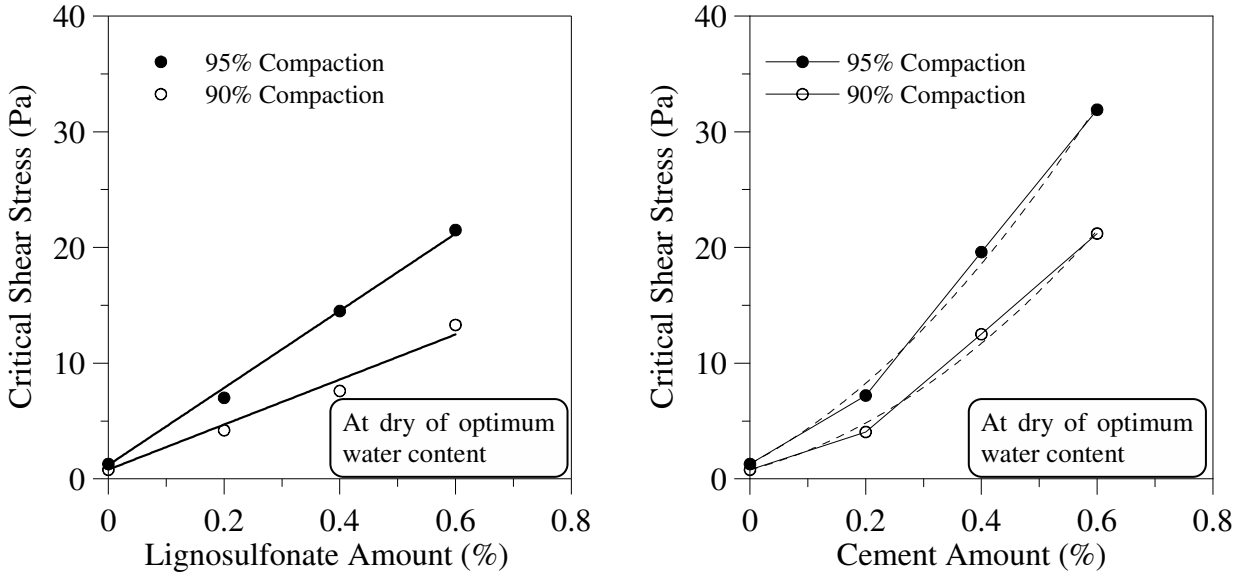

Figure 5.27 Variation of critical shear stress with the amount of (a) lignosulfonate and (b) cement for dispersive clay prepared at dry of optimum water content (Friction factor method)

As described in Figure 5.26, the critical shear stress of soils compacted to 95% and 90% of the maximum dry density and the optimum water content increases linearly with the amount of lignosulfonate, but the critical shear stress of soils treated with cement changes non-linearly with a substantial increase with the addition of 0.4-0.6% of cement (Figure 5.26 (b)). This demonstrates that a significant change in the dispersive characteristics of the clay occurs with the addition of 0.4-0.6% cement, which complies with the findings of the *SCS* dispersion test discussed earlier in this chapter. A similar response was observed for treated and untreated dispersive clay compacted to 95% and 90% of the maximum dry density and dry of optimum, as shown in Figure 5.27. It is clear from Figures 5.26 and 5.27 that the critical shear stress of dispersive clay compacted at the optimum water content is higher than dry of optimum for a given dosage of lignosulfonate or cement and degree of compaction.

5.3.2.2 Hydraulic gradient method

The hydraulic gradient method was also employed to analyse the test data for treated and untreated dispersive clay. As an example, the experimental results obtained for soils compacted at 95% the maximum dry density and the optimum water content are discussed below.

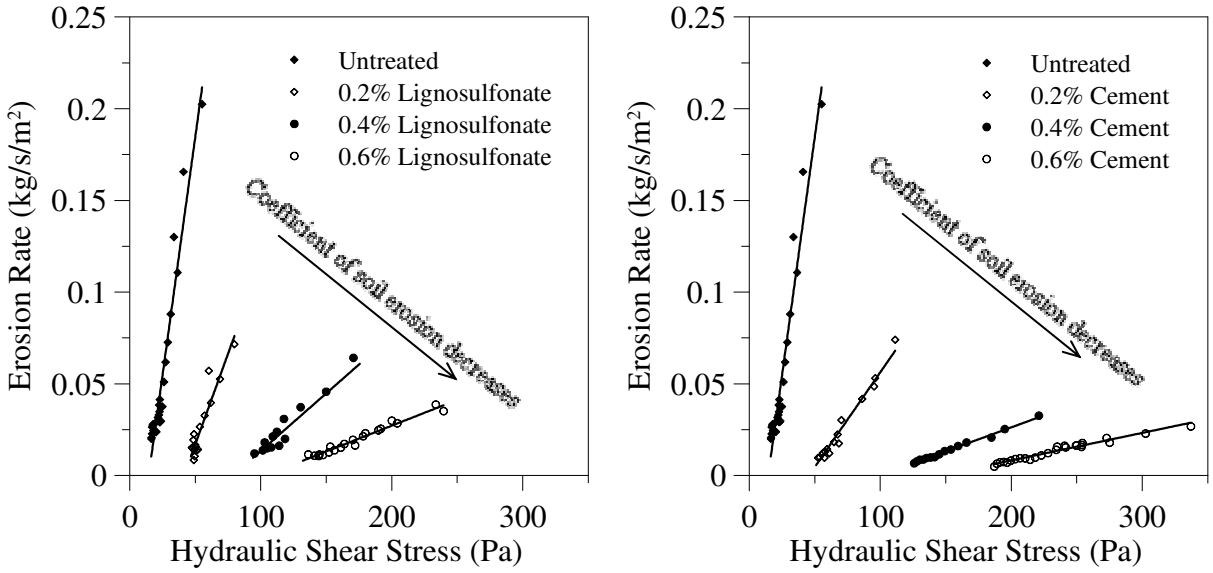

Figure 5.28 Erosion rate versus hydraulic shear stress for (a) lignosulfonate treated and untreated (b) cement treated and untreated soils prepared at 95% of the max. dry density and the optimum water content (Hydraulic gradient method)

Figure 5.28 shows that the critical shear stress increases and the coefficient of soil erosion decreases with the amount of chemical. There were similar trends for all treated and untreated soils compacted to 95% and 90% of the maximum dry density at dry of optimum, and 90% of the maximum dry density at the optimum water content.

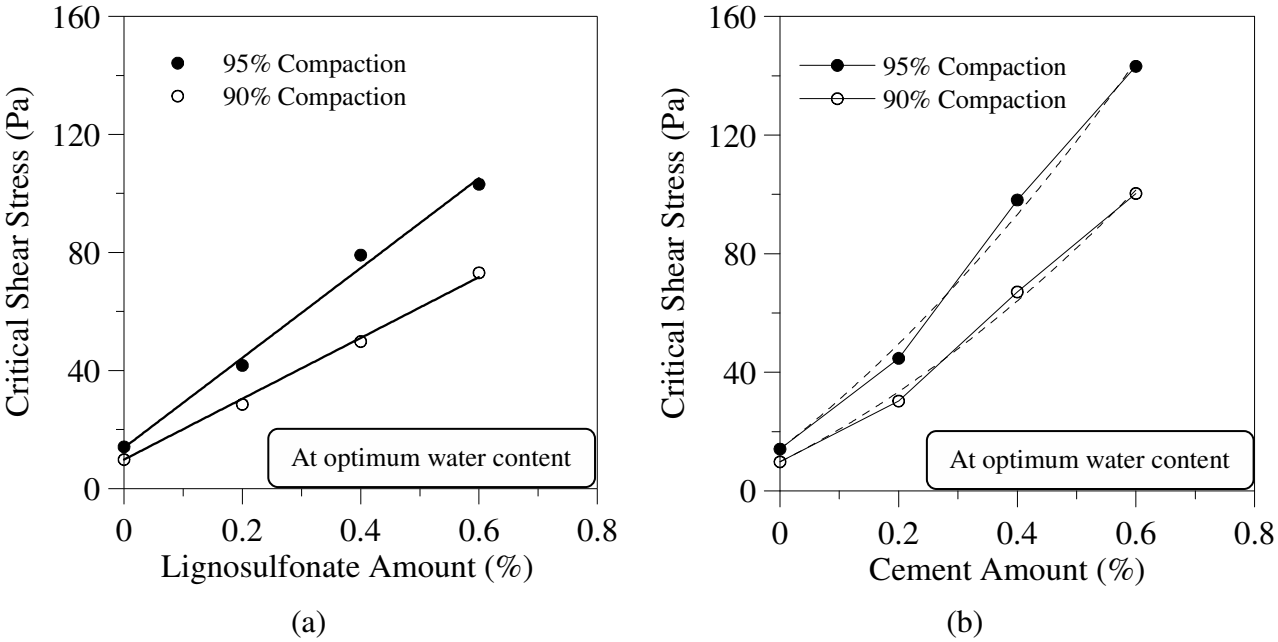

Figure 5.29 Critical shear stress versus amount of (a) lignosulfonate and (b) cement for dispersive clay prepared at the optimum water content (Hydraulic gradient method)

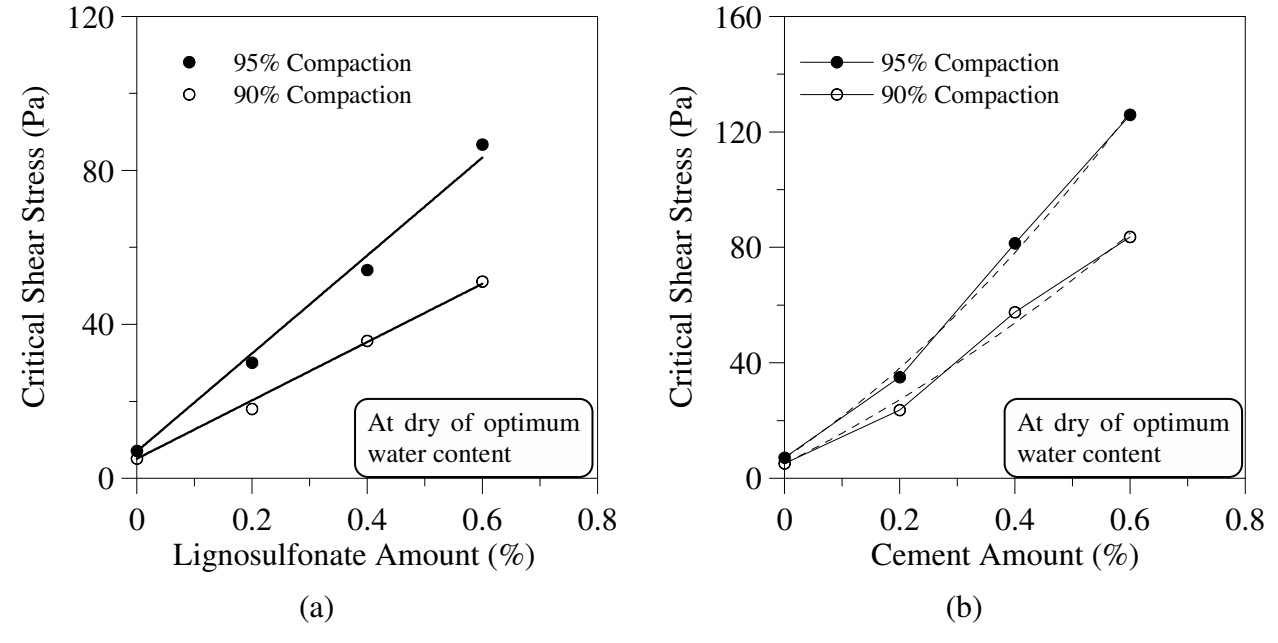

Figure 5.30 Critical shear stress versus the amount of (a) lignosulfonate and (b) cement for dispersive clay prepared at dry of optimum water content (Hydraulic gradient method)

The variation of critical shear stress with the amount of stabiliser at different moulding water contents and degree of compactions are given in Figures 5.29 and 5.30. The response is similar to that obtained from the friction factor method (Figures 5.26 and 5.27). However, the critical shear stress predicted from the hydraulic gradient method is higher than that of from the friction factor method for a given degree of compaction and water content.

5.3.2.3 Development of empirical model to predict the erosion rate of treated dispersive clay

To develop a simple expression for estimating the erosion rate of stabilised dispersive clay, an attempt is made to formulate an empirical relationship between the critical shear stress and the coefficient of soil erosion as conducted for the silty sand.

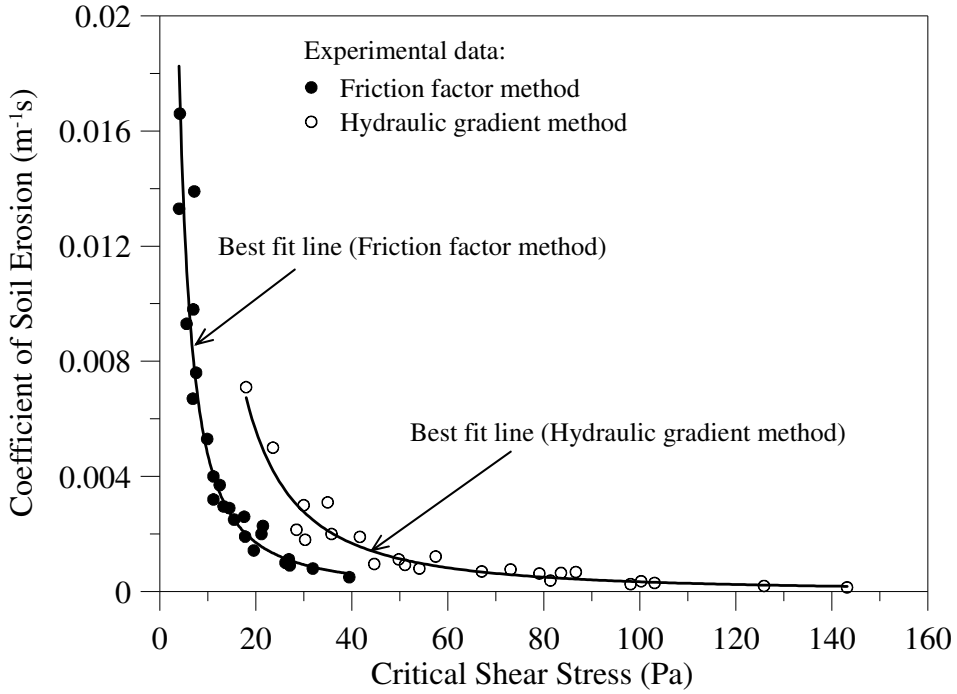

Figure 5.31 Variation of the coefficient of soil erosion with the critical shear stress for treated dispersive clay

Figure 5.31 shows the variation of the coefficient of soil erosion with the critical shear stress obtained from two different analyses for all chemically treated dispersive clay. It shows that a strong relationship exists between the coefficient of soil erosion and the critical shear stress, as seen for the treated silty sand. Hence, the Equation 5.1 can be used to calculate the erosion rate of treated dispersive clay using the values of constants *a* and *b* given in Table 5.9.

Table 5.9 Values of constants *a* and *b* for erosion rate prediction of treated dispersive clay

Method of analysis	*a*	*b*
Friction factor method	0.15	1.48
Hydraulic gradient method	1.03	1.74

The critical shear stress of treated dispersive clay in terms of the critical shear stress of untreated soil and amount of chemical can be obtained from Figures 5.26, 5.27, 5.29, and 5.30. As illustrated, the variation of critical shear stress with the amount of lignosulfonate is almost linear, but is non-linear for cement. Therefore, the relationship for treated silty sand (Equation 5.2) can be used for the lignosulfonate treated dispersive clay. The proportionality coefficients calculated to predict the critical shear stress of lignosulfonate treated dispersive clay are given in Table 5.10. To formulate an expression, the non-linear plot obtained for cement treated soils is fiited with a second order polynomial curve (shown as a dotted line). Hence, the following equation can be employed to calculate the critical shear stress of cement treated dispersive clay.

$$\tau_c = \tau_{c0} + c(CP) + d(CP)^2 \qquad (5.3)$$

where, *CP* (%) is the amount of stabiliser; *c* and *d* are constants; and τ_{c0} (Pa) is the critical shear stress of untreated soil. The values of *c* and *d* are given in Table 5.11.

Table 5.10 Proportionality coefficients (*m*) to predict the erosion rate of lignosulfonate treated dispersive clay

Degree of compaction (%)	Water content (%)	Friction factor method		Gradient method	
		(*m*)	(τ_{c0})	(*m*)	(τ_{c0})
95	Optimum	37.2	3.6	151.6	14.1
	Dry of optimum	33.3	1.3	127.2	7. 0
90	Optimum	23.2	1.8	103.1	9.8
	Dry of optimum	19.5	0.8	76.0	5.0

Table 5.11 Constants *c* and *d* to calculate the erosion rate of cement treated dispersive clay

Degree of compaction (%)	Water content (%)	Friction factor method			Gradient method		
		c	*d*	(τ_{c0})	*c*	*d*	(τ_{c0})
95	Optimum	37.5	38.6	3.6	157.4	100.9	14.1
	Dry of optimum	26.4	42	1.3	134.1	109.8	7.0
90	Optimum	20.3	38.1	1.8	101.3	85.9	9.8
	Dry of optimum	35.7	13.0	0.8	99.8	55.1	5.0

5.4 Results of Tensile Tests

A series of tests were performed to observe the tensile stress-deformation behaviour of silty sand and dispersive clay treated with lignosulfonate and cement. Specimens were tested using a uniaxial tensile testing apparatus, designed and built at University of Wollongong. A detailed description of the apparatus and the number of tests conducted were given earlier in Chapter 4, while the results are presented in detail below.

5.4.1 Tensile Stress-Deformation Behaviour of Treated Silty Sand

The tensile stress-deformation behaviour of samples of silty sand treated with 0.1%, 0.2%, 0.4%, and 0.6% of lignosulfonate and 0.5%, 1.0%, 1.5%, 2.0%, and 3.0% of cement was investigated using the uniaxial tensile testing apparatus. All the tests were performed on silty sand compacted at 95% of the maximum dry density and the optimum water content. The tensile stress-deformation behaviour of silty sand treated with 0.2% lignosulfonate is illustrated in Figure 5.32, which shows that the tensile stress increases to a peak at a displacement of approximately 0.06 mm, and then gradually decreases to zero as all the inter-particle bonds on the fracture plane are broken. Figure 5.33 shows a sample after the tensile failure along a pre-defined fracture plane on the joint.

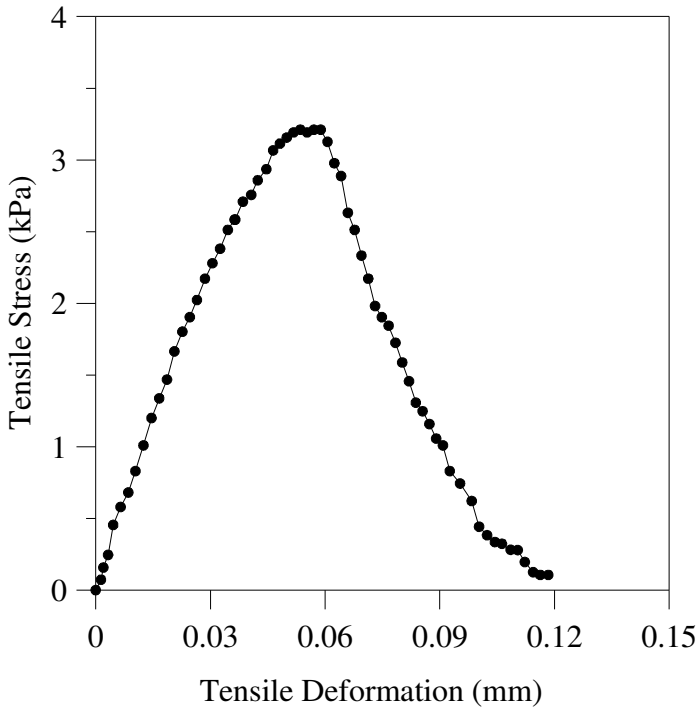

Figure 5.32 Tensile stress-deformation behaviour of silty sand treated with 0.2% of Lignosulfonate

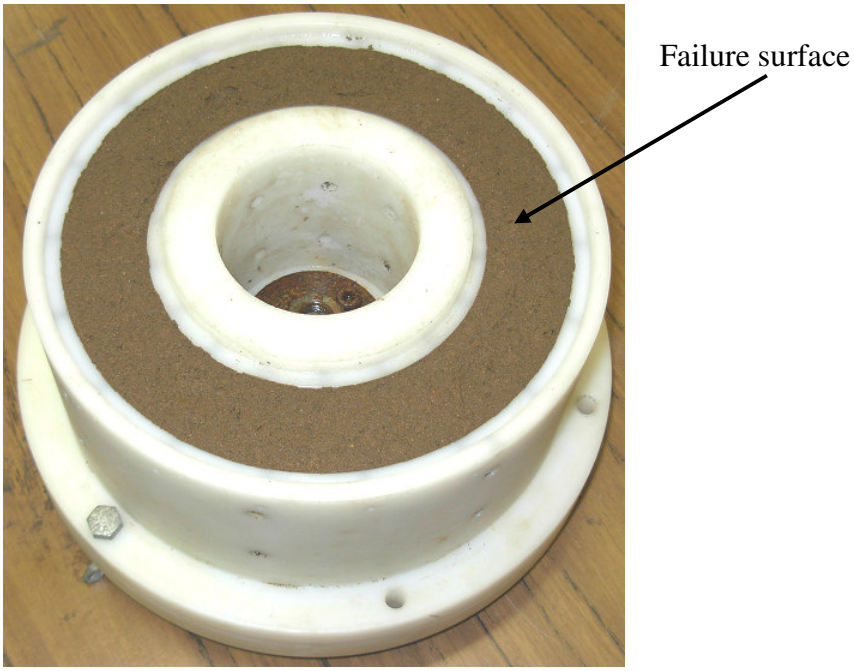

Figure 5.33 A failed sample of treated silty sand

To help understand the effect of chemical stabilisation, the tensile stress-deformation characteristics of all treated silty sand were plotted on the same graph. Figures 5.34 and 5.35 show the tensile stress-deformation behaviour of silty sand treated with lignosulfonate and cement, respectively. As illustrated, the tensile strength of treated soil increases with increasing amounts of lignosulfonate and cement, but the displacement at which the maximum tensile stress occurs decreases with the increasing amounts of cement and lignosulfonate. The variation of the tensile strength of treated soils with the amount of chemical is plotted on Figure 5.36, which shows it to be almost linear for both stabilisers.

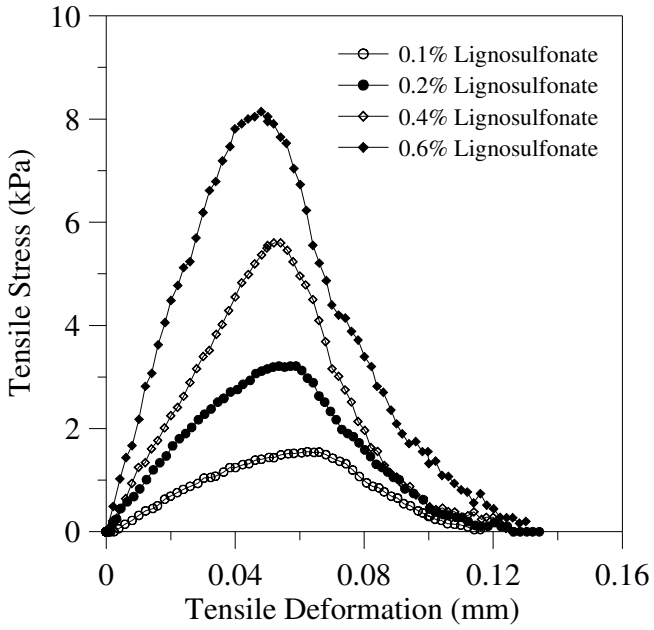

Figure 5.34 Effect of lignosulfonate treatment on the tensile stress-deformation characteristics of silty sand

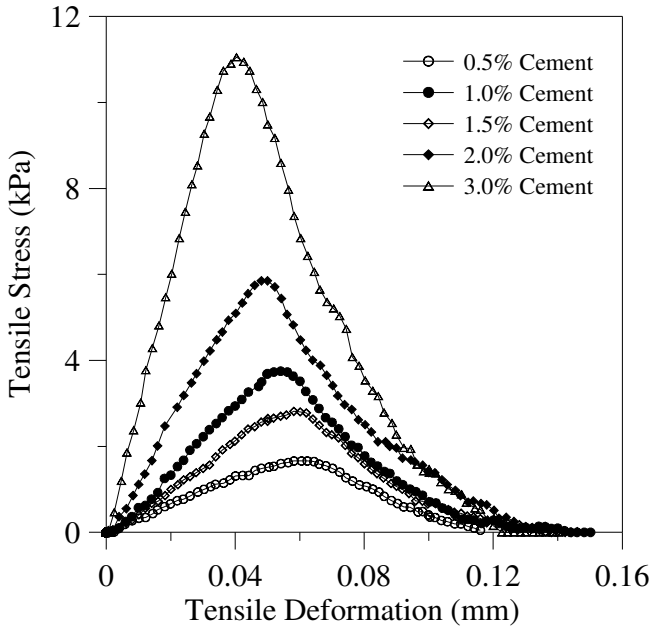

Figure 5.35 Effect of cement treatment on the tensile stress-deformation characteristics of silty sand

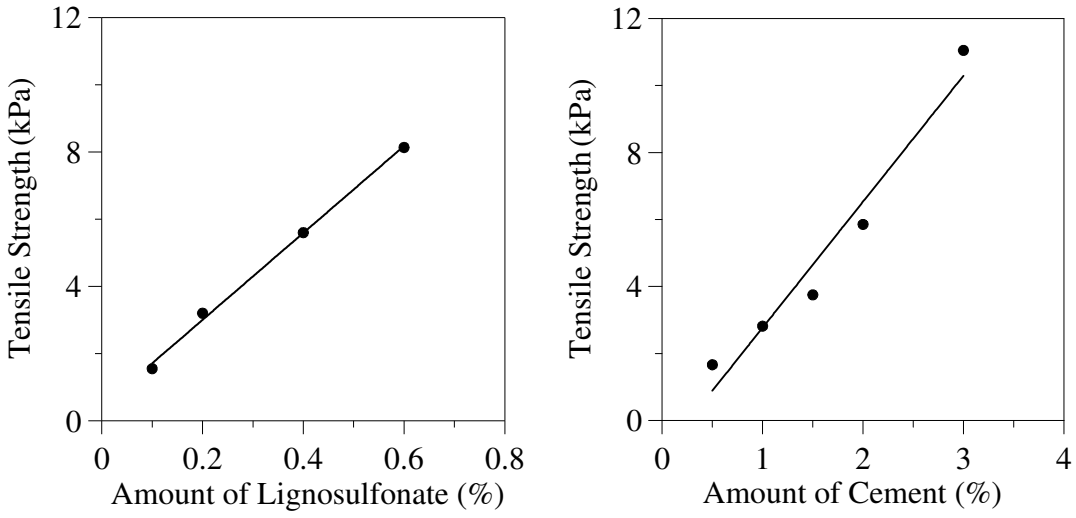

(a) (b)

Figure 5.36 Variation of tensile strength of treated silty sand with the amount of (a) lignosulfonate and (b) cement

The objective of tensile testing was to determine the area under a tensile stress-deformation curve, which represents the energy required to break inter-particle bonds on a unit surface area of the fracture plane. This area is equal to the integral $\int_0^{\delta_{Tf}} \sigma_T \times d\delta_T$ in Equation 3.21 of the erosion model given Chapter 3. Hence, areas under the tensile stress-deformation curves of chemically stabilised silty sand given in Figures 5.34 and 5.35 were calculated to implement them in the erosion model, and their values are given in Table 5.12.

Table 5.12 Calculated area under tensile stress-deformation curves for treated silty sand

	Amount of stabiliser (%)	Area under the tensile stress-deformation curve (J/m^2)
Lignosulfonate treated soil	0.1	0.099
	0.2	0.196
	0.4	0.296
	0.6	0.482
Cement treated soil	0.5	0.103
	1.0	0.169
	1.5	0.213
	2.0	0.340
	3.0	0.594

5.4.2 Tensile Stress-Deformation Behaviour of Treated Dispersive Clay

A number of tensile tests were conducted on treated dispersive clay compacted at 95% of the maximum dry density and the optimum water content. Figures 5.37 and 5.38 show the variation

of the tensile stress-deformation of dispersive clay treated with lignosulfonate and cement, respectively.

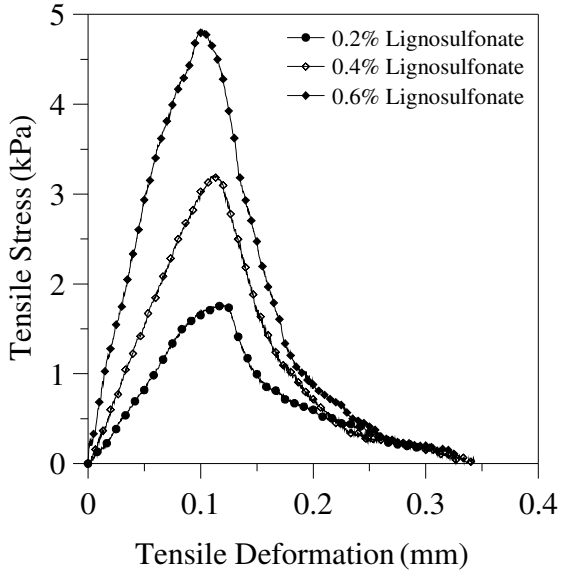

Figure 5.37 Effect of lignosulfonate treatment on the tensile stress-deformation characteristics of dispersive clay

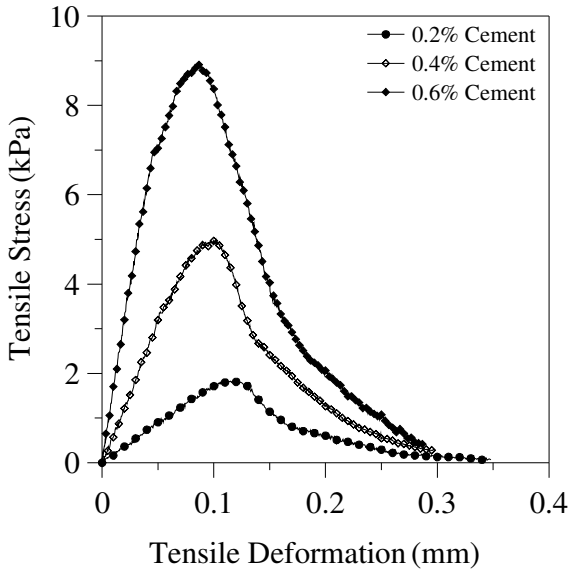

Figure 5.38 Effect of cement treatment on the tensile stress-deformation characteristics of dispersive clay

As indicated in Figures 5.37 and 5.38, the tensile strength of treated soil increases with increasing amounts of lignosulfonate and cement, but the displacement at which the maximum tensile stress occurs decreases with the increasing amounts of these chemical stabilisers. In order to elaborate more on this point, the variation of tensile strength with the amount of cement and lignosulfonate is plotted on the same graph as shown in Figure 5.39. It verifies that the tensile strength of dispersive clay increases almost linearly with lignosulfonate and cement dosage. Areas under the tensile stress-deformation curves of chemically stabilised dispersive clay given in Figures 5.37 and 5.38 were calculated, and their values are given in Table 5.13.

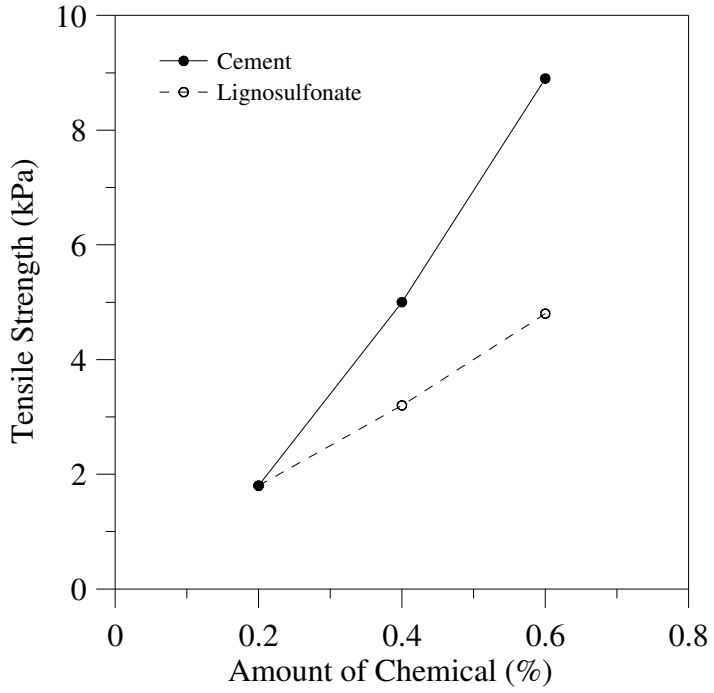

Figure 5.39 Variation of tensile strength of treated dispersive clay with the amount of lignosulfonate and cement

Table 5.13 Calculated area under tensile stress-deformation curves for chemically treated dispersive clay

Soil (Dispersive clay)	Amount of stabiliser (%)	Area under the tensile stress-deformation curve (J/m^2)
Lignosulfonate treated	0.2	0.232
	0.4	0.385
	0.6	0.586
Cement treated	0.2	0.246
	0.4	0.628
	0.6	1.158

5.5 Summary

This chapter mainly discussed the findings of erosion and tensile experimental program conducted on two different erodible soils (silty sand and dispersive clay) stabilised with lignosulfonate and general purpose Portland cement. The results obtained from pinhole tests, compaction tests, unconfined compression tests, *SCS* dispersion tests, and *SEM* tests were also presented. The results of this experimental study are summarised as follows.

- The erosion test results obtained from the *PSAICE* demonstrates that the erosion rate changes linearly with the hydraulic shear stress. The critical shear stress increases with amount of chemical added while the coefficient of soil erosion decreases. The relationship between the critical shear stress and the amount of lignosulfonate is linear

for both types of soils, while silty sand treated with cement responds in a similar fashion. However, the relationship is non-linear for dispersive clay treated with cement.

- Predicting the erosion parameters based on the friction factor method is more accurate than the hydraulic gradient method, because the latter determines the hydraulic shear stress based on the measured gradient, which includes entry losses in the applied head.

- Erosion test results indicate that the coefficient of soil erosion (α) has a strong relationship with the critical shear stress (τ_c) following a decaying power function $\left[\alpha = a / \tau_c^{\,b}\right]$. In addition, an empirical expression has been introduced to evaluate the erosion rate of chemically stabilised soils in terms of the amount of chemical agent added and the magnitude of critical shear stress of the untreated soil.

- An increase in the critical shear stress of silty sand with 0.6% of lignosulfonate is equivalent to that with around 2.5% of cement, however, a small amount of cement compared to that used to stabilise silty sand is sufficient to improve the erosion resistance of dispersive clay. An increase in the critical shear stress with 0.6% cement is higher than from 0.6% of lignosulfonate for dispersive clay.

- The degree of compaction affects the erodibility of treated and untreated soils; the higher the degree of compaction, the greater the critical shear stress, and lower the coefficient of soil erosion.

- Considering the effect of moulding water content on the erosion characteristics of untreated dispersive clay, the erosion resistance of soil compacted at dry of optimum is less than that compacted at the optimum water content. A similar trend was observed for treated dispersive clay.

- The stabilisation mechanisms of cement and lignosulfonate are explained through *SEM* and *SCS* dispersion tests. It was found that lignosulfonate stabilises soils with its binding properties. Cement acts as binder to increase the erosion resistance of silty sand, but it alters the mineralogy of dispersive clay through cation exchange (leading to flocculation) to form a strong clay structure.

- It was found that chemical stabilisation improves the tensile strength of silty sand and dispersive clay. The tensile strength of treated soil increases with increasing amounts of lignosulfonate and cement, but the displacement at which the maximum tensile stress occurs decreases with increasing amounts of these chemicals.

CHAPTER 6

EROSION MODEL VALIDATION

6.1 Introduction

This chapter discusses the verification of the erosion model presented in Chapter 3. The results of erosion tests and uniaxial tensile tests conducted on chemically treated silty sand and dispersive clay were used to validate the model. The results of the erosion tests obtained from the friction factor method were used to validate this model, because, it produced more accurate results than the hydraulic gradient method. This chapter describes the following.

- Developing an expression for the efficiency index in terms of hydraulic parameters, namely, unit stream power and critical unit stream power.
- Formulating an expression for the critical shear stress in terms of tensile strength.
- Using these expressions in the model to check how accurately they predict the erosion rate.

6.2 Verification of Erosion Model

The main reason for validating the model is to investigate any variation in the efficiency index using the appropriate hydraulic parameters. Proffitt *et al.* (1993) reported that the efficiency of overland flow causing erosion changed with the unit stream power, a hydraulic parameter chosen

to describe the state of the flow. In this study, the unit stream power and critical unit stream power were selected for the analysis and their relationship with the efficiency index was explored. The definitions of unit stream power and critical unit stream power are given in Equations 3.26 and 3.27, respectively.

According to Equation 3.23 given in Chapter 3, the efficiency index (ω) can be calculated, if the coefficient of soil erosion (α), the area under the tensile stress-deformation curve $\left[\int_0^{\delta_{Tf}} \sigma_T \times d\delta_T\right]$, the mean particle diameter (d), the dry density of the soil (ρ_d) and the mean flow velocity (v) are known. As discussed in Chapter 5 under section 5.3.1.1, each test on a sample compacted to a certain dry density and water content gives a certain coefficient of soil erosion. It was also observed that the velocity through the crack changed throughout the test, which means that every test produces a set of values for the efficiency indices, unit stream power, and critical unit stream power. The values obtained from tests conducted on samples of chemically treated silty sand were combined to develop a *generalised expression* for the efficiency index. A similar approach was adopted to derive a *generalised expression* for the efficiency index for chemically treated dispersive clay. The following steps were involved in formulating a *generalised expression* for the efficiency index for chemically treated soil (silty sand or dispersive clay).

(i) Variation of the efficiency index with the stream power ratio was plotted for every samples treated with lignosulfonate. A definition of the stream power ratio is given in Equation 6.1. These curves were then normalised using the critical unit stream power to obtain an expression for the efficiency index that was applicable for soil treated with

lignosulfonate. A similar procedure was used to develop a formulation for the efficiency index that was applicable to soil treated with cement.

$$Stream\ Power\ Ratio = P / P_c \qquad (6.1)$$

where, P (W/m^2) is the unit stream power; and P_c (W/m^2) is the critical unit stream power.

(ii) It was found that there was very little difference between the expressions developed for the efficiency index of soil treated with lignosulfonate and cement, and therefore, a *generalised expression* applicable to both was formulated.

Furthermore, a *generalised expression* for the critical shear stress of chemically treated soil in terms of tensile strength was also developed. The model validation is discussed in detail below.

6.2.1 Model Validation Using the Experimental Results of Stabilised Silty Sand

The erosion model was validated based on the results of the erosion and tensile tests on saturated samples of chemically treated silty sand. Only samples prepared at 95% of the maximum dry density and the optimum water content of 10.3% were used for this task. Firstly, a variation of efficiency index with the stream power ratio for samples treated with cement and lignosulfonate was investigated separately in order to explore the effect of stabiliser type. An attempt was then made to formulate a "*generalised expression*" for the efficiency index, which was applicable to

all chemically treated silty sand. The calculated values of the efficiency index for silty sand treated with 0.2% lignosulfonate are given in Table 6.1.

Table 6.1 Calculated values of efficiency index, unit stream power, and critical unit stream power for silty sand treated with 0.2% lignosulfonate

Efficiency index	Unit Stream Power (W/m^2)	Critical unit stream power (W/m^2)	P/P_c
0.0514	50.3	18.3	2.7
0.0507	56.9	18.5	3.1
0.0504	59.8	18.7	3.2
0.0497	69.6	19.0	3.7
0.0495	73.6	19.2	3.8
0.0499	64.5	19.3	3.3
0.0502	58.6	19.4	3.0
0.0503	55.5	19.5	2.8
0.0506	51.2	19.6	2.6
0.0514	44.0	19.6	2.2
0.0522	37.7	19.6	1.9
0.0531	33.2	19.7	1.7
0.0538	30.0	19.7	1.5
0.0543	28.1	19.7	1.4
0.0547	26.5	19.7	1.3
0.0551	25.4	19.7	1.3
0.0554	24.6	19.7	1.2
0.0556	23.9	19.7	1.2
0.0558	23.3	19.7	1.2
0.0560	22.9	19.7	1.2
0.0561	22.6	19.7	1.2
0.0562	22.4	19.7	1.1

The values of the efficiency index, unit stream power, and critical unit stream power were calculated using Equations 3.23, 3.26 and 3.27, respectively. Table 6.1 shows that the efficiency index decreases with an increase in the unit stream power and the stream power ratio $\left(P/P_c\right)$. In order to make this point clear, the variation of the efficiency index with the stream power ratio for silty sand treated with 0.2% lignosulfonate is plotted in Figure 6.1. It shows that the relationship is a power function. It is apparent that the efficiency index should decrease with the stream power ratio, because the higher the unit stream power, the greater the energy loss.

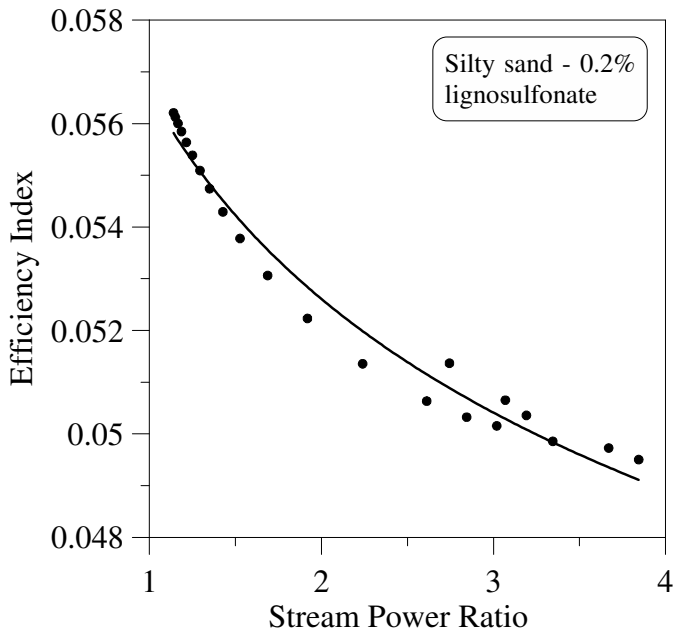

Figure 6.1 Variation of the efficiency index with the stream power ratio for silty sand treated with 0.2% lignosulfonate

A similar procedure was adopted for every other sample of chemically treated silty sand to investigate the variation of the efficiency index under different hydraulic conditions (i.e. under varying unit stream power and critical unit stream power). The response of silty sand treated with

lignosulfonate and cement are illustrated in Figures 6.2 and 6.3, respectively. It is observed that the efficiency index decreases with the amount of chemical stabiliser for a given P/P_c . This is because, the critical unit stream power of treated silty sand increases with an increasing amount of chemical agents, which ultimately increases the unit stream power.

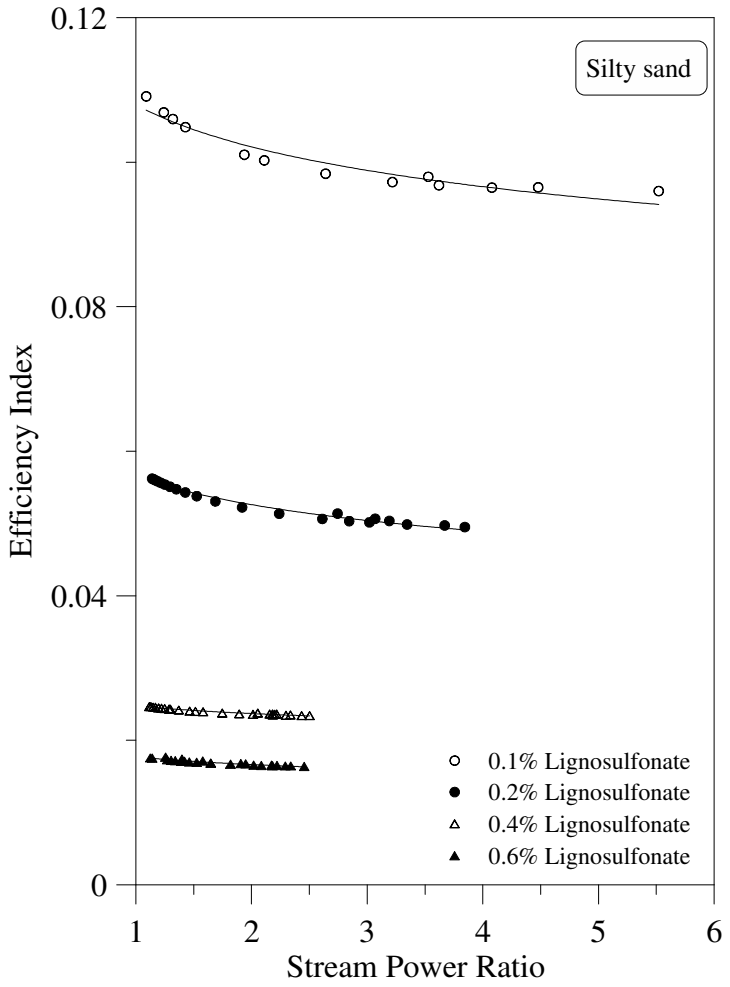

Figure 6.2 Variation of the efficiency index with the stream power ratio for silty sand treated with lignosulfonate

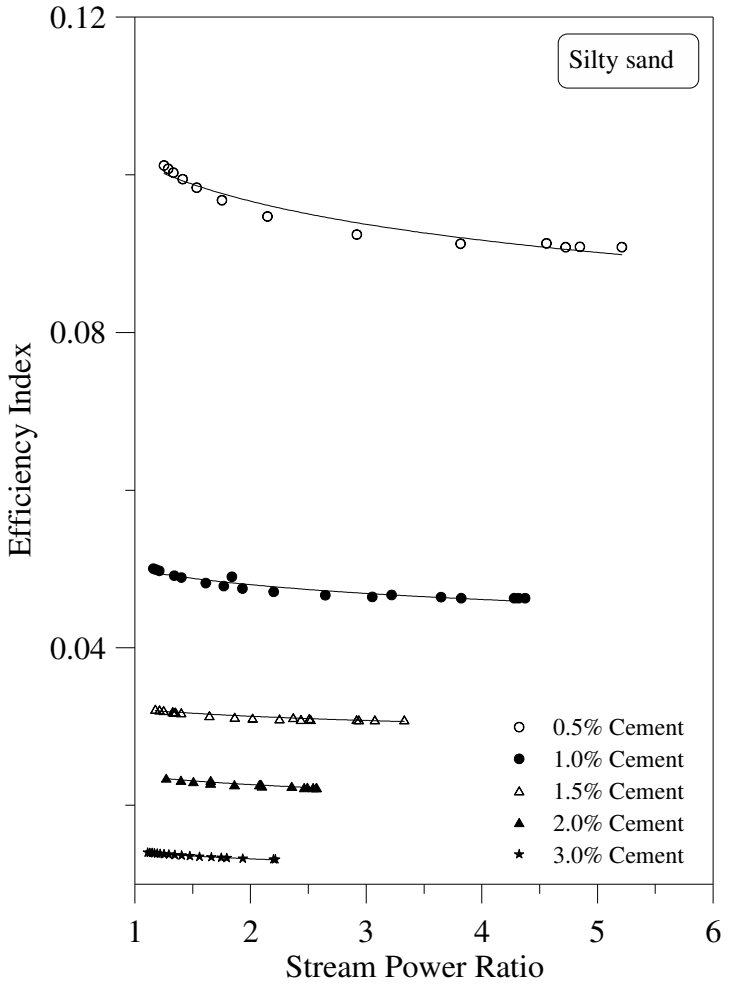

Figure 6.3 Variation of the efficiency index with the stream power ratio for silty sand treated with cement

To develop an expression for the efficiency index applicable to all silty sand treated with lignosulfonate, the efficiency index versus P/P_c curves have been normalised with the respective critical unit stream power, as shown in Figure 6.4. This shows that the product of efficiency index and $P_c^{0.66}$ decreases with the stream power ratio, following a decaying power function. A similar response was observed for all silty sand treated with cement, as shown in Figure 6.5.

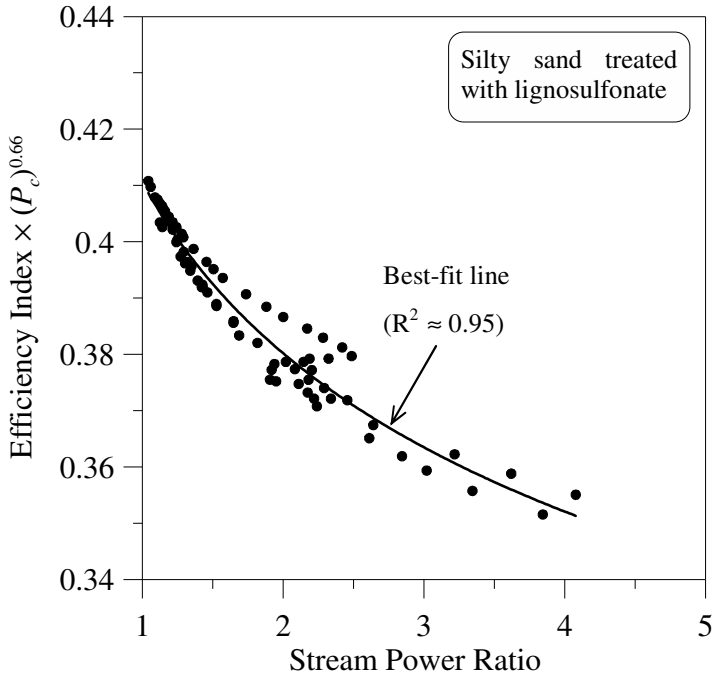

Figure 6.4 A normalised plot for the efficiency index obtained for silty sand treated with lignosulfonate

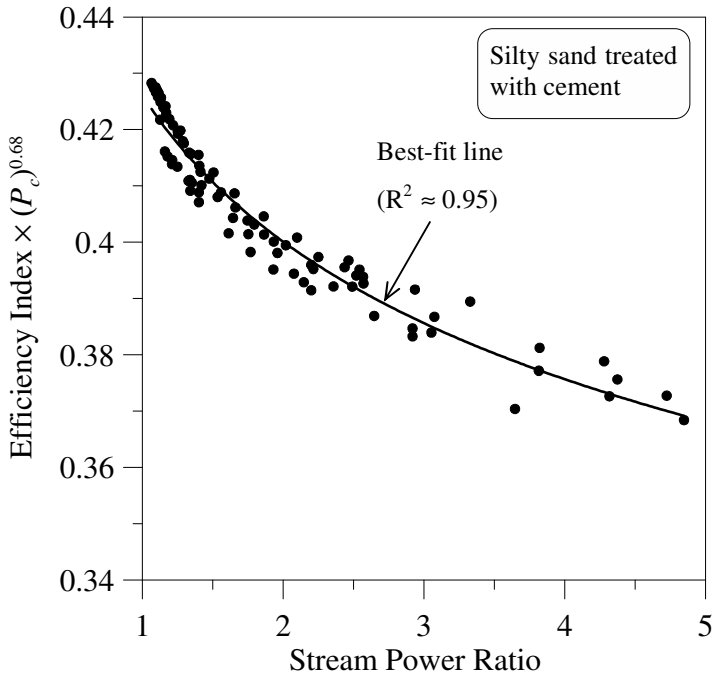

Figure 6.5 A normalised plot for the efficiency index obtained for silty sand treated with cement

It is clear from Figures 6.4 and 6.5 that the normalised plots remain as a decaying power function irrespective of stabiliser type. Therefore, the expression for the efficiency index for silty sand treated with lignosulfonate or cement can be written as:

$$\omega = \frac{\lambda}{P^{\beta} P_c^{\gamma}} \tag{6.2}$$

where, the indices λ, β and γ are constants, and their values are given in Table 6.2 for soils treated with lignosulfonate and cement.

Table 6.2 Values of λ, β and γ for chemically stabilised silty sand

Type of stabiliser	λ	β	γ
Lignosulfonate	0.41	0.11	0.55
Cement	0.43	0.09	0.59

Since the set of values of λ, β and γ obtained for soils treated with lignosulfonate and cement are not too different to each other, a normalised curve for all chemically treated soils can be plotted on Figure 6.6 to obtain a *generalised expression* for the efficiency index for both types of chemical treatment. As observed from Figure 6.6, this *generalised expression* is similar to Equation 6.2 with λ=0.42, β=0.09 and γ=0.58.

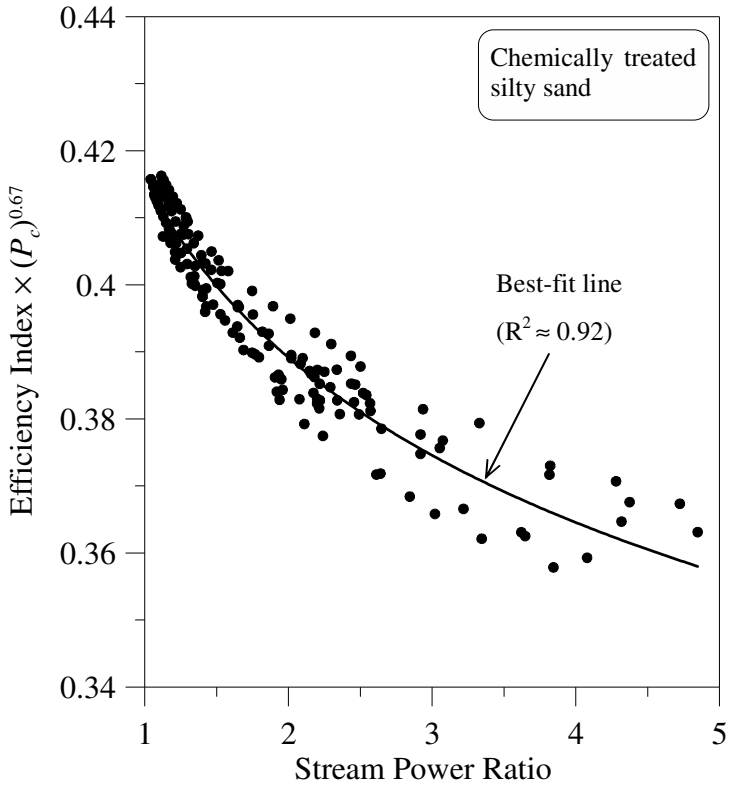

Figure 6.6 A normalised plot for the efficiency indices obtained for chemically treated silty sand

The tensile strengths of all treated silty sand were plotted against their corresponding critical shear stresses, as shown in Figure 6.7. This shows that the critical shear stress changes linearly with the tensile strength, therefore, the *generalised expression* for the critical shear stress can be written as:

$$\tau_c = A + B \times \sigma_{Tf} \tag{6.3}$$

where, σ_{Tf} (kPa) is the tensile strength of the soil. In this study, the empirical constants $A = 0.3$ Pa and $B = 4.1$.

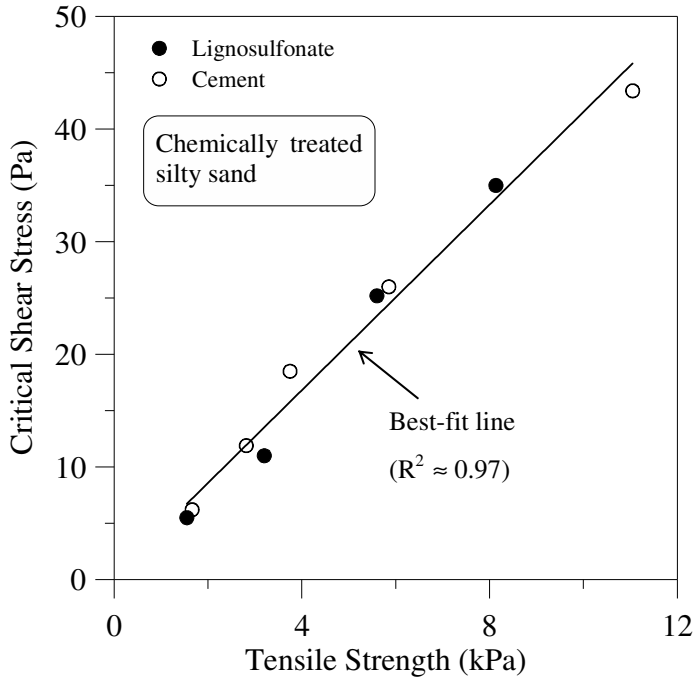

Figure 6.7 Variation of the critical shear stress with the tensile strength for chemically stabilised silty sand

Substituting the *generalised expressions* developed for the efficiency index and the critical shear stress in Equation 3.21 gives the erosion rate as:

$$\dot{\varepsilon} = \frac{\lambda \lfloor \tau_a - A - B\sigma_{Tf} \rfloor \, v\rho_d}{P^{\beta} P_c^{\gamma} \left[\frac{3}{D} \times \int_0^{\delta_{Tf}} \sigma_T \times d\delta_T + \frac{v^2}{2} \rho_d \right]} \tag{6.4}$$

Equation 6.4 can be used to calculate the erosion rate of chemically treated silty sand by substituting 0.3, 4.1, 0.42, 0.09, and 0.58 for A, B, λ, β, and γ, respectively. To verify whether Equation 6.4 can capture the erosion process of chemically stabilised silty sand with minimal error, a variation in the erosion rate with the hydraulic shear stress was predicted based on the model, and then compared with the experimental results. A range of mean flow velocities were

selected to produce a set of hydraulic shear stresses, and Equation 6.4 was then applied to calculate the erosion rate of silty sand treated with 3.0% cement. The results are given in Table 6.3.

Table 6.3 Predicted erosion rates using the model for silty sand treated with 3.0% cement

Selected velocity (m/s)	Hydraulic shear stress (Pa)	Unit Stream Power (W/m^2)	Critical unit stream power (W/m^2)	P/P_c	Efficiency index	Erosion rate ($kg/s/m^2$)
3.50	46.55	162.9	159.0	1.0	0.014	0.002
3.55	47.78	169.6	159.1	1.1	0.014	0.004
3.60	49.00	176.3	159.3	1.1	0.014	0.007
3.65	50.24	183.1	159.4	1.1	0.014	0.010
3.69	51.45	190.0	159.6	1.2	0.014	0.013
3.74	52.66	197.1	159.8	1.2	0.014	0.016
3.79	53.86	204.1	160.1	1.3	0.014	0.018
3.84	55.05	211.3	160.4	1.3	0.014	0.021
3.89	56.38	219.1	160.5	1.4	0.014	0.024
3.94	57.59	226.7	160.7	1.4	0.014	0.027
3.98	58.80	234.3	161.0	1.5	0.013	0.030
4.03	60.01	242.0	161.3	1.5	0.013	0.032
4.08	61.20	249.7	161.7	1.5	0.013	0.035
4.13	62.39	257.6	162.0	1.6	0.013	0.038
4.18	63.58	265.6	162.4	1.6	0.013	0.040
4.23	64.76	273.7	162.8	1.7	0.013	0.043
4.27	65.92	281.8	163.2	1.7	0.013	0.046
4.32	67.10	290.0	163.6	1.8	0.013	0.048
4.37	68.26	298.3	164.0	1.8	0.013	0.051
4.42	69.41	306.7	164.4	1.9	0.013	0.053
4.47	70.56	315.2	164.9	1.9	0.013	0.056
4.52	71.70	323.8	165.3	2.0	0.013	0.058
4.56	72.83	332.4	165.8	2.0	0.013	0.061
4.61	73.96	341.2	166.3	2.1	0.013	0.063
4.66	75.09	350.0	166.7	2.1	0.013	0.066
4.71	76.21	358.9	167.2	2.1	0.013	0.068
4.76	77.33	367.9	167.7	2.2	0.013	0.070
4.81	78.44	377.0	168.2	2.2	0.013	0.073

The erosion rate and the hydraulic shear stress for soil treated with 3.0% cement, observed from the experiment and calculated based on the model given in Equation 6.4, are shown in Figure 6.8. It demonstrates that the proposed model captures erosion reasonably well. The coefficient of soil erosion obtained from the model is 0.0022, which is close to 0.002 obtained from the experimental procedure. The critical shear stress calculated from the model is 45.8 Pa, while it is 43.4 Pa from the experimental observation. In order to verify whether the model can predict the erosion rate over a wide range of hydraulic shear stresses, the erosion rate calculated by the model and experiments on all chemically treated soils were plotted against the hydraulic shear stress. The values for soils treated with lignosulfonate and cement are plotted in Figures 6.9 and 6.10, respectively. The results indicate that the model can predict the erosion rate with reasonable accuracy under a wide range of hydraulic shear stresses, as further verified by the experiments.

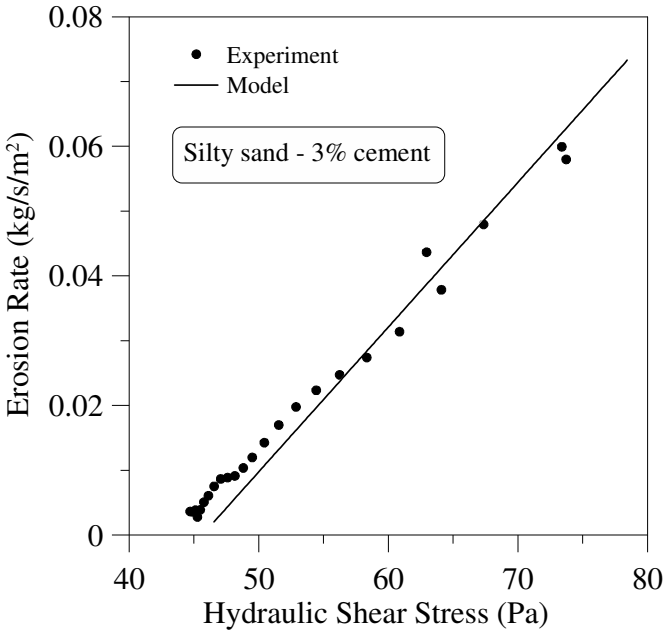

Figure 6.8 Variation of the erosion rate with the hydraulic shear stress for silty sand treated with 3.0% cement

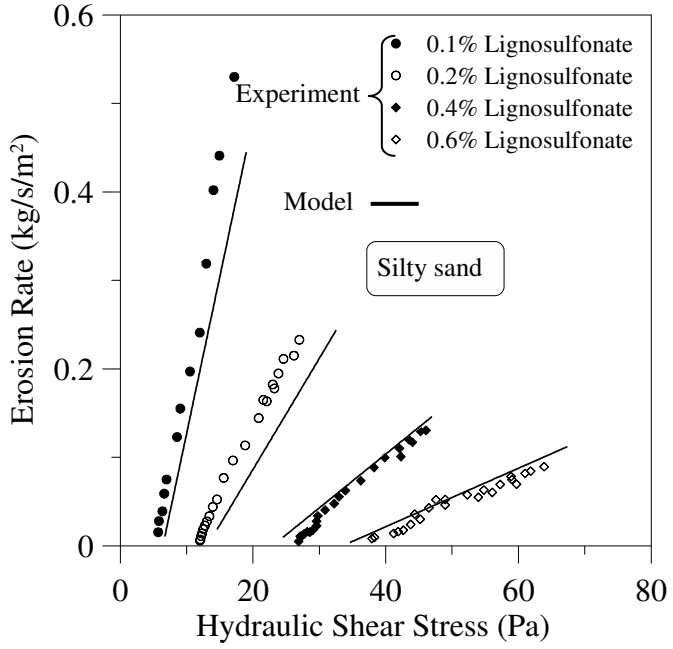

Figure 6.9 Variation of the erosion rate with the hydraulic shear stress for silty sand treated with lignosulfonate

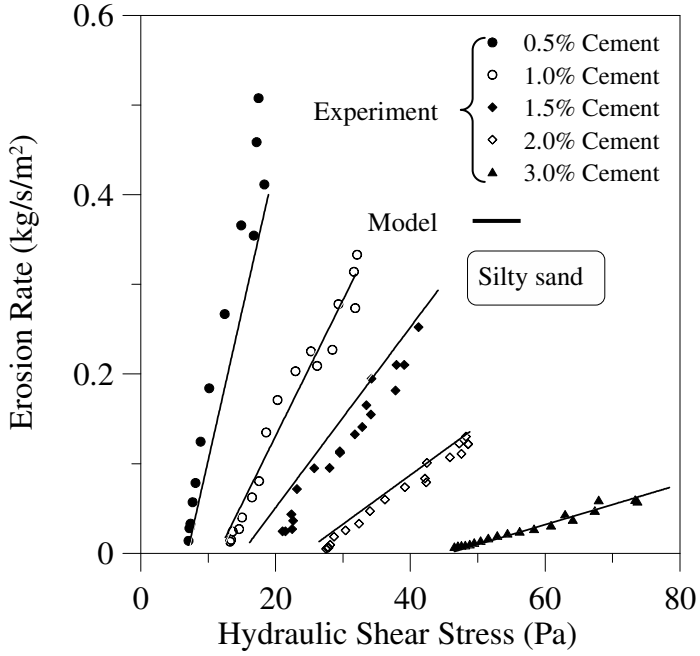

Figure 6.10 Variation of the erosion rate with the hydraulic shear stress for silty sand treated with cement

6.2.2 Model Validation Based on the Experimental Results of Stabilised Dispersive Clay

The procedure used to formulate a *generalised expression* for the efficiency index and the critical shear stress for stabilised silty sand (as described earlier in this chapter) was reproduced for chemically treated dispersive clay. A whole analysis was conducted on samples compacted to 95% of their maximum dry density and the optimum water content. The variation of the efficiency index with the stream power ratio for dispersive clay treated with lignosulfonate and cement is plotted in Figures 6.11 and 6.12, respectively. It can be noted that the efficiency index decreases with the stream power ratio, while it reduces with the amount of chemical stabiliser for a given stream power ratio, as observed for chemically stabilised silty sand.

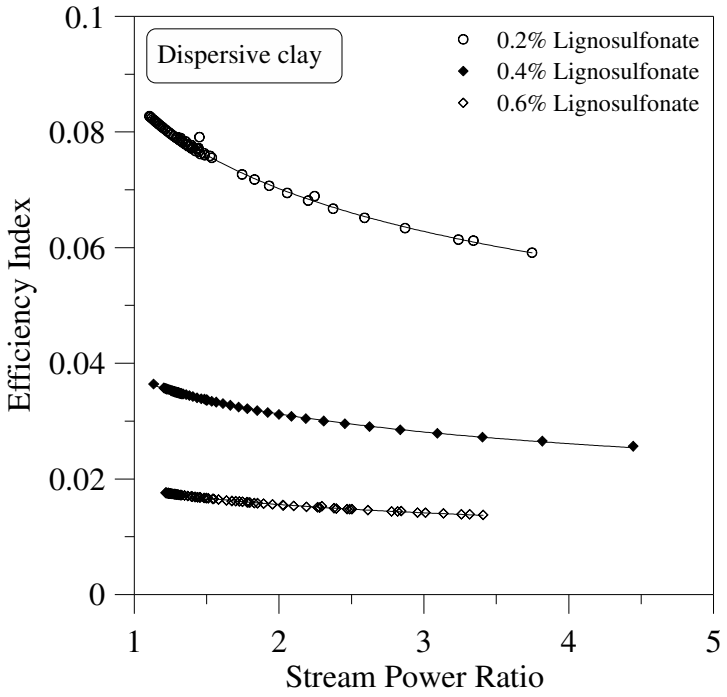

Figure 6.11 Variation of the efficiency index with the stream power ratio for dispersive clay treated with lignosulfonate

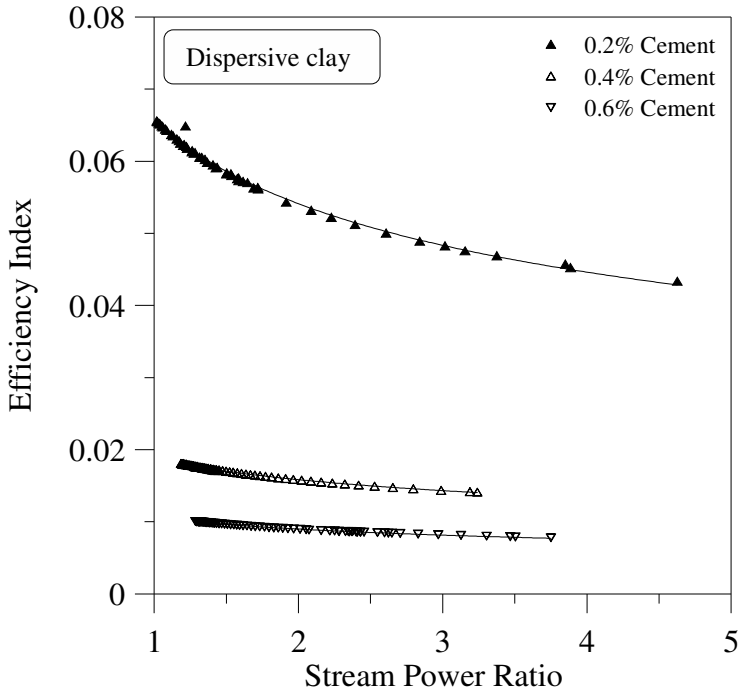

Figure 6.12 Variation of the efficiency index with the stream power ratio for dispersive clay treated with cement

The efficiency index versus stream power ratio curves obtained for dispersive clay treated with lignosulfonate and cement have been normalised and plotted in Figures 6.13 and 6.14, respectively. It is clear from these figures that expressions for the efficiency index of dispersive clay treated with lignosulfonate and cement are similar to stabilised silty sand, as given in Equation 6.2 with different values of λ, β and γ ,which are given Table 6.4.

Table 6.4 Values of λ, β and γ for chemically treated dispersive clay

Type of stabiliser	λ	β	γ
Lignosulfonate	1.40	0.28	0.70
Cement	1.27	0.24	0.73

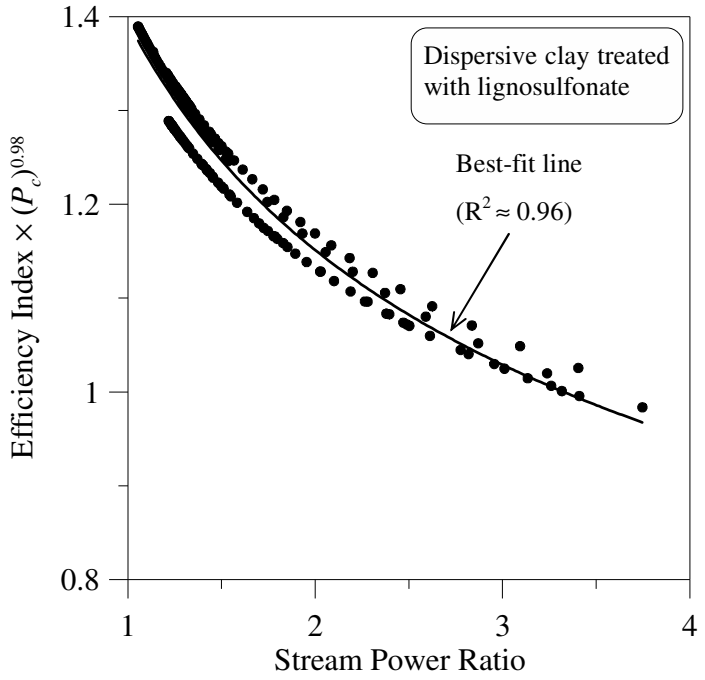

Figure 6.13 A normalised plot for the efficiency index (dispersive clay treated with lignosulfonate)

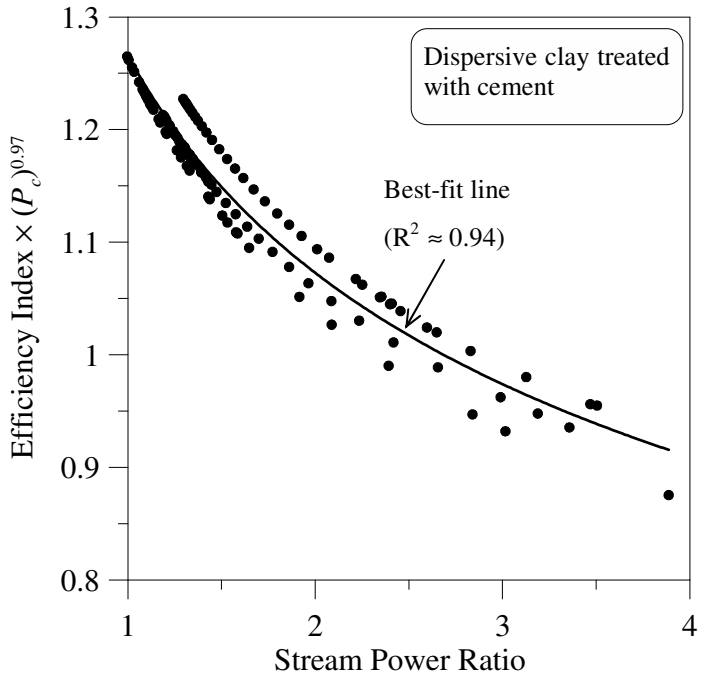

Figure 6.14 A normalised plot for the efficiency index (dispersive clay treated with cement)

To develop a *generalised expression* for the efficiency index that is applicable to all samples of chemically treated dispersive clay, every efficiency index versus stream power ratio curves have been normalised and plotted on the same graph as shown in Figure 6.15. As illustrated in the figure, Equation 6.2 can be used to describe the trend with $\lambda = 1.3$, $\beta = 0.26$, and $\gamma = 0.71$.

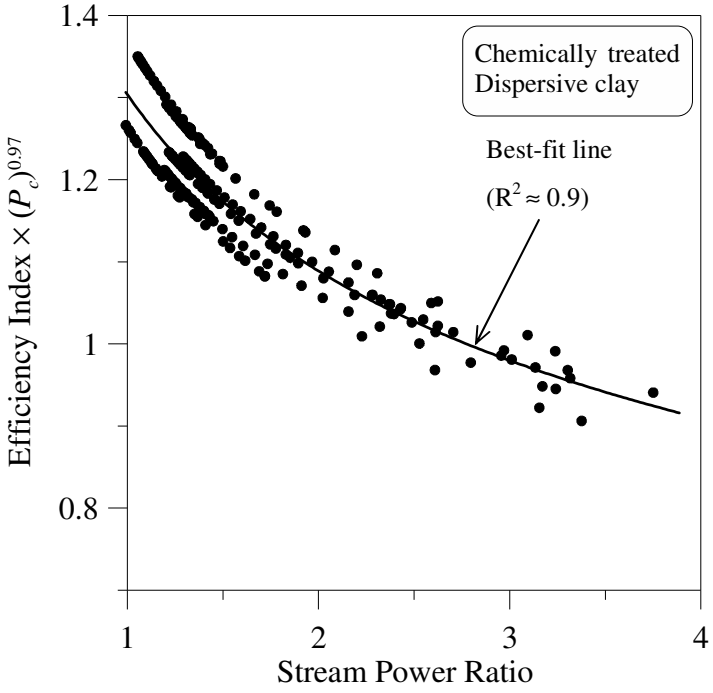

Figure 6.15 A normalised plot for the efficiency index (chemically treated dispersive clay)

An empirical expression for the critical shear stress in terms of tensile strength was developed for chemically stabilised dispersive clay. Figure 6.16 illustrates that the critical shear stress changes linearly with the tensile strength and therefore, the corresponding *generalised expression* for the critical shear stress of chemically treated dispersive clay can be given by Equation 6.4, with $A = 4.2$ pa and $B = 4.2$.

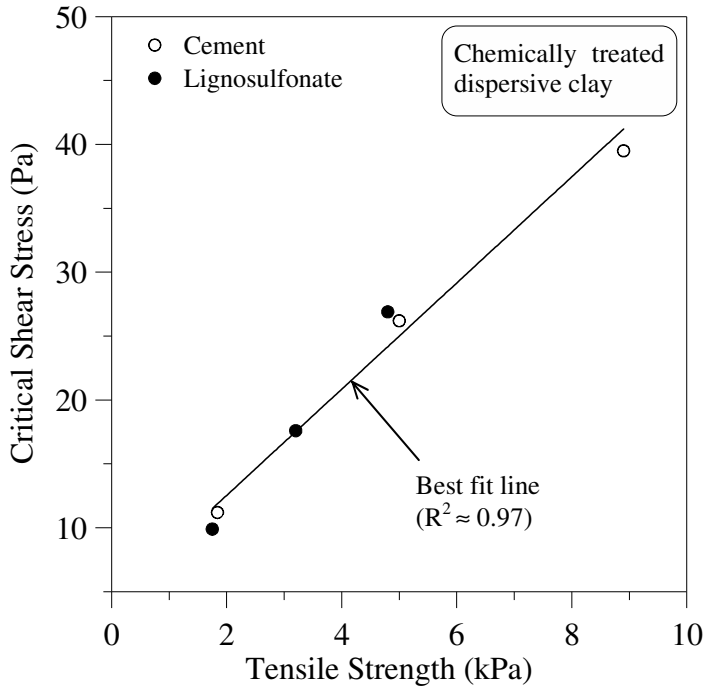

Figure 6.16 Variation of the critical shear stress with the tensile strength of chemically stabilised dispersive clay

Generalised expressions developed for the critical shear stress and the efficiency index for chemically stabilised dispersive clay were incorporated into Equation 6.4 to predict the erosion rate, as performed for stabilised silty sand. The values of A, B, λ, β and γ used for the analysis were 4.2, 4.2, 1.3, 0.26, and 0.71, respectively. Variations in the erosion rate with the hydraulic shear stress obtained from the model for specimens of dispersive clay treated with lignosulfonate and cement are plotted in Figures 6.17 and 6.18, respectively. The results demonstrate that the model can be used to calculate the erosion rate of chemically stabilised dispersive clay over a wide range of hydraulic shear stresses with negligible error.

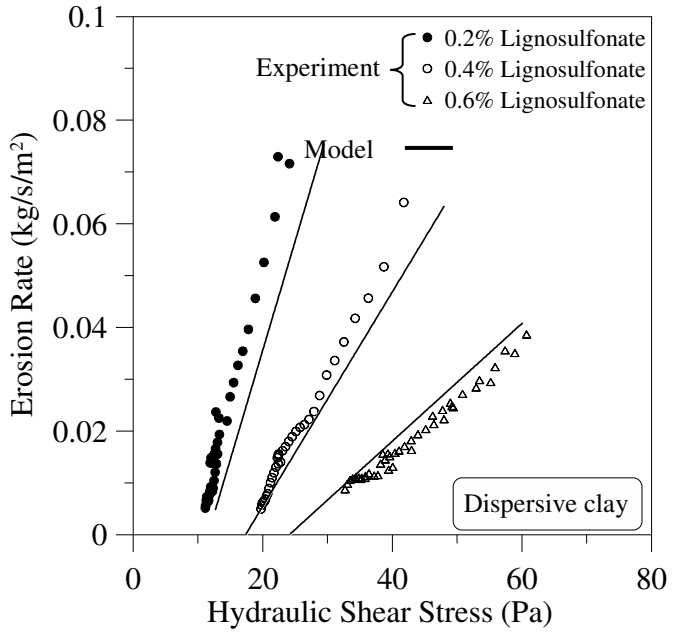

Figure 6.17 Variation of the erosion rate with the hydraulic shear stress for dispersive clay treated with lignosulfonate

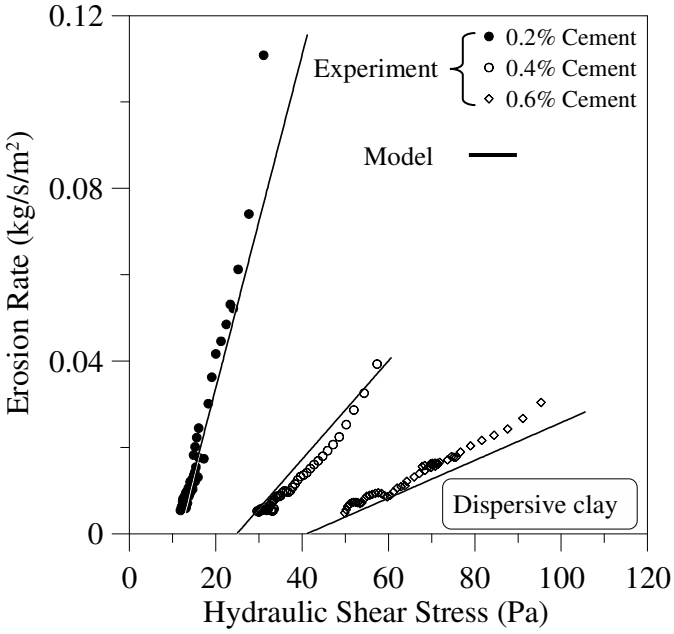

Figure 6.18 Variation of the erosion rate with the hydraulic shear stress for dispersive clay treated with cement

6.3 Summary

This chapter described the development of a *generalised expressio*n for the efficiency index in terms of hydraulic parameters (unit stream power and critical unit stream power), and the critical shear stress as a function of tensile strength. The following conclusions can be drawn from the model validation.

- The efficiency index changes as a power function of stream power ratio $\left(P/P_c\right)$ irrespective of the soil and type of stabiliser. For any given soil, its magnitude decreases with the amount of cement or lignosulfonate for a certain value of P/P_c .

- The efficiency index versus stream power ratio curves obtained for chemically treated silty sand (irrespective of stabiliser type) can be converted into a common decaying power function through normalisation, yielding a *generalised expression* for the efficiency index. A similar trend was observed for stabilised dispersive clay.

- The *generalised expression* developed for the critical shear stress in terms of tensile strength is linear for chemically stabilised silty sand and dispersive clay.

- The proposed erosion model, incorporating generalised expressions for the efficiency index and the critical shear stress, captures the erosion process with reasonable accuracy over a wide range of hydraulic shear stresses, as verified by the experiments.

CHAPTER 7

CONCLUSIONS AND RECOMMENDATIONS

7.1 General

Understanding the behaviour of erodible soils and identifying appropriate techniques to reduce their erodibility is very important, when evaluating the safety of engineering structures such as embankment dams. Moreover, developing an erosion model that incorporates the strength properties of soil will provide an effective means of predicting erosion rate. This thesis study presented an extensive experimental program that investigated the erosional behaviour of silty sand and dispersive clay treated with lignosulfonate and general purpose Portland cement. Every erosion test was performed on saturated samples using a newly built Process Simulation Apparatus for Internal Crack Erosion (*PSAICE*). The experimental program also incorporated a series of tensile tests using the uniaxial tensile testing apparatus that was designed and built at University of Wollongong. Further, the compaction characteristics, stress-strain behaviour, and stabilisation mechanism of the chemical additives were studied through a preliminary investigation, which included compaction tests, unconfined compression tests, Scanning Electron Microscopy (*SEM*) tests, and Soil Conservation Service (*SCS*) dispersion tests.

In this study, a theoretical erosion model was developed in terms of the tensile stress-deformation properties, the mean particle diameter, the dry density and the mean flow velocity.

The model was validated using the experimental data. Specific conclusions drawn from this program and modelling are summarised in the following sections.

7.2 Results of Preliminary Investigation and Tensile Test

- The *SEM* tests conducted on treated and untreated silty sand revealed that lignosulfonate and cement act as a binder to increase resistance to erosion. The cement alters the mineralogy of dispersive clay through cation exchange (leading to flocculation) to form a stronger structure, while the lignosulfonate acts as a binder. The results of the *SCS* dispersion tests on samples of dispersive clay treated with cement showed that the cement encourages flocculation, which reduces the "percent dispersion".

- The maximum dry density and the optimum water content of silty sand are barely affected by chemical stabilisation. Similar results were observed for dispersive clay treated with lignosulfonate, but when treated with cement there was a decrease in the maximum dry density and an increase in the optimum water content.

- The standard pinhole test demonstrated that around 0.6% of lignosulfonate by dry weight of soil is sufficient to convert silty sand into a completely erosion resistant soil, while 2.0% cement is required to achieve the same effect. However, 0.6% of cement is enough to make the dispersive clay non-erodible, but the same amount of lignosulfonate does not make the soil non-erodible. It is clear that altering the clay mineralogy with cement is more effective than just binding the dispersive clay with lignosulfonate.

- The tensile strength of treated soil increases with the amount of stabiliser, while the tensile deformation at which the maximum tensile stress occurs decreases with increasing amount of these chemicals.

7.3 Erosional Behavior of Chemically Stabilised Erodible Soils

- The results of the erosion test from the *PSAICE* demonstrated that the erosion rate changes linearly with the hydraulic shear stress. A similar erosional behaviour was reported by previous researchers (e.g. Arulananthan *et al.* 1975; Sargunan 1977).

- When the friction factor and hydraulic gradient methods were used to calculate the hydraulic shear stress, there were two different values of critical shear stress for a given soil sample. The hydraulic gradient method overestimates the critical shear stress, because it includes the entry losses in the applied head. Hence, the friction factor method is better method for predicting erosion rate.

- The critical shear stress increases with an increasing amount of chemical stabilisers, while the coefficient of soil erosion decreases. The relationship between the critical shear stress and the amount of lignosulfonate is linear for both types of soils. There is a similar response when silty sand is treated with cement. However, the relationship for dispersive clay treated with cement is non-linear.

- The amount of lignosulfonate required to achieve a given increase in the critical shear stress of silty sand is significantly less than cement, but only a small amount of cement compared to that used for stabilising silty sand is sufficient to increase the erosion

resistance of dispersive clay. An increase in the critical shear stress of dispersive clay with 0.6% of cement is higher than with 0.6% of lignosulfonate.

- The results of erosion tests clearly showed that the coefficient of soil erosion has a strong relationship with the critical shear stress, following a *decaying power function*. An empirical expression has been formulated to evaluate the critical shear stress of chemically stabilised soils in terms of the amount of chemical agent added and the magnitude of critical shear stress of untreated soil.

- The erosion of chemically treated and untreated soils is affected by the degree of compaction such that the higher the compaction the greater the critical shear stress and the lower the coefficient of soil erosion. The difference between the critical shear stress of soil compacted to 95% of the maximum dry density and soil compacted to 90% increases with the amount of stabiliser.

- Initial moulding water content plays a significant role on the erosion characteristics of saturated dispersive clay. The erosion resistance of the soil moulded at the dry of optimum is less than that of the soil moulded at the wet of optimum and the optimum water content.

7.4 Theoretical Erosion Model

Important features of the erosion model and conclusions drawn from its validation are summarised below.

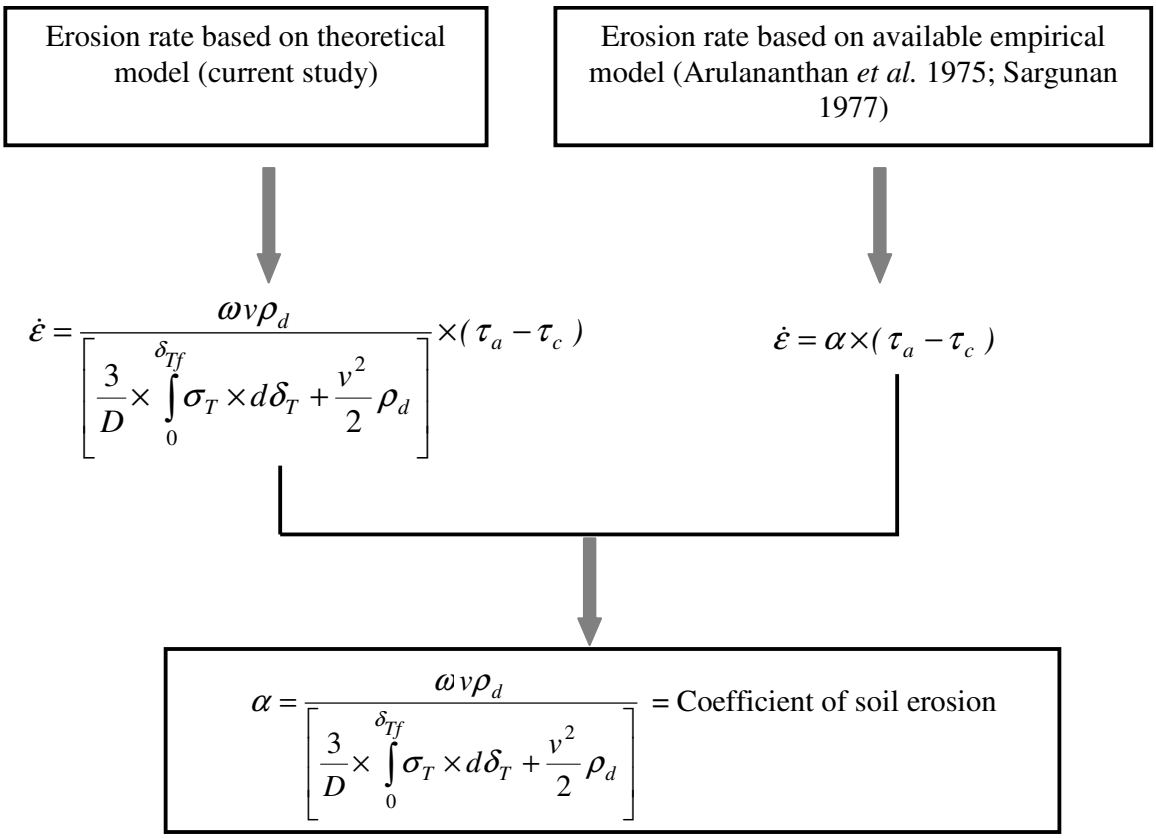

Figure 7.1 Summary of the theoretical erosion model

- As described in Figure 7.1, the theoretical model developed using the law of the conservation of energy can be compared with an empirical relationship previously proposed by several investigators (e.g. Arulananthan *et al.* 1975; Sargunan 1977).

- Verification of the model showed that only a fraction of flow energy (i.e. efficiency index) is effectively used during erosion. For all chemically stabilised silty sand and dispersive clay, the efficiency index varies from 0.008-0.110 depending on the hydraulic conditions.

- The efficiency index (ω) changes as a power function of the stream power ratio (i.e. the ratio between the unit stream power and critical unit stream power) irrespective of the type of stabiliser and soil. However, its magnitude decreases with the amount of cement or lignosulfonate for a given stream power ratio.

- The model validation indicated that the efficiency index versus stream power ratio curves obtained for chemically treated silty sand (irrespective of stabiliser type) can be normalised into a decaying power function known as the *generalised expression* for the efficiency index. A similar trend was observed for stabilised dispersive clay.

- A generalised *expression* for the critical shear stress of stabilised silty sand and dispersive clay in terms of tensile strength was formulated, and the relationship was found to be linear.

- The erosion model, incorporating *generalised expressions* that were developed for the efficiency index and the critical shear stress, captures erosion over a wide range of hydraulic shear stresses with reasonable accuracy.

- The proposed model can be used to predict the erosion rate under given hydraulic conditions, if the tensile stress-deformation characteristics, mean particle diameter, and compacted density of the soil are known.

7.5 Recommendations for Future Research

- Experimental studies can be conducted to investigate the effectiveness of different chemical additives such as lime, gypsum, cement, lignosulfonate, and fly ash to

control erosion of several erodible soils ranging from dispersive clay to non-cohesive. Based on the findings, a data base can be created to assist engineers in the construction aspects of earth structures.

- Internal erosion in earth structures occurs through concentrated leaks (e.g. cracks), seepage erosion through internally unstable soil, backward erosion due to seepage, and blow out (Fell *et al.* 2003). This current study only focused on erosion through cracks. Therefore, further study on internal erosion through internally unstable soils will help to complete a more comprehensive picture of internal erosion and piping in embankment dams. Unstable soils with coarse and fine, but no intermediate particles, can be selected for the study (or commercial soils with the correct proportions). Performing a series of erosion tests on different soils (by changing their fine and coarse contents) will be useful for developing a criterion, which can be used to identify the internally unstable soils.

- The theoretical model developed in this study can be modified for other types of erosion such as surface erosion. To validate the model, a series of surface erosion tests using flume, and tensile tests with the apparatus used in the current study can be conducted. The findings would be applied in the design of channels in cohesive soils.

- The concept of the current erosion model can be applied to the seepage erosion scenarios in different geotechnical and geo-environmental conditions such as erosion through the core of a dam and transportation of fine particles (e.g. contaminant transport) through the sub-surface. The seepage erosion occurs because of flow through the pore tubes that exist in the soil mass. The model developed in this study

considers erosion through a crack, which could be treated as one of the pore tubes existing in the soil mass. Since these two situations are apparently similar, developing a comprehensive model that captures erosion by seepage with appropriate modifications to the current model is encouraged.

- The effect of in-situ stresses on the characteristics of soil erosion was not considered in this study. Conducting a series of tests by modifying the current experimental setup to apply in-situ stresses to the sample will help to understand how they affect erosion.

REFERENCES

Ajaz, A. and Parry, R.H.G. (1974). "An unconfined direct tension test for compacted clays", *Journal of Testing and Evaluation*, Vol. 2(3), 163-172.

Ajaz, A. and Parry, R.H.G. (1975). "Stress-strain behaviour of two compacted clays in tension and compression", *Geotechnique*, Vol. 25(3), 495-512.

Arulanandan, K., Loganathan, P., and Krone, R.B. (1975). "Pore and eroding fluid influences on surface erosion of soil", *Journal of the Geotechnical Engineering Division*, ASCE, Vol. 101(GT1), 51-66.

AS 1289.3.8.1 (1997). "Determination of Emerson class number of a soil", Australian standard.

ASTM D 4647 (2004). "Identification and classification of dispersive clay soils by the pinhole test", *Annual book of ASTM standards: Section 4, Construction*, Vol. 04.08: 826-833.

Atkinson, J.H, Charles, J.A. and Mhach, H.K (1990). "Examination of erosion resistance of clays in embankment dams", *Quarterly Journal of Engineering Geology*, London, Vol. 23, 103-108.

Barua, D.K. (2004). "Discussion of simple formula to estimate settling velocity of natural sediments, by Jimenez, J.A. and Madsen, O.S.", Journal of Water way, Port, Coastal and Ocean Engineering, ASCE, Vol. 130(4), 219-221.

Balasubramaniam, A.S., Bergado, D.T., Buensuceso, B.R. and Yang, W.C. (1989). "Strength and deformation characteristics of lime-treated soft clays", *Geotechnical Engineering*, Vol. 20, 49-65.

Biggs, A.J.W. and Mahony, K.M (2004). "Is Soil Science Relevant To Road Infrastructure?" *13th International Soil Conservation Organization Conference – Brisbane*, July 2004 Conserving Soil and Water for Society: Sharing Solutions, Paper No 410.

Bishop, A.W, and Garga, V.K. (1969). "Drained tension tests on London clay", Geotechnique, Vol. 19(3), 309-313.

Briaud, J.L., Ting, F.C.K., Chen, H.C., Gudavalli, R., Perugu, S. and Wei, G. (1999). "SRICOS: Prediction of scour rate in cohesive soils at bridge piers", *Journal Geotechnical and Geoenvironmental Engineering*, ASCE, Vol. 125(4), 237-246.

Briaud, J.L., Ting, F.C.K., Chen, H.C., Cao, Y., Han, S.W. and Kwak, K.W. (2001). "Erosion function apparatus for scour rate predictions", *Journal Geotechnical and Geoenvironmental Engineering*, ASCE, Vol. 127(2), 105-113.

Chapuis, R.P. and Gatien, T. (1986). "An improved rotating cylinder technique for quantitative measurements of the scour resistance of clays", *Canadian Geotechnical Journal*, Vol. 23, 83-87.

Chemstab, (2003). "Technical Manual", *CHEMSTAB* Consulting Pty Ltd, Horsley, NSW Australia.

Chew, S.H., Kamaruzzaman, A.H.M. and Lee, F.H. (2004). "Physiochemical and Engineering Behaviour of cement treated clays" *Journal of Geotechnical and Geoenvironmental Engineering*, ASCE, Vol. 130(7), 696-706.

Christensen, R.W. and Das, B.M. (1973). "Hydraulic erosion of remolded cohesive soils", *In soil Erosion: Causes and mechanisms; Prevention and Control, Special Report 135*, Highway Research Board, 8-19.

Crouch, R.J. (1977). "Tunnel-Gully erosion and urban development: A case study", *Dispersive clays, related piping, and erosion in geotechnical projects, ASTM STP 623*, Sherard and Decker, Eds., 58-68.

Dascal, O. and Hurtubise, J. (1977). "Chemical treatment of a sensitive cemented clay (Champlain clay)", *Dispersive clays, related piping, and erosion in geotechnical projects, ASTM STP 623*, Sherard and Decker, Eds., 69-73.

Dass, R.N., Yen, S.C., Das, B.M., Puri, V.K., and Wright, M.A. (1994). "Tensile stress-strain characteristics of lightly cemented sand", *Geotechnical Testing Journal*, Vol. 17(3), 305-314.

Decker, R.S., Dunnigan, L.P. (1977). "Development and use of the soil conservation service dispersion test", *Dispersive clays, related piping, and erosion in geotechnical projects, ASTM STP 623*, Sherard and Decker, Eds., 94-109.

Dunn, I.S. (1959). "Tractive resistance of cohesive channels", *Journal of the soil mechanics and foundations division*, ASCE, Vol. 85(SM3), 1-24.

Elliot, G.L. (1977). "Amelioration of tunneling susceptible soils in the hunter valley, New South Wales, by modification of clay double-layer interactions", *Dispersive clays, related piping, and erosion in geotechnical projects, ASTM STP 623*, Sherard and Decker, Eds., 110-120.

Fell, R., Wan, C.F., Cyganiewicz, J. and Foster, M. (2003). "Time for the development of internal erosion and piping in embankment dams", *Journal of Geotechnical and Geoenvironmental Engineering*, ASCE, Vol.129(4), 307-314.

Foster, M.A. (1999). "The probability of failure of embankment dams by internal erosion and piping", *PhD Thesis*, University of New South Wales, Australia.

Hanson, G.J. (1991). "Development of a jet index to characterise erosion resistance of soils in earthen spillways", Soil and Water Division, *Transactions of the ASAE*, Vol. 34(5), 2015-2020.

Hanson, G.J. and Robinson, K.M. (1993). "The influence of soil moisture and compaction on spillway erosion", Soil and Water Division, *Transactions of the ASAE*, Vol. 36(5), 1349-1352.

Hjeldnes, E.I. and Lavania, B.V.K. (1980). "Cracking, leakage, and erosion of earth dam materials", *Journal of Geotechnical Engineering Division*, ASCE, Vol. 106(GT2), 117-135.

ICOLD. (1990). "Dispersive soils in embankment dams", *ICOLD*, Bulletin no: 77, France.

Indraratna, B. (1996). "Utilization of lime, slag and fly ash for improvement of a colluvial soil in New South Wales, Australia", *Journal of Geotechnical & Geological Engineering*, Vol. 14, 169-191.

Indraratna, B., Balasubramaniam A.S. and Khan M.J. (1995). "Effect of fly ash with lime and cement on the behaviour of a soft clay", *Quarterly Journal of Engineering Geology*, Vol. 28, 131-142.

Indraratna, B., Nutalaya, P. and Kuganenthira, N. (1991). "Stabilisation of a dispersive soil by blending with flyash", *Quarterly Journal of Engineering Geology*, Vol. 24, 275-290.

Ingles, O.G (1962). "Bonding forces in soils part 3; A theory of tensile strength for stabilized and naturally coherent soils", *Proceedings of the 1st conference of the Australian Road Research Board,* Vol. 1, 1025-1047.

Kamphuis, J.W. and Hall, K.R. (1983). "Cohesive material erosion by unidirectional current", *Journal of Hydraulic Engineering*, ASCE, Vol. 109(1), 49-61.

Kandiah, A. and Arulanandan, K. (1974). "Hydraulic erosion of cohesive soils", *Transportation Research Record*, No: 497, 60-68.

Karol, R.H. (2003) "*Chemical Grouting and Soil Stabilisation*", *3rd Edition*, Marcel Dekker Inc. New York, Basel, USA.

Kawamura, M. and Diamond, S. (1975). "Stabilisation of clay soils against erosion loss", *Clays and clay minerals*, Vol. 23, 444-451.

Krishnayya, A.V.G., Eisenstein, Z. and Morgenstern, N.R. (1974). "Behaviour of compacted soil in tension", *Journal of the Geotechnical Engineering Division*, ASCE, Vol. 100(GT9), 1051-1061.

Kuganenthira, N. (1990). "Engineering behaviour of fly ash and its effectiveness in stabilising dispersive soils", *MEng. Thesis*, AIT, Thailand.

Leonards, G.A. and Narain, J. (1963). "Flexibility of clay and cracking of earth dams", *Journal of the Soil Mechanics and Foundations Division*, ASCE, Vol. 89(SM2), 47-97.

Lim, S.S. (2006). "Experimental investigation of erosion in variably saturated clay soils", *PhD Thesis*, University of New South Wales, Australia.

Lo, S.R. and Wardani, S.P.R. (2002). "Strength and dilatancy of a silt stabilized by a cement and fly ash mixture", Canadian Geotechnical Journal, Vol. 39, 77-89.

Locke, M.R. (2001). "Analytical and laboratory modelling of granular filters for embankment dams", *PhD Thesis*, University of Wollongong, Australia.

Lohnes, R.A. and Coree, B.J. (2002). "Determination and evaluation of alternative methods for managing and controlling highway-related dust", *Final Report TR 449*, Iowa Highway Research Board.

Lyle, W.M. and Smerdon, E.T. (1965). "Relation of Compaction and other soil properties to erosion resistance of soils", *Transactions of the ASAE*, 419-422.

Machan, G., Diamond, S. and Leo, E. (1977). "Laboratory study of the effectiveness of cement and of lime stabilisation for erosion control", *Transportation Research Record*, Vol. 641, 24-28.

McDaniel, T.N. and Decker, R.S. (1979). "Dispersive soil problem at Los Esteros dam", *Journal of the Geotechnical Engineering Division*, ASCE, Vol. 105(GT9), 1017-1030.

Mitchell, J.K. (1976). "Fundamentals of soil behaviour", John Wiley & Sons, Inc. New York, USA.

Narain, J. and Rawat, P.C. (1970). "Tensile strength of compacted soils", *Journal of the Soil Mechanics and Foundations Division*, ASCE, Vol. 96(SM6), 2185-2190.

Parker, D.B., Michel, T.G. and Smith, J.L. (1995). "Compaction and water velocity effects on soil erosion in shallow flow", *Journal of Irrigation and Drainage Engineering*, ASCE, Vol. 121(2), 170-178.

Pengelly, A.D., Boehm, D.W., Rector, E. and Welsh, J.P. (1997). "Engineering experience with in-situ modification of collapsible and expansive soils", *Unsaturated soil engineering practice, ASCE Geotechnical Special Publication no: 68*, 277-298.

Perry, J.P. (1977). "Lime treatment of dams constructed with dispersive clay soils", Soil and Water Division, *Transactions of the ASAE*, 1093-1099.

Phillips, J.T. (1977). " Case histories of repairs and design for dams built with dispersive clay", *Dispersive clays, related piping, and erosion in geotechnical projects, ASTM STP 623*, Sherard and Decker, Eds., 330-340.

Proffitt, A.P.B, Hairsine, P.B and Rose, C.W. (1993). "Modelling soil erosion by overland flow: Application over a range of hydraulic conditions", Soil and Water Division of ASAE, Vol. 36(6), 1743-1753.

Puppala, A.J. and Hanchanloet, S. (1999). "Evaluation of a new chemical (SA-44/LS-40) treatment method on strength and resilient properties of a cohesive soil", paper presented at Transportation Research Board Annual Meeting.

Rajasekaran, G., Murali, K. and Srinivasaraghavan, R. (1997). "Fabric and mineralogical studies on lime treated marine clays", *Ocean Engineering Journal*, Vol. 24(3), 227-234.

Reddi, L.N. and Bonala, M.V.S. (1997), "Critical Shear stress and its relationship with cohesion for sand kaolinite mixtures", *Canadian Geotechnical Journal*, Vol. 34, 26-33.

Rosewell, C.J. (1977). "Identification of susceptible soils and control of tunnelling failure in small earth dams", *Dispersive clays, related piping, and erosion in geotechnical projects, ASTM STP 623*, Sherard and Decker, Eds., 362-369.

Ryker, N.L. (1977). "Encountering dispersive clays on soil conservation service projects in Oklahoma", *Dispersive clays, related piping, and erosion in geotechnical projects, ASTM STP 623*, Sherard and Decker, Eds., 370-389.

Sanders, T.G., Addo, J.Q., Ariniello, A. and Heiden, W.F. (1997). "Relative effectiveness of road dust suppressants", *Journal of Transportation Engineering*, Vol. 123(5), ASCE, 393-397.

Sargunan, A. (1977). ''Concept of critical shear stress in relation to characterisation of dispersive clays.'', *Dispersive clays, related piping, and erosion in geotechnical projects, ASTM STP 623*, Sherard and Decker, Eds., 390–397.

Shaikh, A., Ruff, J.F., Charlie, W.A. and Abt, S.R (1988). "Erosion rate of dispersive and non dispersive clays", *Journal of Geotechnical Engineering Division*, ASCE, Vol. 114(5), 589–600.

Sherard, J.L., Decker, R.S. and Ryker, N.L. (1972). "Piping in earth dams of dispersive clay", *Proceedings, Specialty conference on performance of earth and earth-supported structures*, ASCE, Vol. 1(1), 589-626.

Sherard, J.L., Dunnigan, L.P., Decker, R.S. and Steele, E.F. (1976a). "Pinhole test for identifying dispersive soils", *Journal of the Geotechnical Engineering Division*, ASCE, Vol. 102(GT1), 69-85.

Sherard, J.L., Dunnigan, L.P., and Decker, R.S. (1976b). "Identification and nature of dispersive soils", *Journal of the Geotechnical Engineering Division*, ASCE, Vol. 102(GT4), 287-301.

Shrestha, P.L. and Arulanandan, K. (1989). "Discussions on Erosion rate of dispersive and non dispersive clays" by Shaikh, A., Ruff, J.F., Charlie, W.A. and Abt, S.R, *Journal of Geotechnical Engineering Division*, ASCE, Vol. 115(12), 1824-1825.

Tingle, J.S., and Santori, R.L. (2003). "Stabilisation of Clay Soils with Nontraditional Additives" *Transportation Research Record*, National Research Council, Washington, D.C., Vol. 1819, 72-84.

Uddin, K. (1995). "Strength and deformation characteristics of cement treated Bangkok clay", *PhD thesis*, Asian Institute of Technology, Thailand.

Uddin, K., Balasubramaniam, A.S. and Bergado, D.T. (1997). "Engineering behaviour of cement treated Bangkok soft clay, *Geotechnical Engineering*, Vol. 28(1), 89-119.

Uddin, K. and Buensuceso, B.R. (2002). "Lime treated clay: Salient engineering properties and a conceptual model", *Soils and Foundations*, Japanese Geotechnical Society, Vol. 42(5), 79-89.

Udomchoke, V. (1991). "Origin and engineering characteristics of the problem soils in the Khorat basin, Northern Thailand", *PhD thesis*, Asian Institute of Technology, Bangkok.

US Army Corps of Engineer (1995). "Manual on Chemical grouting", No: EM 1110-1-3500, paragraph 2-6.

Wan, C.F. and Fell, R. (2002). Investigation of internal erosion and piping of soils in embankment dams by the slot erosion test and the hole erosion test", *UNICIV report No: R-412*, University of New South Wales, Australia.

Wan, C.F. and Fell, R. (2004). "Investigation of rate of erosion of soils in embankment dams", *Journal of Geotechnical and Geoenvironmental Engineering*, ASCE, 130(4), 373-380.

APPENDIX A

EXPERIMENTAL PROCEDURE FOR EROSION TESTING

A.1 General

This appendix describes the procedure to carry out erosion testing using Process Simulation Apparatus for Internal Crack Erosion (*PSAICE*). The following are elaborated.

- Determination of particle size distribution of eroded soil
- Safe operating procedure
- Detailed drawing of the apparatus

A.2 Determination of Particle Size Distribution of Eroded Soil

As described in Chapter 4, it was necessary to determine the particle size distribution of eroded soil to calculate the hydraulic shear stress. Collecting all sediments during a continuous erosion test was difficult, because, every test yielded a large volume of effluent. Hence, an additional erosion test was carried out on an identical soil sample to determine the particle size distribution. Test was conducted for a short period of time to collect 2-3 liters of effluent without loosing the sediment into drain. The effluent was then condensed (evaporation) to get sufficient concentration for the testing, if required. Consequently, the effluent was put into a beaker and stirred with the help of magnetic stirrer. While stirring, a 100-150 ml sub-sample was collected,

and it was then analysed using the Malvern Mastersizer to get the particle size distribution of the eroded soil (Figure A.1).

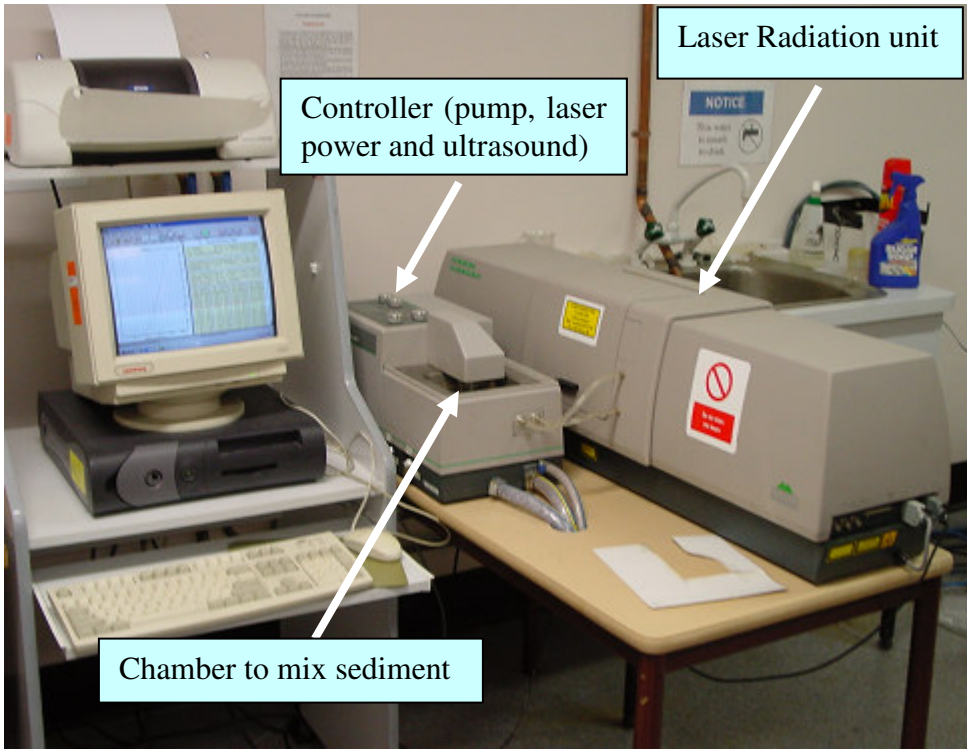

Figure A.1 Photograph of the Malvern Mastersizer

A.3 Safe Operating Procedure

HAZARDS:

Moving parts (tank), Electric shock

PERSONAL PROTECTION EQUIPMENT:

Gloves, Protection shoes

PRE START:

- Keep all electric cables off the floor where water can spill during the test
- Assemble the soil sample and the turbidity meter with the pipeline network
- Close the inlet valve and outlet valve, and open air release valves
- Fill the whole system with eroding fluid until the air is released completely
- Switch on the power to the turbidity meter and the electronic balance, and check their working conditions
- Release the outlet valve and bring the moving head tank to the required position
- Pump the eroding fluid into the head tank until it spills over the weir

START:

- Once the readings of the turbidity meter, pressure transducers, and electronic balance come to stable values, Log on the data taker and balance talk software
- Turn on the inlet valve gently to its full open position

END OF TESTING:

- Stop the pump and release the water from the collection tank at the outlet
- Switch off the power to the turbidity meter and release it from the set up
- Remove all water from the pipeline and then take the soil sample out

PLEASE NOTE:

Before operating the apparatus, all UG/PG students and any unauthorized persons must complete induction program and sign both the Safety Awareness and Training Confirmation forms.

A.4 Detailed Drawing of the *PSAICE*

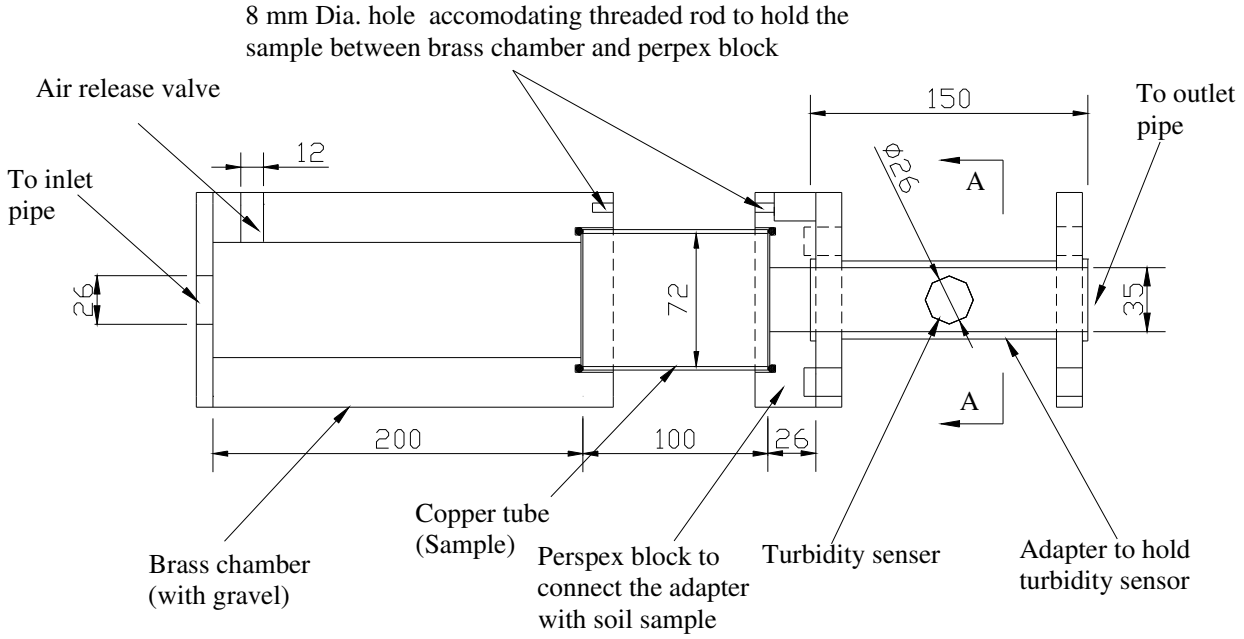

LONGITUDINAL SECTION OF BRASS CHAMBER, COPPER TUBE, PERSPEX BLOCK AND ADAPTER FOR TURBIDITY PROBE

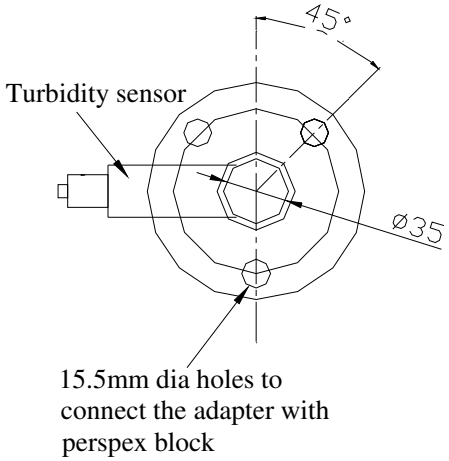

END ELEVATION A-A
(Only adapter details are shown)

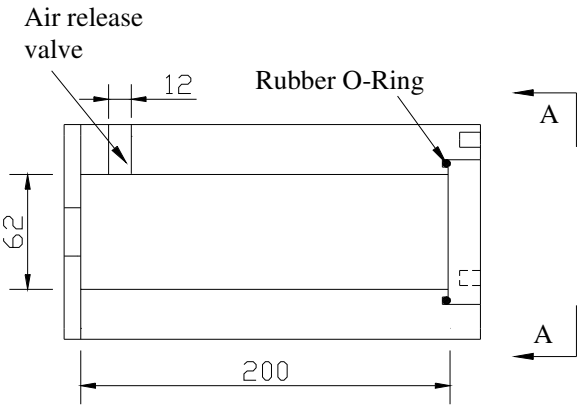

LONGITUDINAL SECTION OF
BRASS CHAMBER

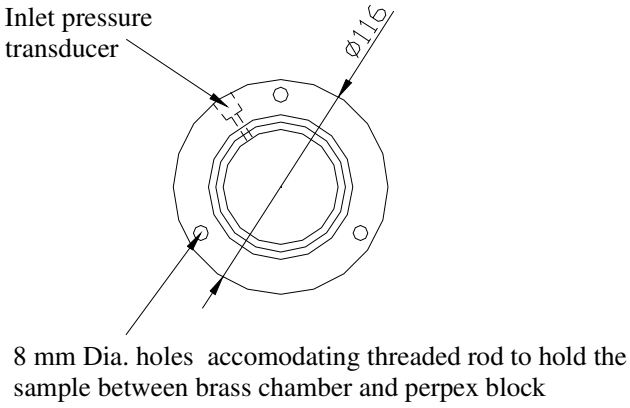

END ELEVATION A-A

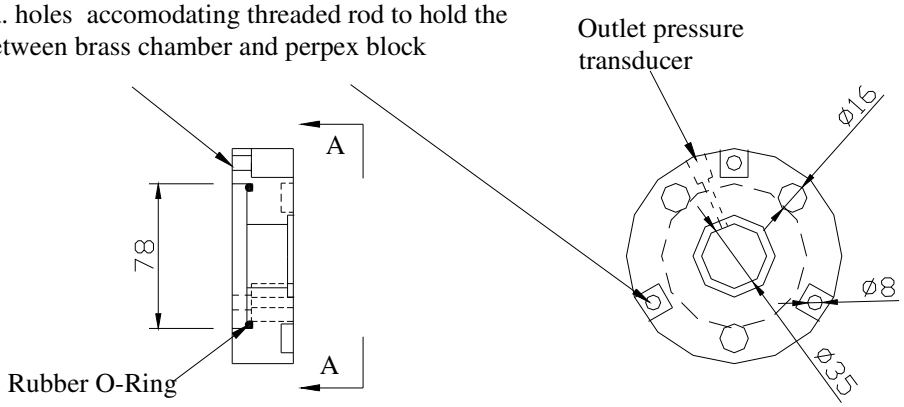

LONGITUDINAL SECTION
OF PERSPEX BLOCK

END ELEVATION A-A

APPENDIX B

SAFE OPERATING PROCEDURE AND DETAILED DRAWING OF TENSILE TESTING APPARATUS

B.1 Safe Operating Procedure

HAZARDS:

- Possible crushing during soil compaction using AVERY machine
- Falling of top half of the apparatus at the end of tensile testing

PERSONAL PROTECTION EQUIPMENT:

Gloves, Protection shoes

PRE START:

Prepare the sample by static compaction using AVERY

START:

- Switch on the INSTRON machine at least ½ an hour before the test
- Fix the lower half of the apparatus with INSTRON using a pin
- Fix the upper half of the apparatus and load cell with INSTRON using a pin
- Set the LVDT and apply the load, then Log the data

END OF TESTING:

- Bring the upper half of the apparatus to its initial position (make sure that compressive force is not applied on the load cell)
- Release the pin and move the INSTRON platen UP to get enough clearance to remove the top half of the apparatus
- Switch OFF INSTRON and remove the lower half of the apparatus by releasing the pin

PLEASE NOTE:

Before operating AVERY and INSTRON, all UG/PG students and any unauthorized persons must complete induction program and sign both the Safety Awareness and Training Confirmation forms.

B.2 Detailed Drawing of the Apparatus

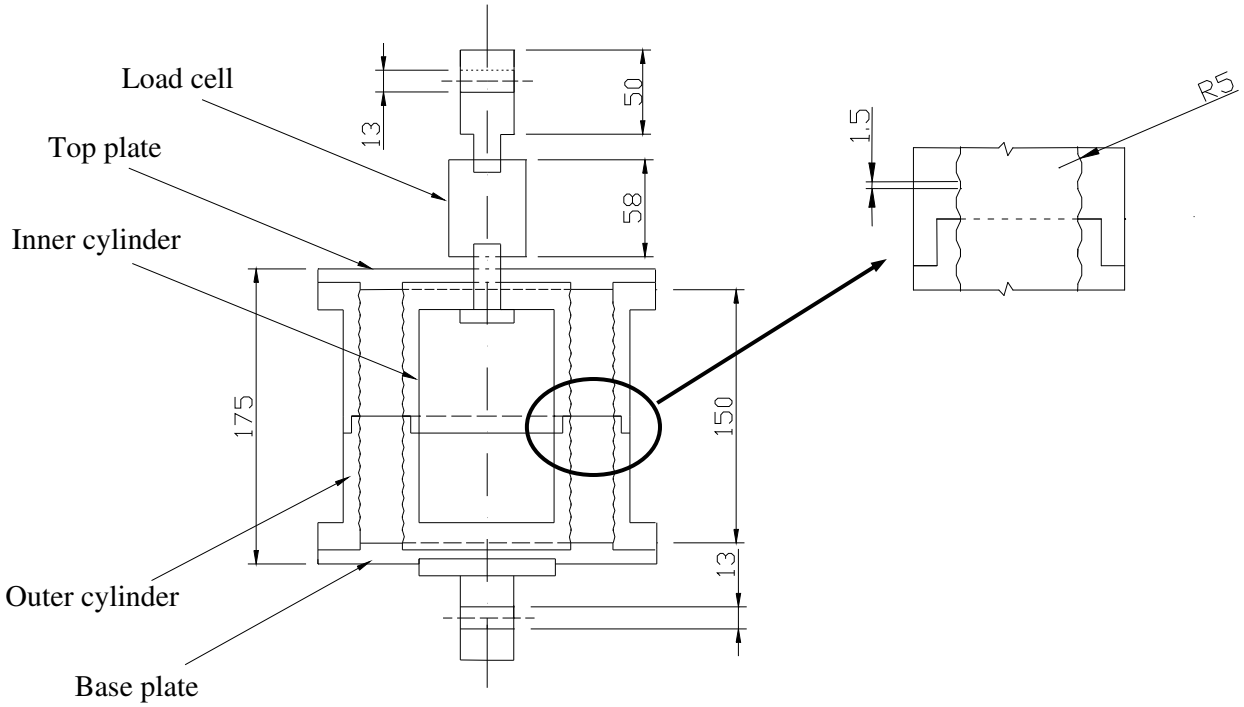

Cross section of Tensile testing apparatus

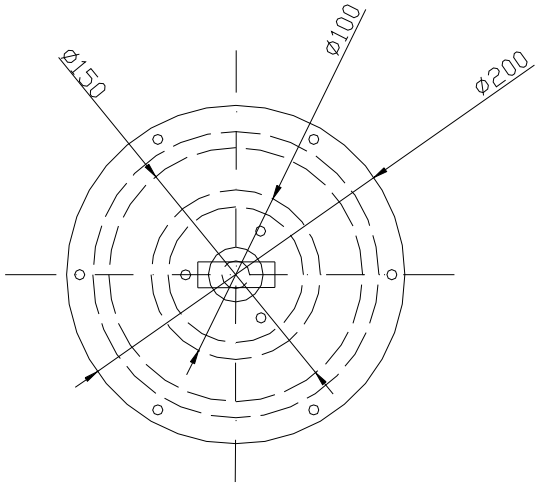

Plan view of Tensile testing apparatus

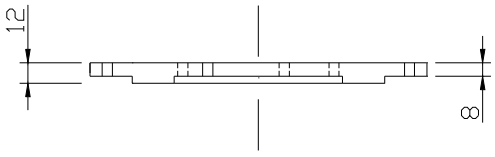

Cross section of Top plate

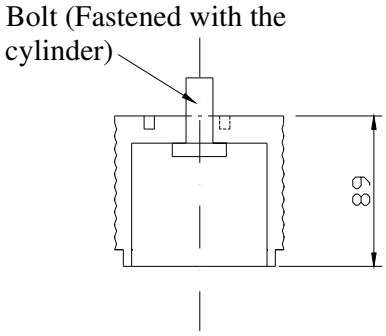

Cross section of Inner cylinder (Top half)

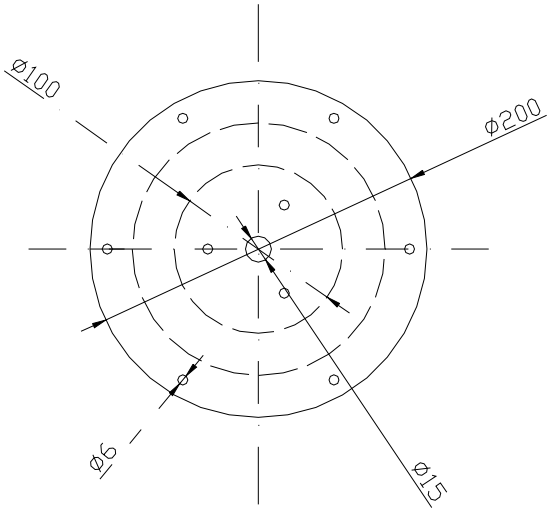

Plan view of Top plate

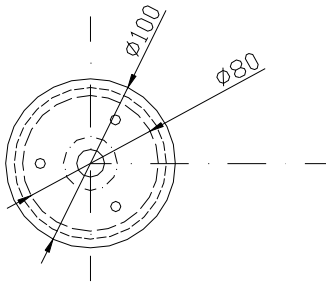

Plan view of Inner cylinder (Top half)

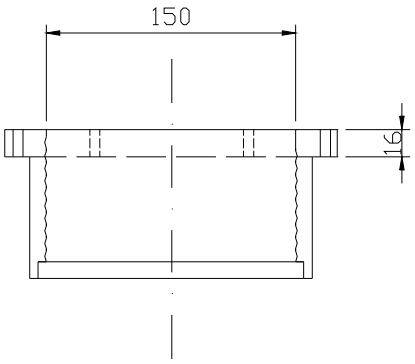

Cross section of Outer cylinder (Top half)

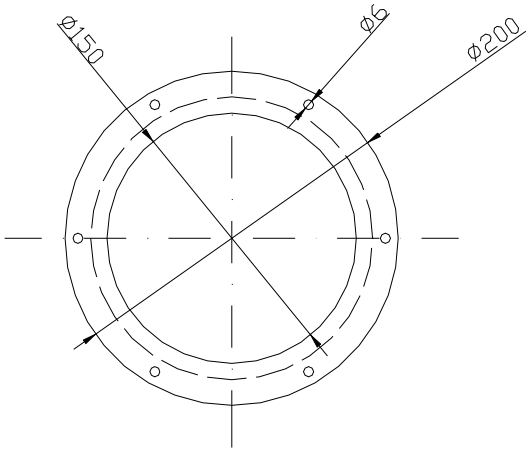

Plan view of Outer cylinder (Top half)

APPENDIX C

MATERIAL SAFETY DATA SHEET FOR LIGNOSULFONATE MIXTURE

C.1 Introduction to Chemical Stabiliser

Recommended use:	Soil conditioner and stabiliser
Chemical family	Lignosulfonate mixture

C.2 Hazardous Identification

Non-hazardous substance and Non-dangerous goods.

Not classified as hazardous according to the criteria of NOHSC

C.3 Composition/Information on Ingredients

Appearance:	Dark brown liquid with vanilla-like odor

Ingredients:

Chemical Name, CAS No	**Proportion**	**Risk phrases**
Lignosulfonate mixture	30-60%	-
Minor ingredients	<5%	-
Water	To make total of 100%	-

All constituents of this material are listed on the Australian Inventory of Chemical Substances (AICS)

C.4 First Aid Measures

Poison information center in each state can provide additional assistance for scheduled poisons. Phone: 131126 from anywhere in Australia.

Ingestion:

Rinse mouth with water. Give 2-3 glasses of water to drink. Do NOT induce vomiting. Seek medical advice immediately.

Eye contact:

Immediately flush the contaminated eye(s) with lukewarm, gently flowing water for AT LEAST 15 minutes, by the clock.

Skin Contact:

Wash contaminated skin with plenty of water. Remove contaminated clothing and wash before re-use. If irritation persists, seek medical advice.

Inhalation:

Remove source of contamination or move victim to fresh air. Administer oxygen if breathing is difficult. Obtain medical advice.

Other first aid:

Provide general supportive measures (comfort, warmth, rest). Consult a physician and/or the nearest Poison Information Center.

Notes to physician: Treat symptomatically.

C.5 Fire Fighting Measures

Special Hazards:

Non-combustible material.

Fire fighting further advice:

Non-combustible. Water-based solution.

Suitable extinguishing media:

Water fog (or if unavailable fine water or spray), foam, dry agent (carbon dioxide, dry chemical powder).

C.6 Accidental Release Measures

Small Spills:

Contain sand or diatomaceous earth. Collect and seal in properly labeled drums. Wash remaining area with large volumes of water.

Large Spills

PRECAUTIONS Restrict access to area. Clear area of unprotected personnel. Provide adequate protective equipment and ventilation.

Remove chemicals which can react with the spilled material. Spills are slippery.

CLEANUP Contain spill or leak. Do not allow entry into sewers or waterways. Spilled solutions should be contained by dyking with inert material, such as sand or earth. Solutions can be recovered or carefully diluted with water.

C.7 Handling and Storage

Handling:

Avoid contact with eyes or skin. Avoid breathing vapors or mists. Wash thoroughly after handling. Keep containers closed when not in use.

Storage conditions:

Store in suitable labeled containers. Keep containers tightly closed when not in use and empty. Protect from damage.

C.8 Exposure Controls/Personal Protection

Exposure standards:	No values assigned by NOHSC Australia.
Engineering controls:	Use in well-ventilated area. Keep containers closed when not in use.
Personal protection:	Wear goggles or safety glasses with side protection. Wear protective clothing and nitrile or neoprene gloves.

C.9 Physical & Chemical Properties

Appearance:	Dark brown liquid
Odor threshold:	Not available
Specific gravity:	Approx 1.2
Flammability limits:	Non-flammable
pH:	3.8 approx.

C.10 Stability and Reactivity

Incompatibility:	None
Hazardous decomposition products:	Sulphur dioxide
Hazardous polymerization:	Does not occur
Corrosivity to metals:	Non-corrosive
Explosion data- sensitivity to mechanical impact	N/A
Explosion data- sensitivity to static charge	N/A
Fire Hazard comments:	Will not burn or support combustion
Fire extinguishing agents:	Use extinguisher appropriate to the material which is burning
Fire fighting procedures:	Water can be used to extinguish a fire in an area where product is stored
Combustion products:	Oxides of carbon and sulphur

C.11 Toxicological Information

Acute effects:

Ingestion:	May cause local irritation to the gastro-intestinal tract and abdominal pain to occur
Eye contact:	Spray and mist may cause eye irritation
Skin contact:	May cause skin irritation
Inhalation:	Not established. May cause irritation

Long term effects: There have no documented effects due to long-term exposure to product

Toxicity data: No data

C.12 Ecological Information

Avoid contaminating waterways.

C.13 Disposal Consideration

Refer State Land Waste Management Authority. Decontaminate empty containers before disposal, by triple rinsing with water, using rinse water in further processing or neutralise rinse water.

C.14 Regulatory Information

Not classified as hazardous according to the criteria of NOHSC. Not scheduled per SUSDP. Not a dangerous good according to ADG code.

R-Prases: Nil

S-Phrases: Nil

C.15 Other Information

References:

1. National code of practice for the preparation of MSDS (NOHSC: 2011(2003))
2. List of Designated Hazardous Substances (NOHSC: 10005: 1999).

3. ADG Code 6th edition

4. Suppliers MSDS